Elastic and inelastic contributions to the diffuse scattering

Alexeï Bosak

European Synchrotron Radiation Facility

Introduction

Technical issues

Applied examples

- zinc
- quartz
- magnetite
- prussian blue
- BMT

Conclusions

Introduction

Starting point: diffraction

crystal

$$\sum_{i,j,k}\delta(\mathbf{r}-\mathbf{r}_1 i-\mathbf{r}_2 j-\mathbf{r}_3 k)\otimes\rho(\mathbf{r})\cdot\mathrm{shape}(\mathbf{r})$$

infinite lattice with basis vectors $\mathbf{r}_1$, $\mathbf{r}_2$, $\mathbf{r}_3$

density distribution in the unit cell

crystal shape

FT

$$\sum_{i,j,k}\delta(\mathbf{Q}-\mathbf{q}_1 i-\mathbf{q}_2 j-\mathbf{q}_3 k)\cdot\int_{UC}\rho(\mathbf{r})\exp(2\pi i\mathbf{r}\mathbf{Q})d\mathbf{r}\otimes SHAPE(\mathbf{Q})$$

infinite lattice with basis vectors $\mathbf{q}_1$, $\mathbf{q}_2$, $\mathbf{q}_3$

structure factor

FT of crystal shape

ESRF

Starting point: diffraction

$$\sum_{ijk}\delta(\mathbf{Q}-\mathbf{q}_1 i-\mathbf{q}_2 j-\mathbf{q}_3 k)\cdot\int_{UC}\rho(\mathbf{r})\exp(2\pi i\mathbf{rQ})d\mathbf{r}\otimes SHAPE(\mathbf{Q})$$

infinite lattice with basis vectors $\mathbf{q}_1, \mathbf{q}_2, \mathbf{q}_3$

structure factor

FT of crystal shape

large crystal => $SHAPE(\mathbf{Q})\rightarrow\delta(\mathbf{Q})$

FT(crystal) becomes a set of δ *functions with different prefactors*
nothing between Bragg reflections!

structure factor

$$F(\mathbf{Q})=\sum_d f_d(\mathbf{Q})\exp(2\pi\mathbf{Q}\mathbf{r}_d)$$

⟶

structure factor including thermal blurring

$$F(\mathbf{Q})=\sum_d f_d(\mathbf{Q})\exp(2\pi\mathbf{Q}\mathbf{r}_\mathbf{d})\exp(-W_d(\mathbf{Q}))$$

Starting point: diffraction

$CaCO_3$ single crystal
room temperature

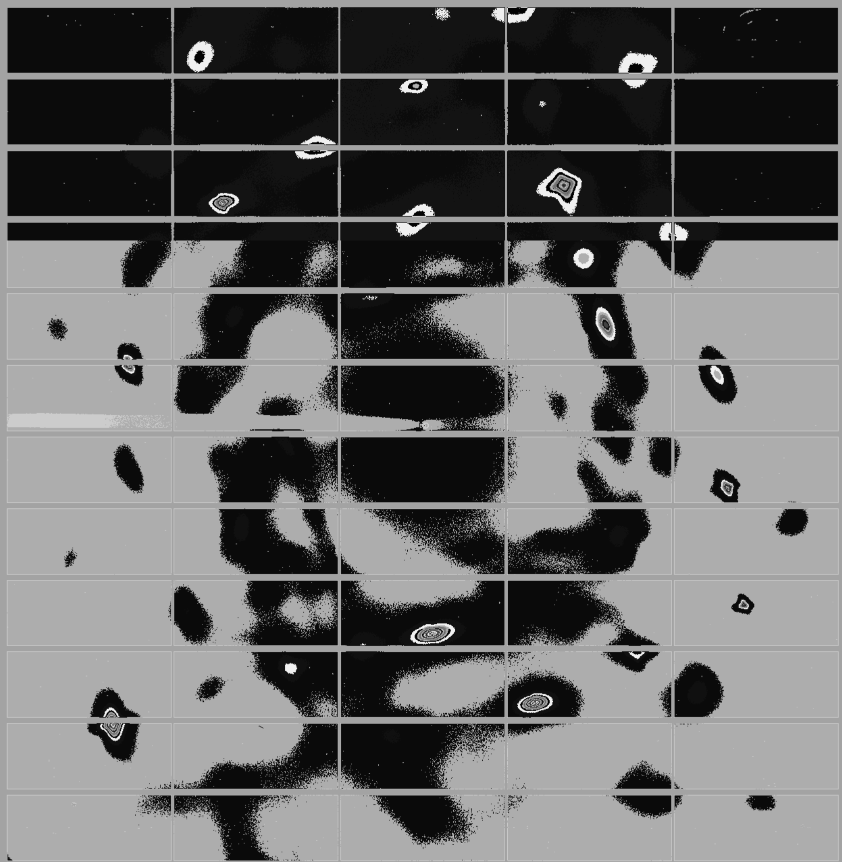

raw image taken with PILATUS 6M detector
X06SA SLS

Step forward: thermal vibrations

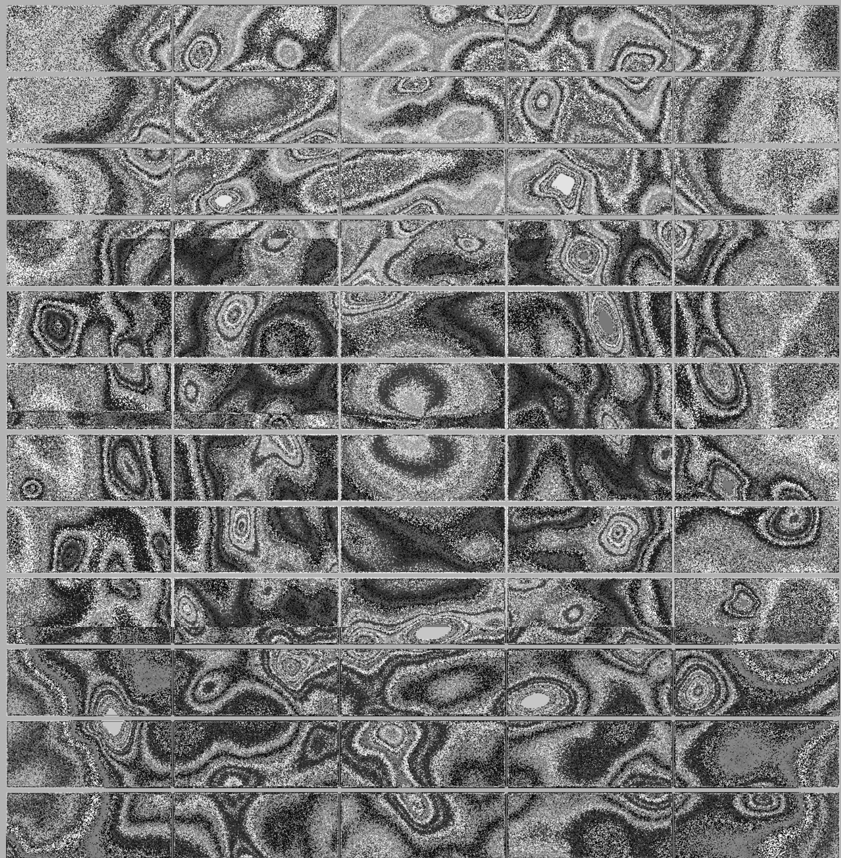

raw image taken with PILATUS 6M detector
X06SA SLS

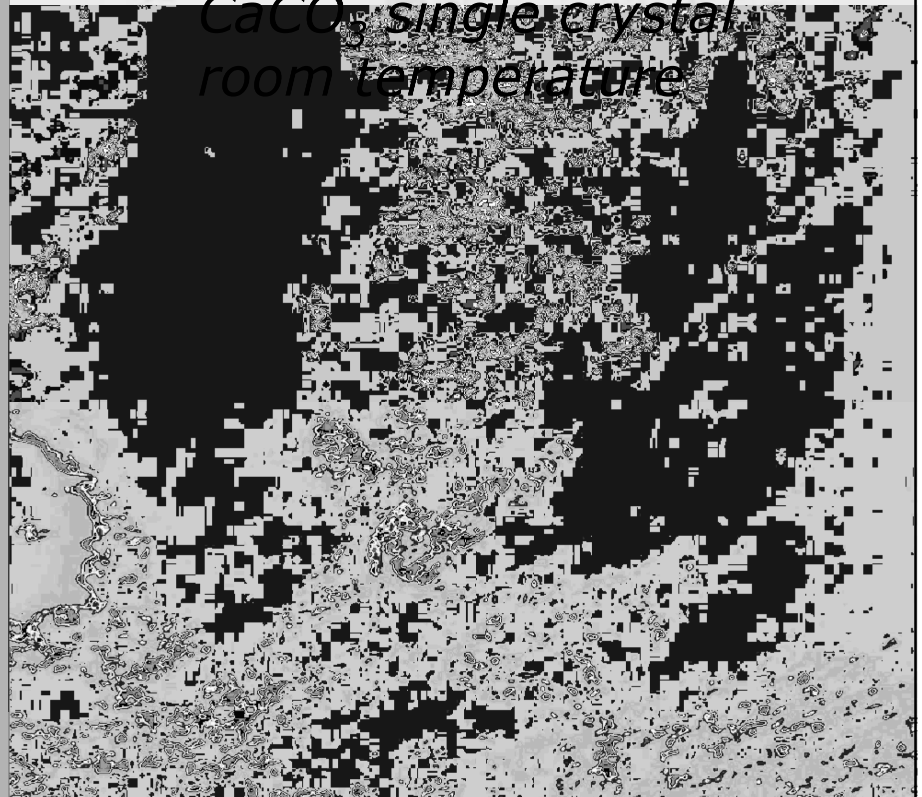

$CaCO_3$ single crystal
room temperature

Scattering on thermal vibrations (3D)

$$\mathbf{D}(\mathbf{q})\hat{\boldsymbol{\sigma}}^{j}(\mathbf{q}) = \hat{\boldsymbol{\sigma}}^{j}(\mathbf{q})\omega_j^2$$

dynamical equation decribes the modes allowed to propagate in crystal

ω_j *- mode frequency,* $\hat{\boldsymbol{\sigma}}^{j}(\mathbf{q})$ *mode eigenvector*

$\int S(\mathbf{Q},\omega)d\omega$ *- thermal diffuse scattering (TDS)*

$$I(\mathbf{Q}) \propto \sum_{j=1}^{3N} \frac{1}{\omega_j} \coth\left(\frac{\hbar\omega_j}{2kT}\right) \left| \sum_{d=1}^{N} f_d(Q) \exp(-W_d(\mathbf{Q}) + i\mathbf{Q}\cdot\mathbf{d})(\mathbf{Q}\cdot\hat{\sigma}_d^j(\mathbf{q})) M_d^{-1/2} \right|^2$$

or

$$I(\mathbf{Q}) \propto \mathbf{Q}^T \cdot \mathbf{Z}(\mathbf{Q}) \frac{\hbar}{2\sqrt{\boldsymbol{D}(\mathbf{q})}} \coth\left(\frac{\hbar\sqrt{\boldsymbol{D}(\mathbf{q})}}{2kT}\right) \mathbf{Z}^{*}(\mathbf{Q}) \cdot \mathbf{Q}$$

$$Z_{\alpha\alpha}(\mathbf{Q}) = f_{[\alpha/3]}(\mathbf{Q}) \exp(-W_{[\alpha/3]}(\mathbf{Q}) + i\mathbf{Q}\cdot\mathbf{r}_{[\alpha/3]}) M_{[\alpha/3]}^{-1/2}$$

A. Bosak, D. Chernyshov, Acta Cryst. A ***64****, 598 (2008)*

Thermal diffuse scattering in silicon

raw image taken with PILATUS 6M detector
X06SA SLS

area detectors -> revival of TDS since 1999

M. Holt, Z. Wu, H. Hong, P. Zschack, P. Jemian, J. Tischler, H. Chen, T.-C. Chiang
Phys. Rev. Lett. **83**, *3317 (1999)*

fitting of single images with lattice dynamics model

new age with pixel detectors?

FULL reciprocal space can be explored in few minutes

Step forward: chemical disorder + distortions

$$I_{\rm diff}(q) \propto e^{-2B_{\rm th}q^2}\left[I_{\rm DS}(q) + I_{\rm TDS}(q)\right]$$

assuming small lattice distortions

$$I_{\rm DS}(q) \propto \left\langle \left|\Delta c_q + i\bar{f}q \cdot u_q\right|^2 \right\rangle$$

chemical disorder

distortions

Huang scattering

$$I_H(Q) - N_d |F(\tau)|^2 \frac{Q^2}{q^2} \sum_{\alpha=1}^{\nu} \left(m_i C^{-1}_{qij} P_{qj} n_l\right)^2$$

$$C_{ij} = c_{ipqj} n_p n_q$$

structure factor

elastic dipole force tensor

Huang scattering

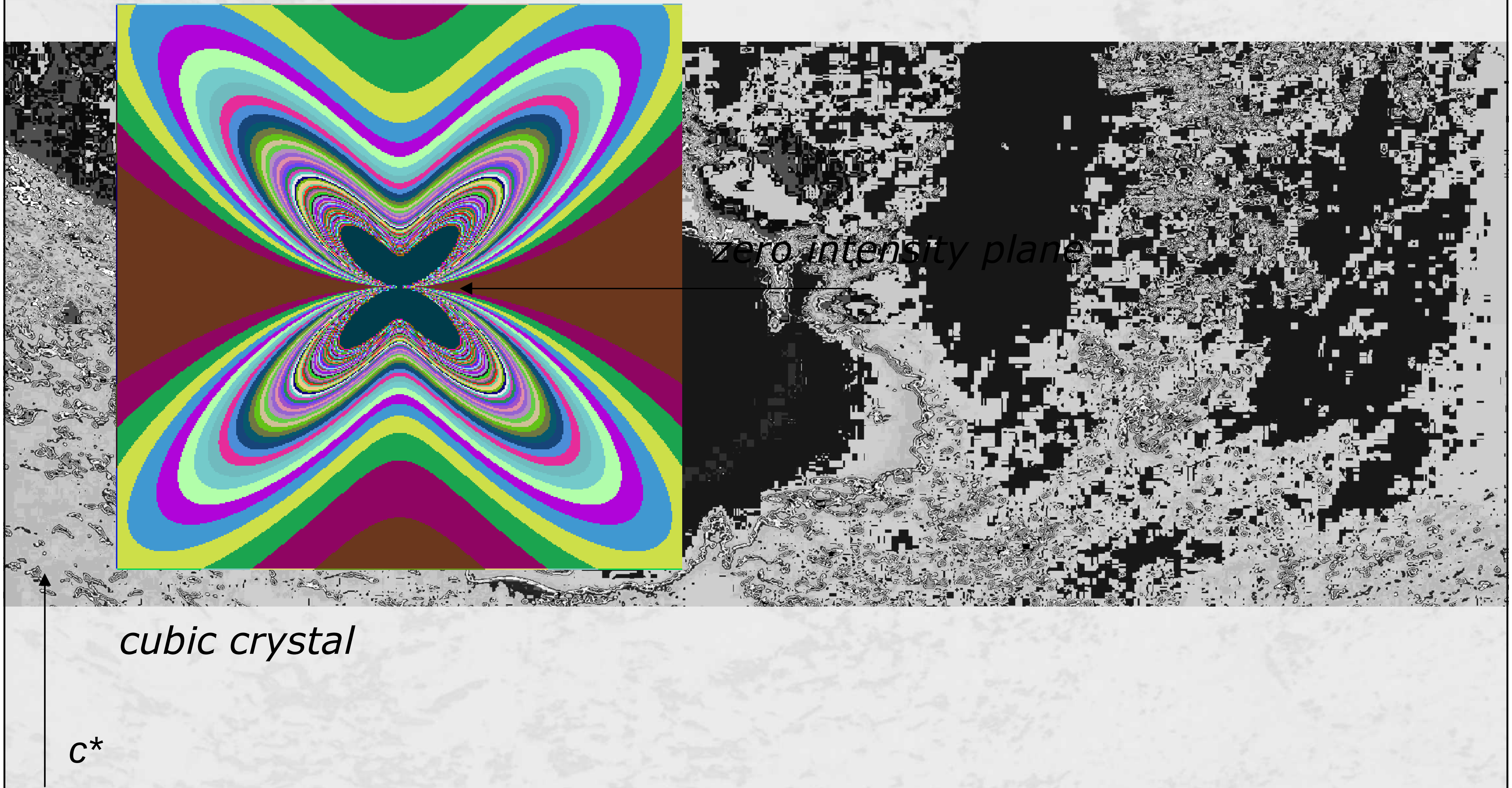

Huang scattering

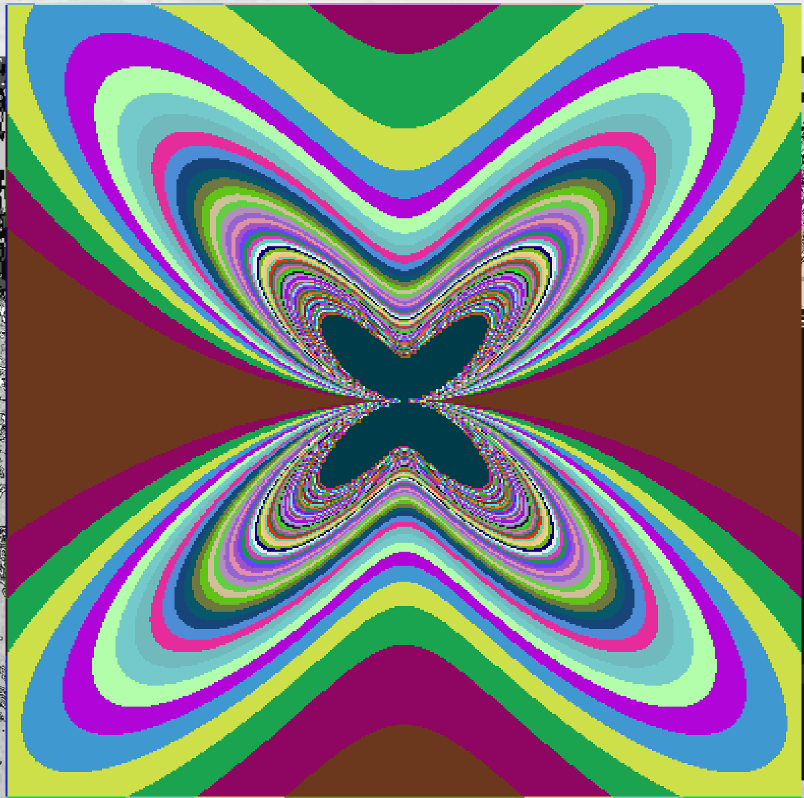

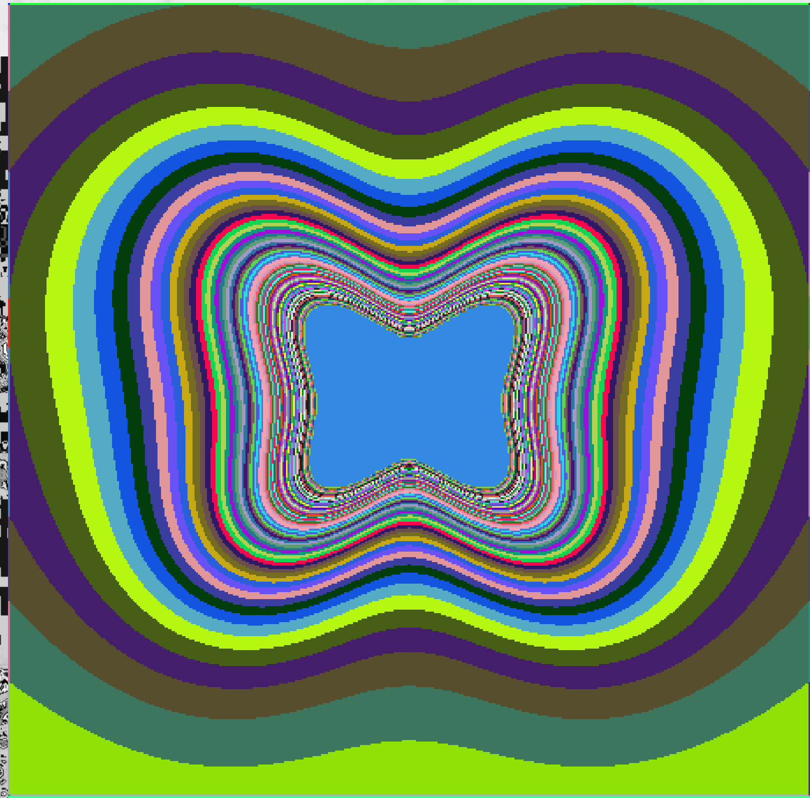

cubic crystal

*c**

do not mix with TDS!

Experimental issues

Reciprocal space exploration

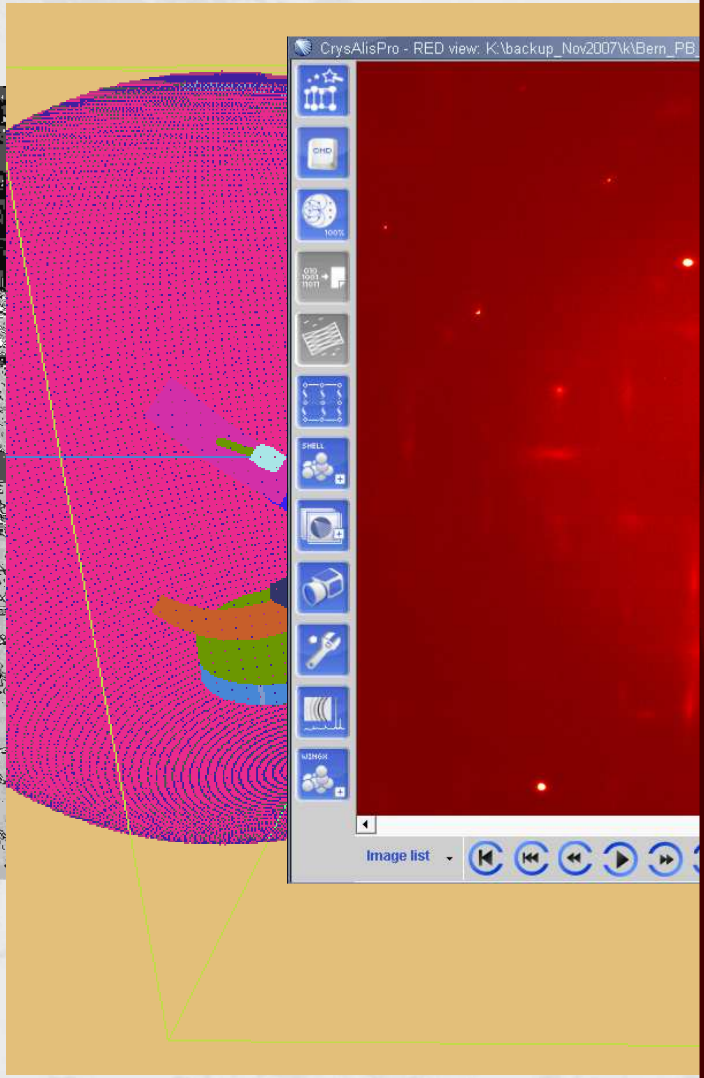

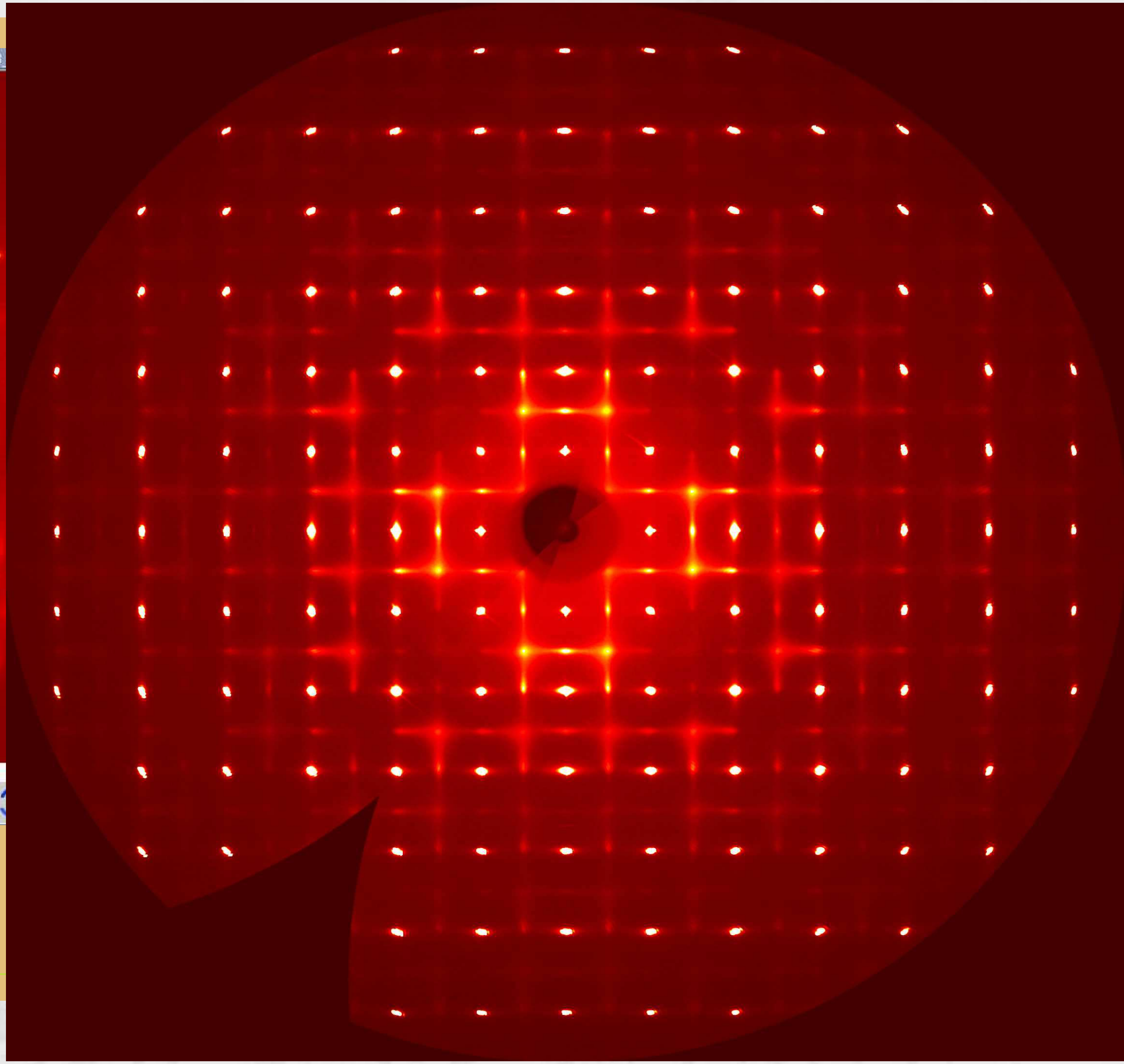

2D patterns $\rightarrow$ 3D

flat image
MAR
EDF
BSL
CBF
…

sphere

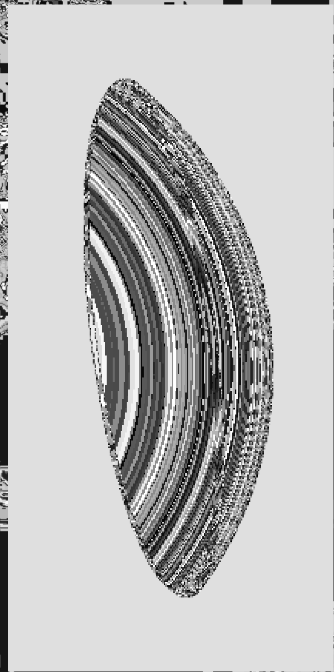

space filling

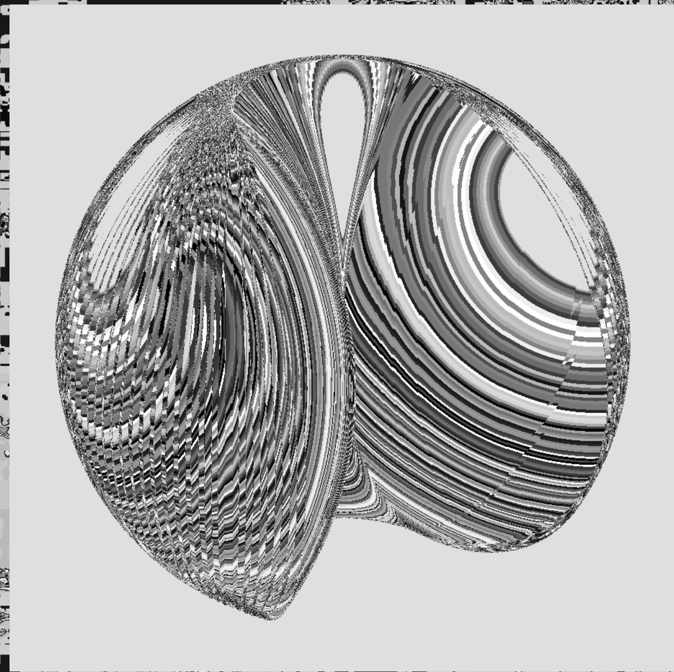

CCP4 map format

UCSF Chimera

VRML
X3D
POV-Ray
…

Energy-resolved scattering

Brockhouse (1955)

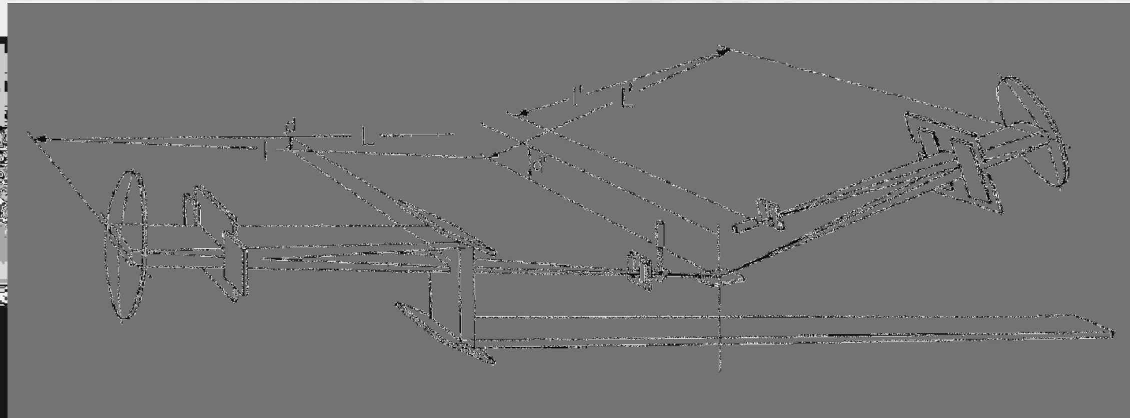

The instrument INELAX at the HARWI wiggler line of HASYLAB.

Burkel, Dorner and Peisl (1987)

Thermal neutrons:

E_i = 25 meV

k_i = 38.5 nm^{-1}

$\Delta E/E$ = 0.01 – 0.1

large beams: few mm or larger

Hard X-rays:

E_i = 18 keV

k_i = 91.2 nm^{-1}

$\Delta E/E \leq 1 \times 10^{-7}$

small beams: 100 μm or smaller

IXS kinematics

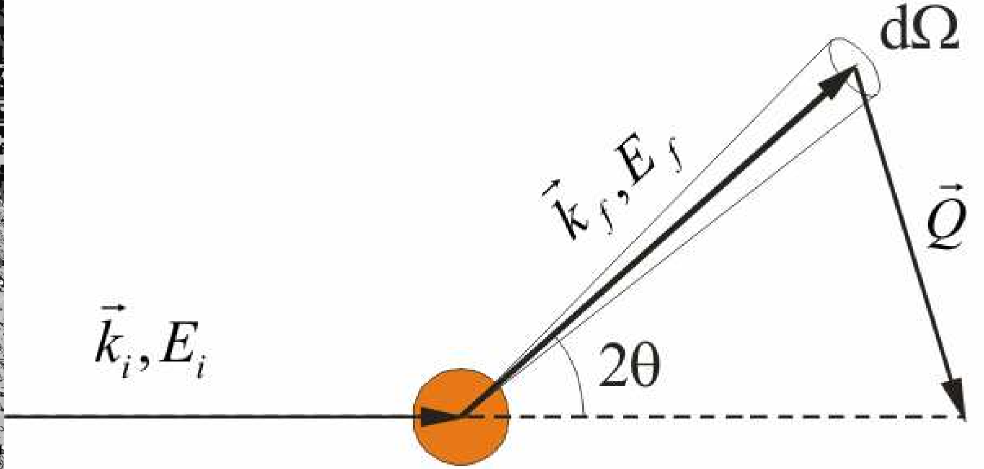

$E = E_i - E_f$
energy conservation

$\vec{Q} = \vec{k}_f - \vec{k}_i$
momentum conservation

$\Delta k/k \sim 10^{-7}$

$|\vec{Q}| = 2|\vec{k}_i|\sin(\theta)$

energy and momentum transfers are uncoupled

NB: for neutrons $E = E_i - \frac{\hbar^2}{2m_n}(\vec{k}_i - \vec{Q})^2$

Experimental IXS setup

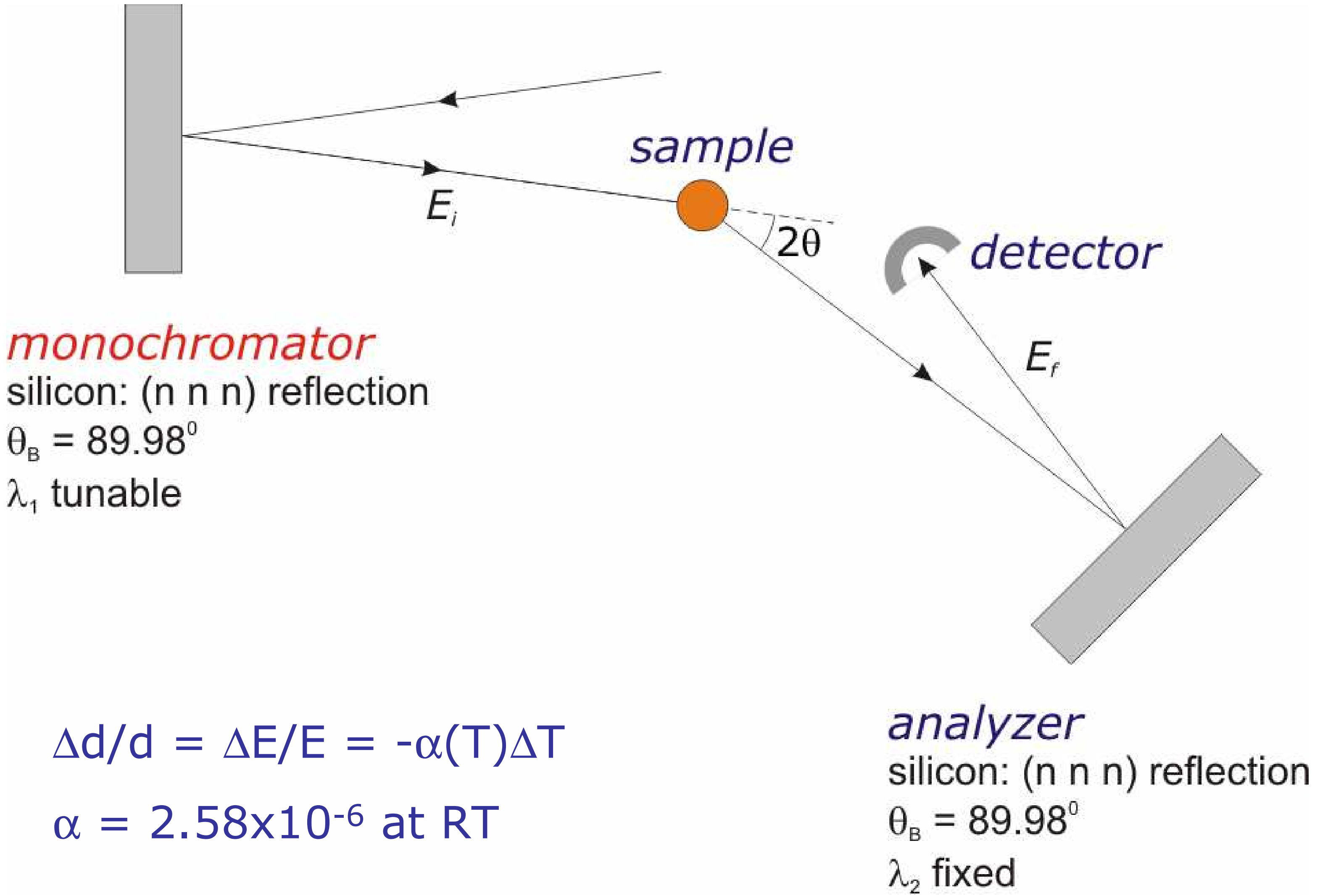

$\Delta d/d = \Delta E/E = -\alpha(T)\Delta T$

$\alpha = 2.58\text{x}10^{-6}$ at RT

ESRF: ID16 and ID28

Applied examples

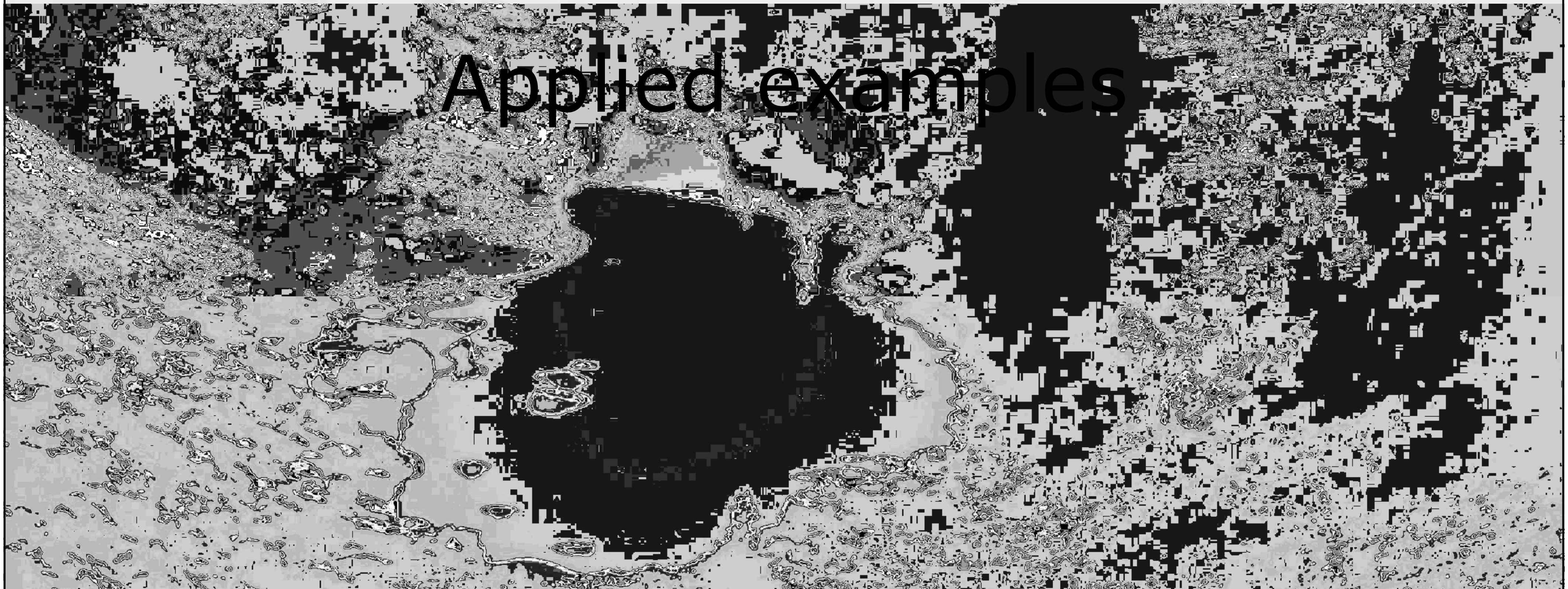

α-quartz lattice dynamics :

TDS + IXS + modeling

Departure point: boson peak

Lemma: boson peak in glass originates from TA singularity of "parent" crystal

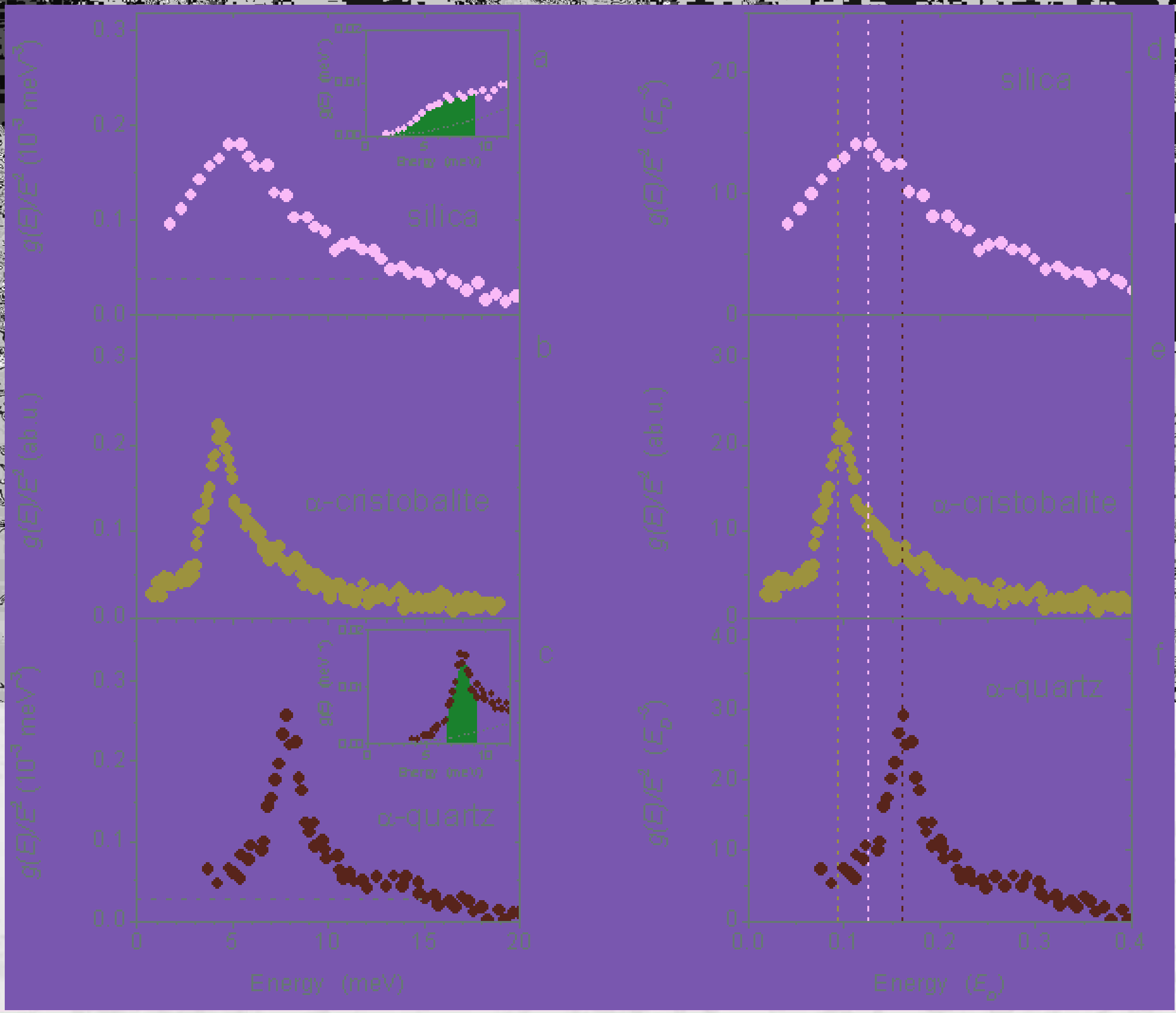

credits: A. Chumakov (ESRF ID18)

A.I. Chumakov, A. Monaco, G. Monaco, W.A. Crichton, A. Bosak, R. Rüffer, A. Meyer, F. Kargle, L. Comez, D. Fioretto, H. Giefers, S. Roitsch, G. Wortmann, M.H. Manghnani, A. Hushur, J. Balogh, Q. Williams, K. Parliński, P.T. Jochym, and P. Piekarz

Equivalence of the boson peak in glasses to the transverse van Hove singularity in crystals, submitted

X-VDOS: incoherent approximation with IXS

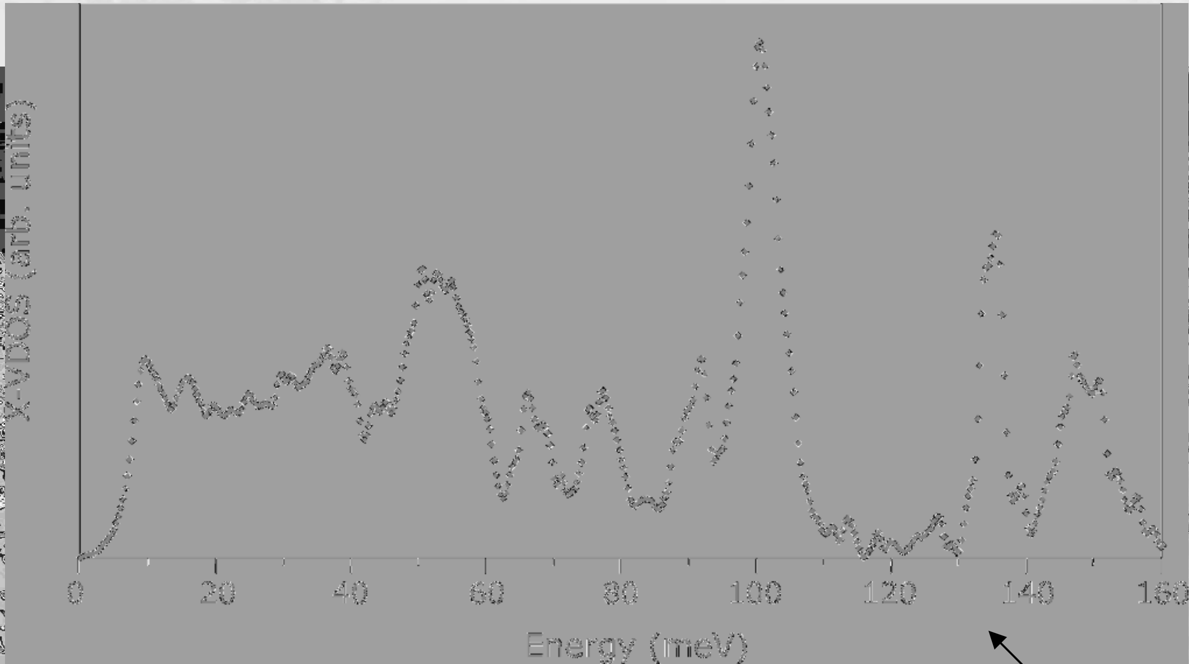

Harris et al., 2000

ID28@ESRF

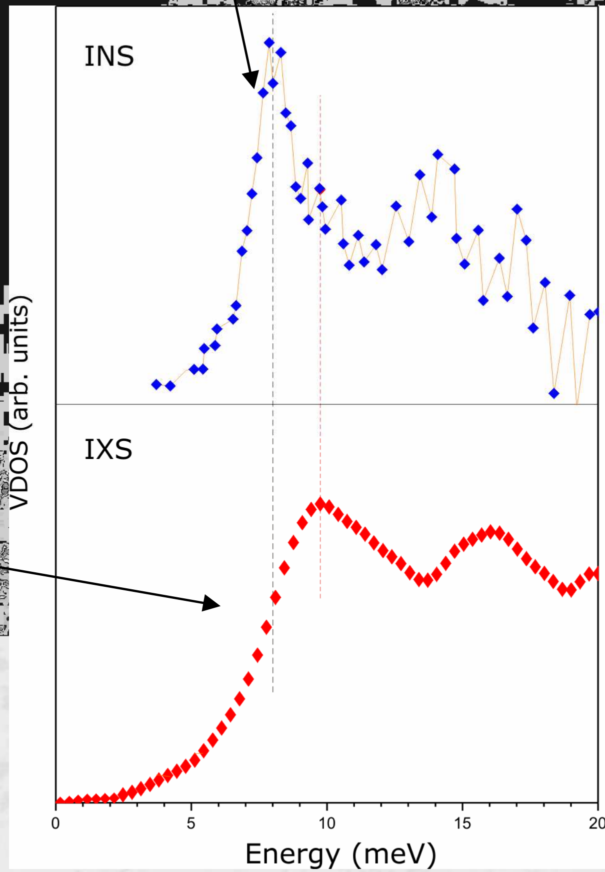

…obvious difference in peak position and spectral shape

Questions

- to which Q corresponds the low-energy peak in VDOS (related to boson peak problem)?

- are the “soft” directions always high-symmetry directions?

Available lattice dynamics data

- Raman data (+ temperature dependence)
- BLS data (+ temperature dependence)
- INS single crystal data (Γ-K-M, Γ-M, Γ-A + temperature dependence)
- INS powder data (low energy, incoherent approximation)
- IXS single crystal data (Γ-K-M, Γ-M, Γ-A)
- diffuse scattering data for selected directions (inelastic nature)

BUT

- to which Q corresponds the low-energy peak in VDOS (related to boson peak problem)?
- are the “soft” directions always high-symmetry directions?

Where does 1st VDOS peak come from?

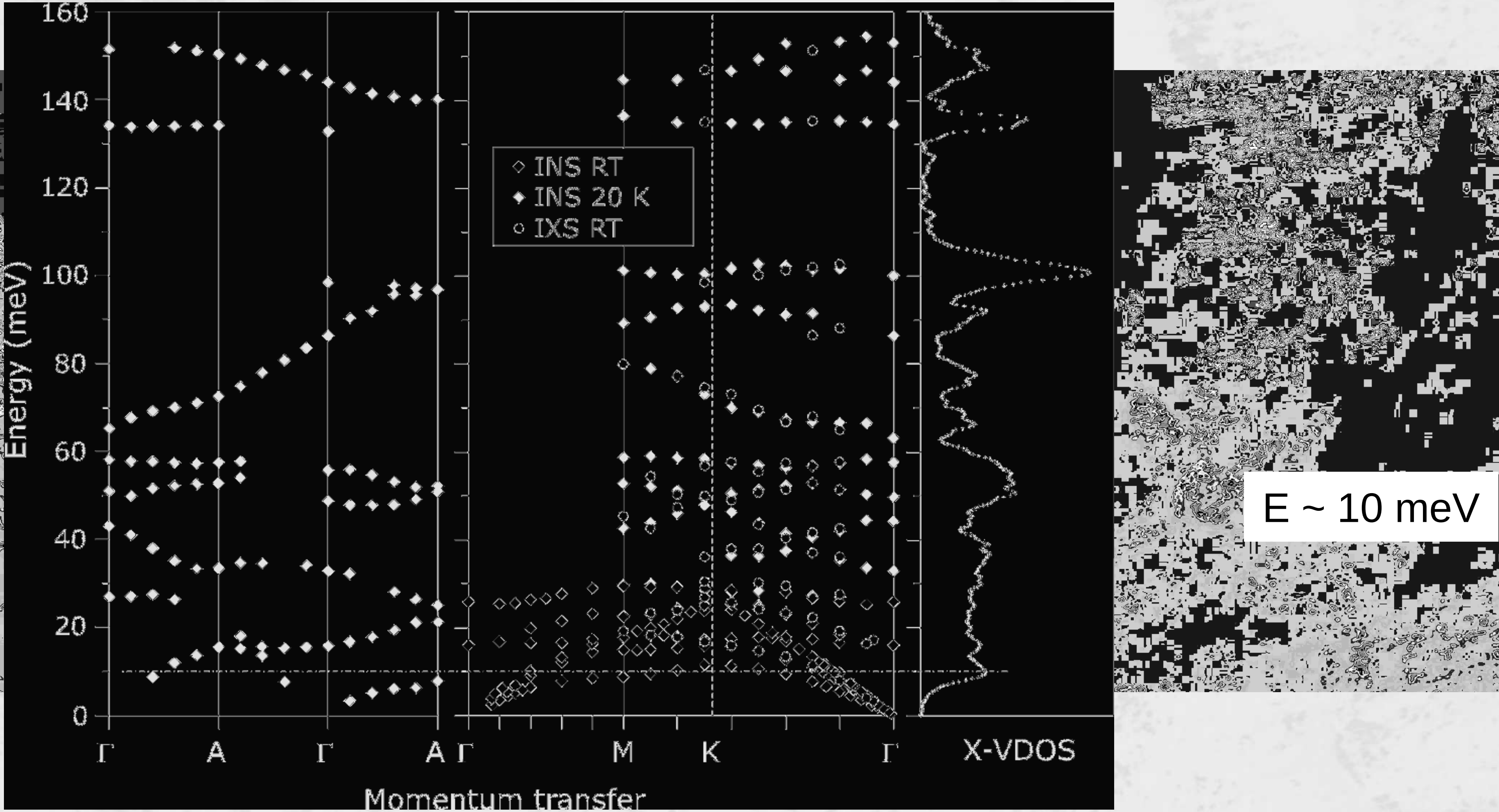

[Dorner et al., 1980; D. Strauch and B. Dorner, 1993; C. Halcoussis, 1997]

no high symmetry direction is responsible for the 1st VDOS peak

Preparing the roadmaps: TDS

- quartz single crystal 1x1x10 mm^3
- SNBL at ESRF BM01A beamline
- SLS X06SA beamline
- PILATUS 6M detector
- wavelength ~0.7 Å
- angular step 0.1 deg, 3600 images, 0.25 s exposure
- primary treatment with CrysAlis Oxford Diffraction package
- 3D reconstruction with original software, visualization with USCF Chimera, rendering with Pov-Ray

Room temperature TDS isosurface

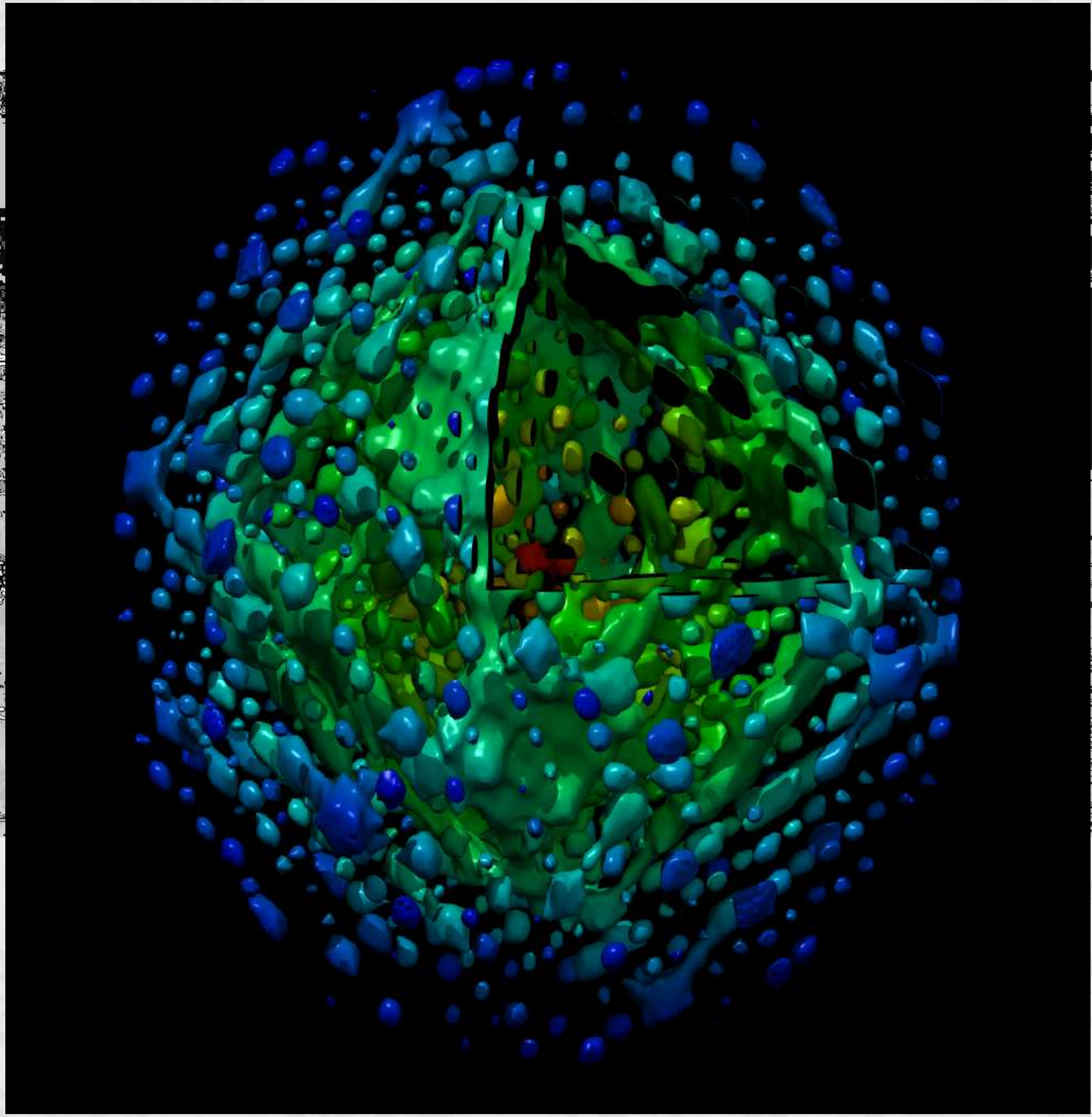

TDS distribution in high-symmetry planes

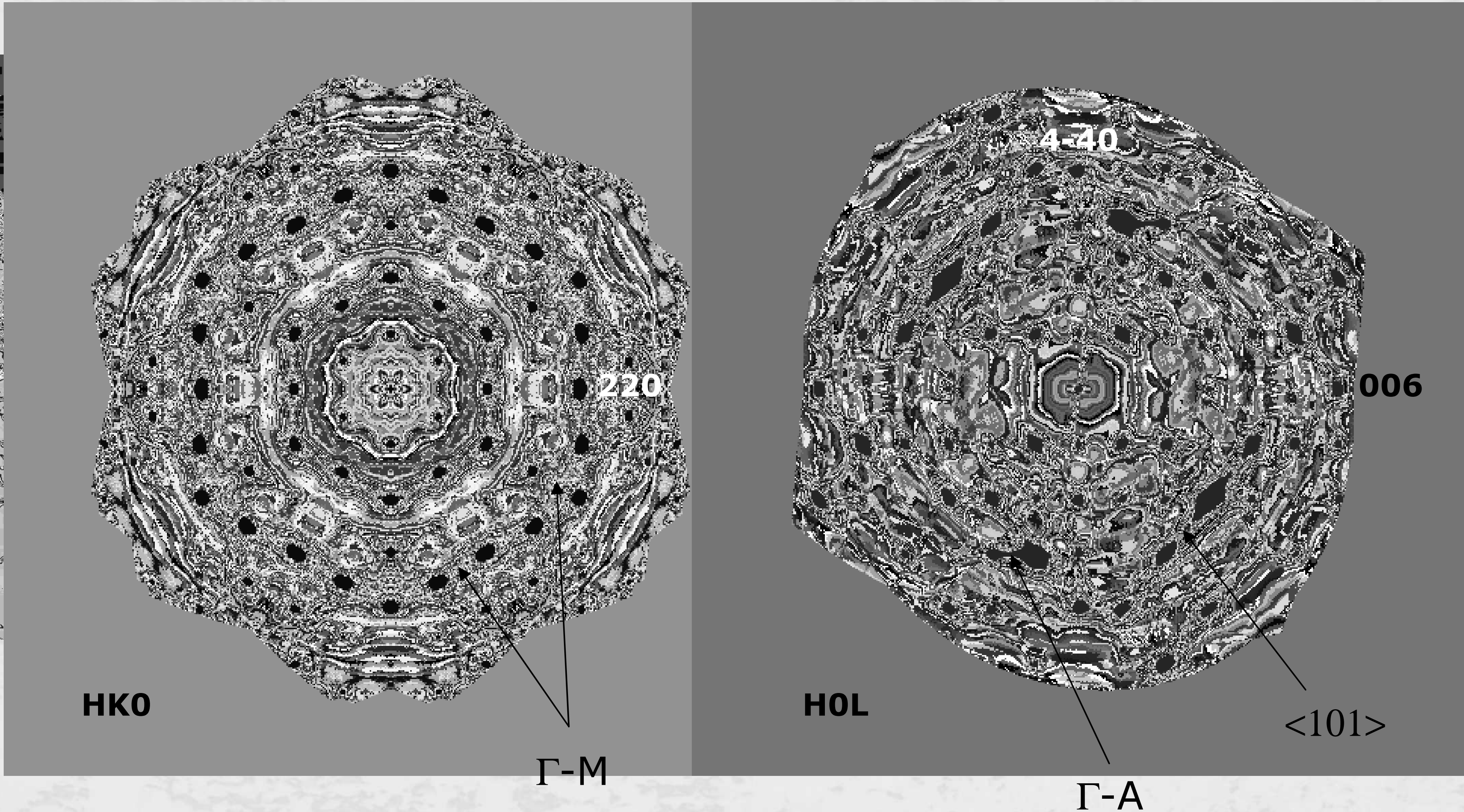

TDS distribution in high-symmetry planes

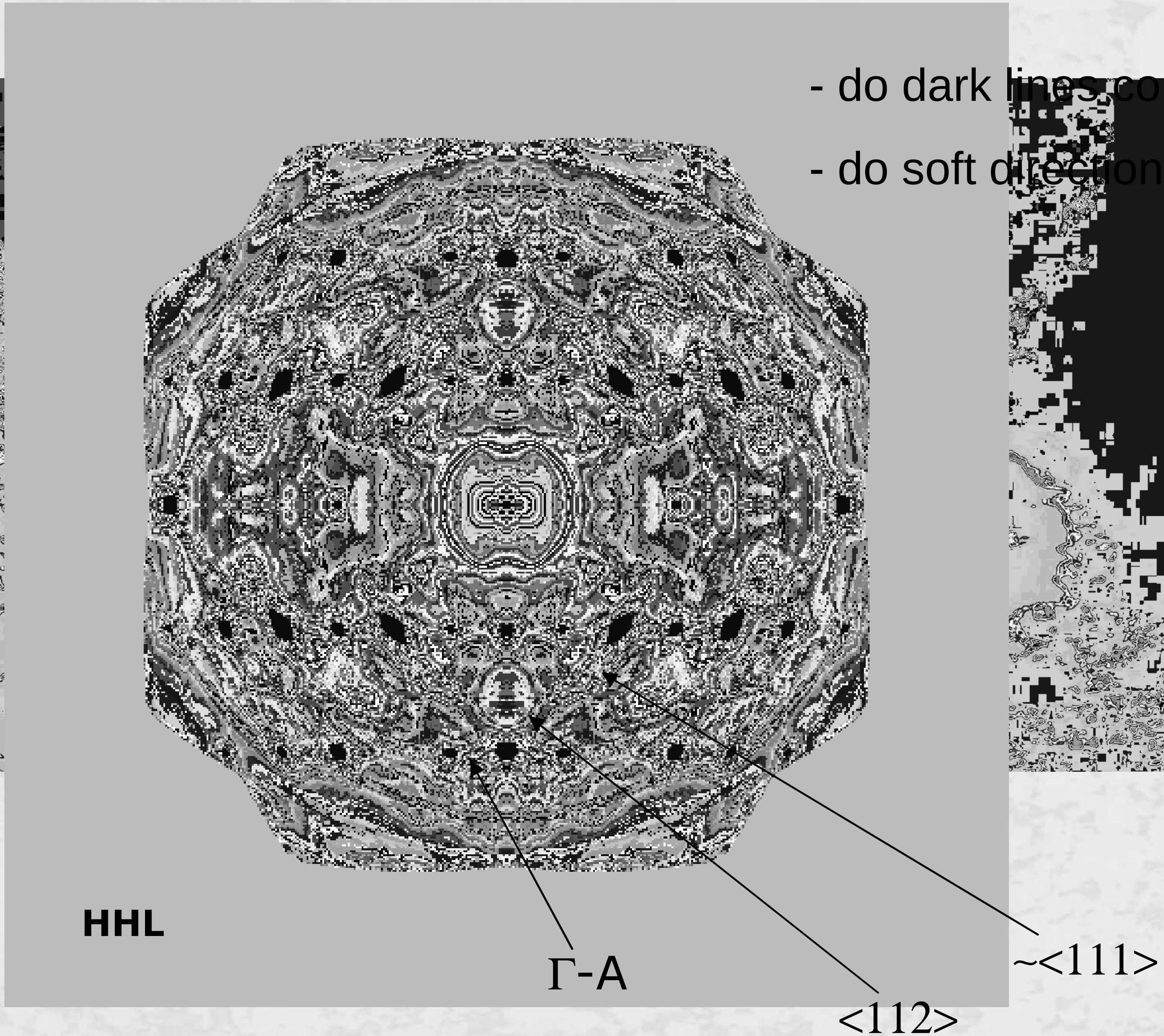

- do dark lines correspond to soft directions?
- do soft directions give rise to VDOS peaks?

Preparing the roadmaps: LD calculations

ab initio calculations

CASTEP package

calculation over the dense mesh

(16000 points in the irreducible BZ part)

peak in VDOS => saddle point on the dispersion surface [Van Hove, 1952]

$$\omega - \omega_C = (q - q_0)^T \cdot S \cdot (q - q_0)$$

ε_1, ε_2, ε_3 – eigenvalues of S

saddlepoint: $\varepsilon_1, \varepsilon_2 > 0, \varepsilon_3 < 0$ or $\varepsilon_1, \varepsilon_2 < 0, \varepsilon_3 > 0$

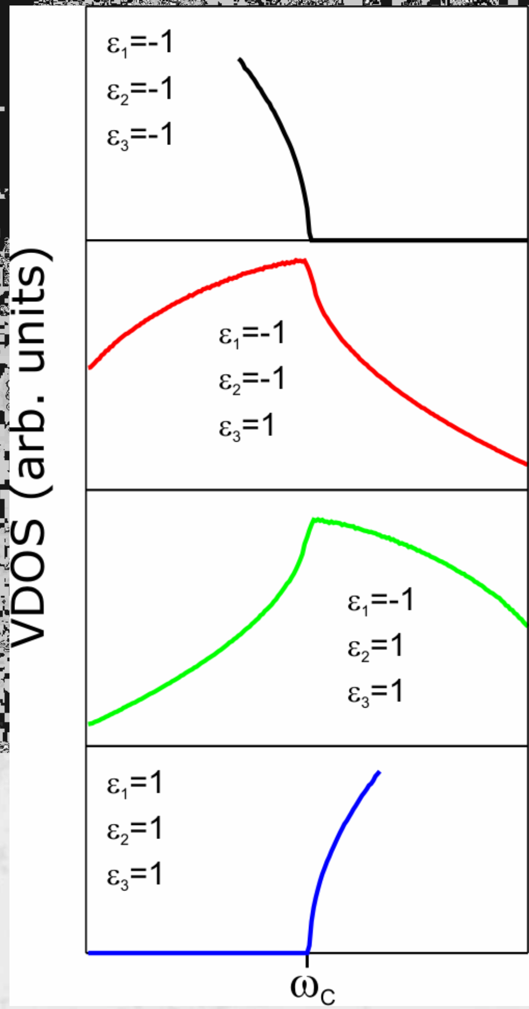

Preparing the roadmaps: LD calculations

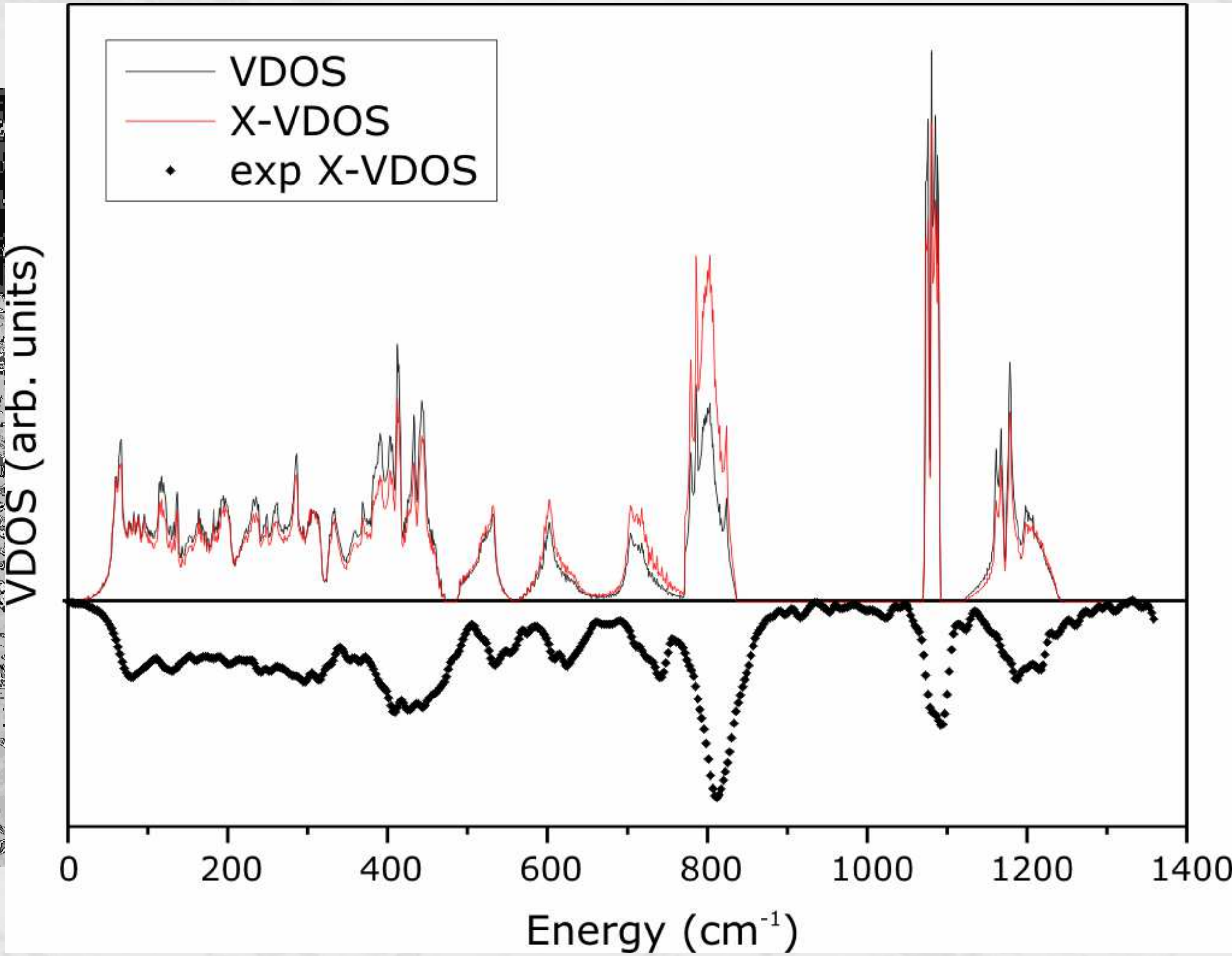

1st peak at ~8 meV

reasonable agreement – so the calculation can be helpful?

X-VDOS is quite close to real VDOS

Exploration of suspicious points and directions

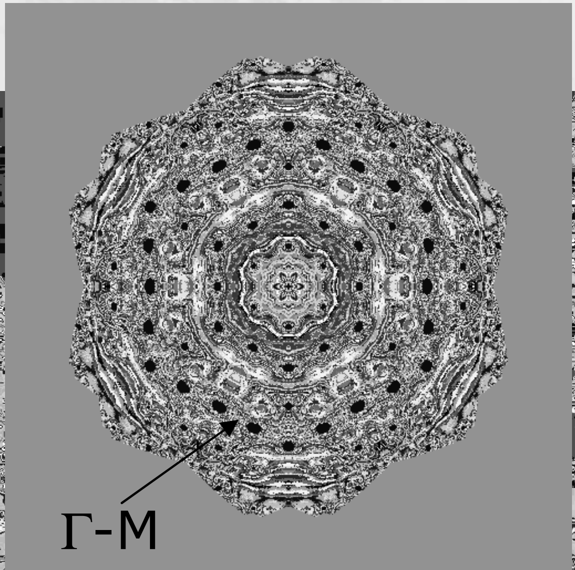

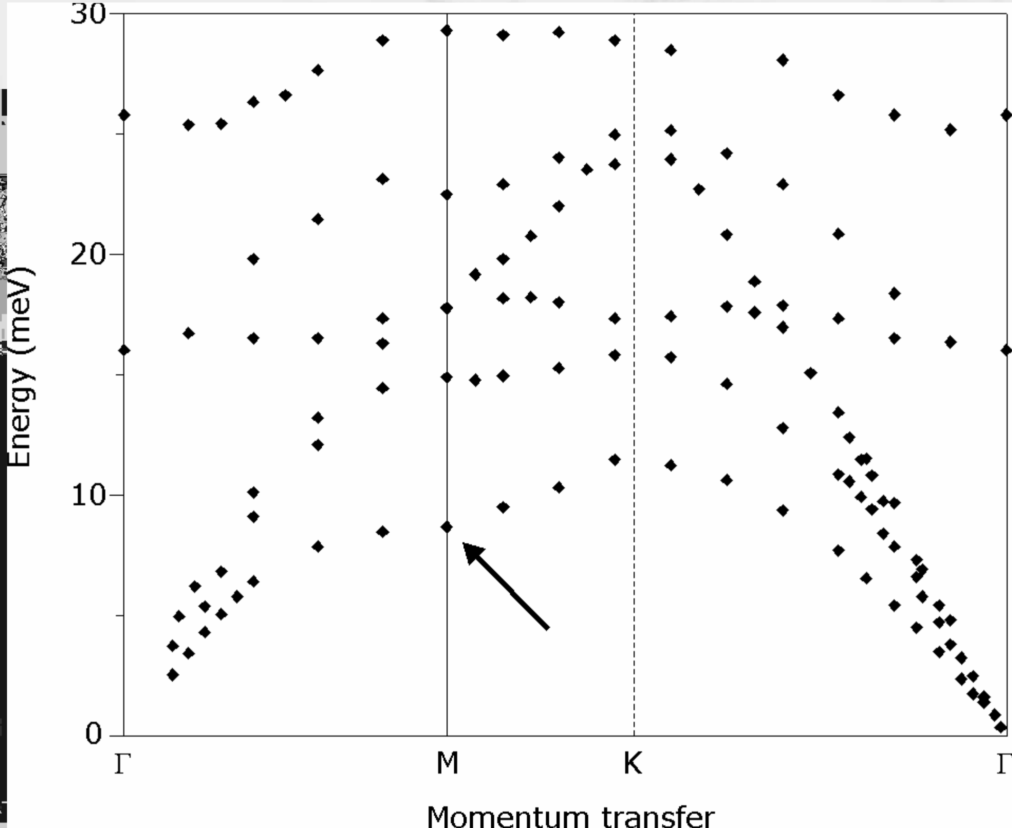

INS: M is saddle point with energy of ~8.7 meV

Exploration of suspicious points and directions

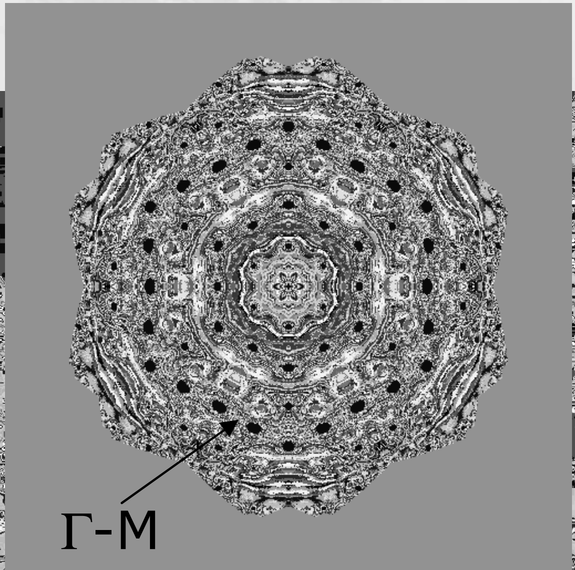

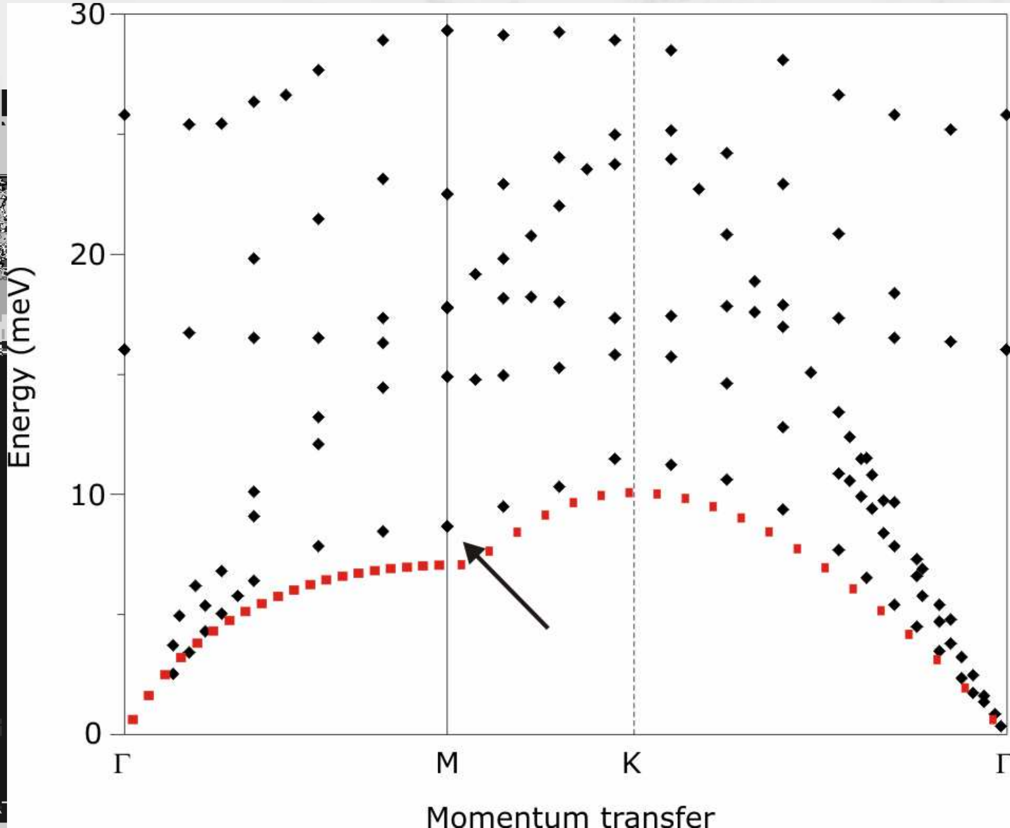

INS: M is saddle point with energy of ~8.7 meV
CASTEP: saddle point, slightly lower energy (~7 meV)
does not fit with VDOS peak

IXS experiment

quartz single crystal 1x1x10 mm^3

ESRF ID28 beamline

5 adjacent analyzers used

wavelength ~0.7 A

fitting with fixed excitation width

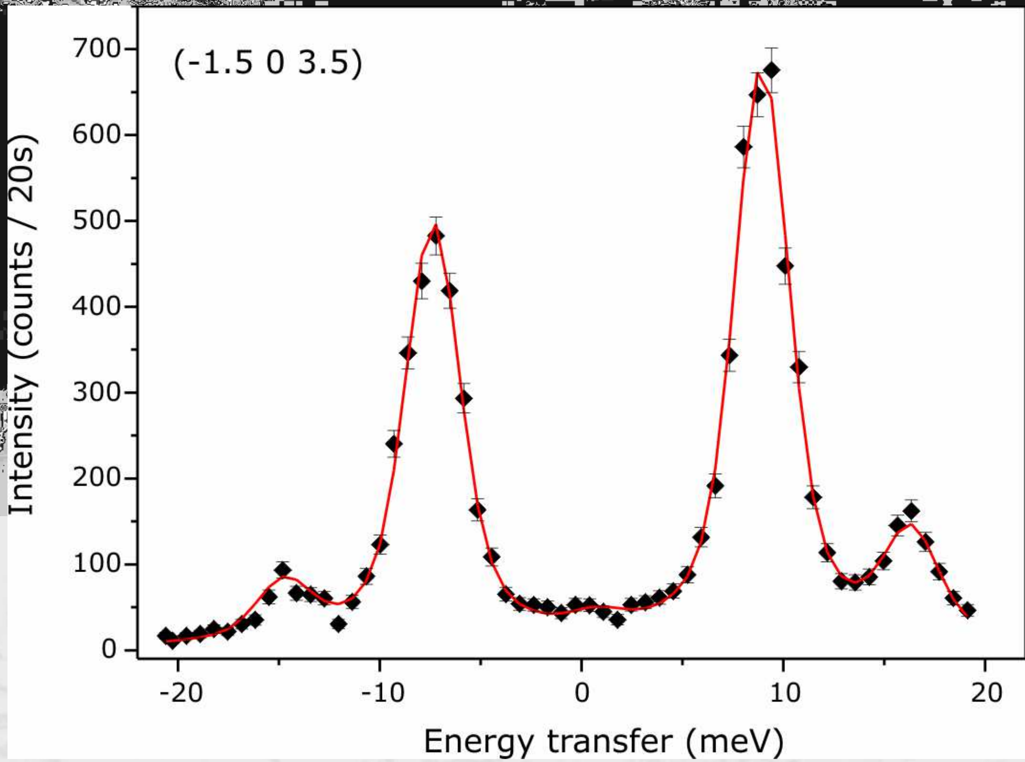

Exploration of suspicious points and directions

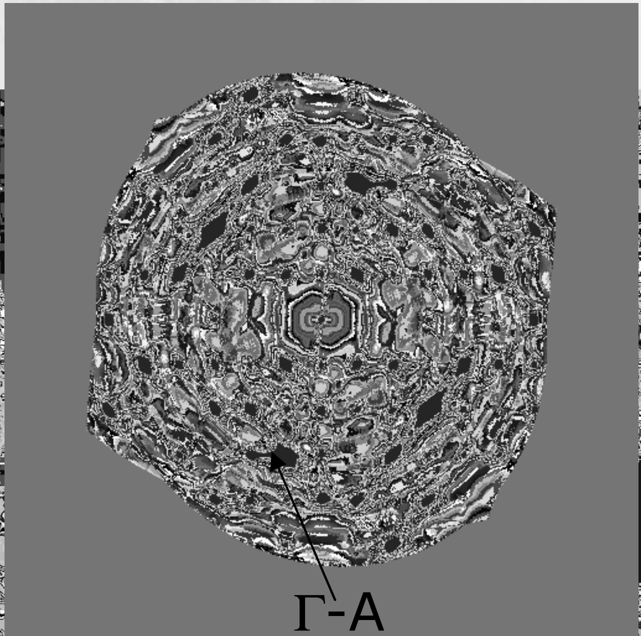

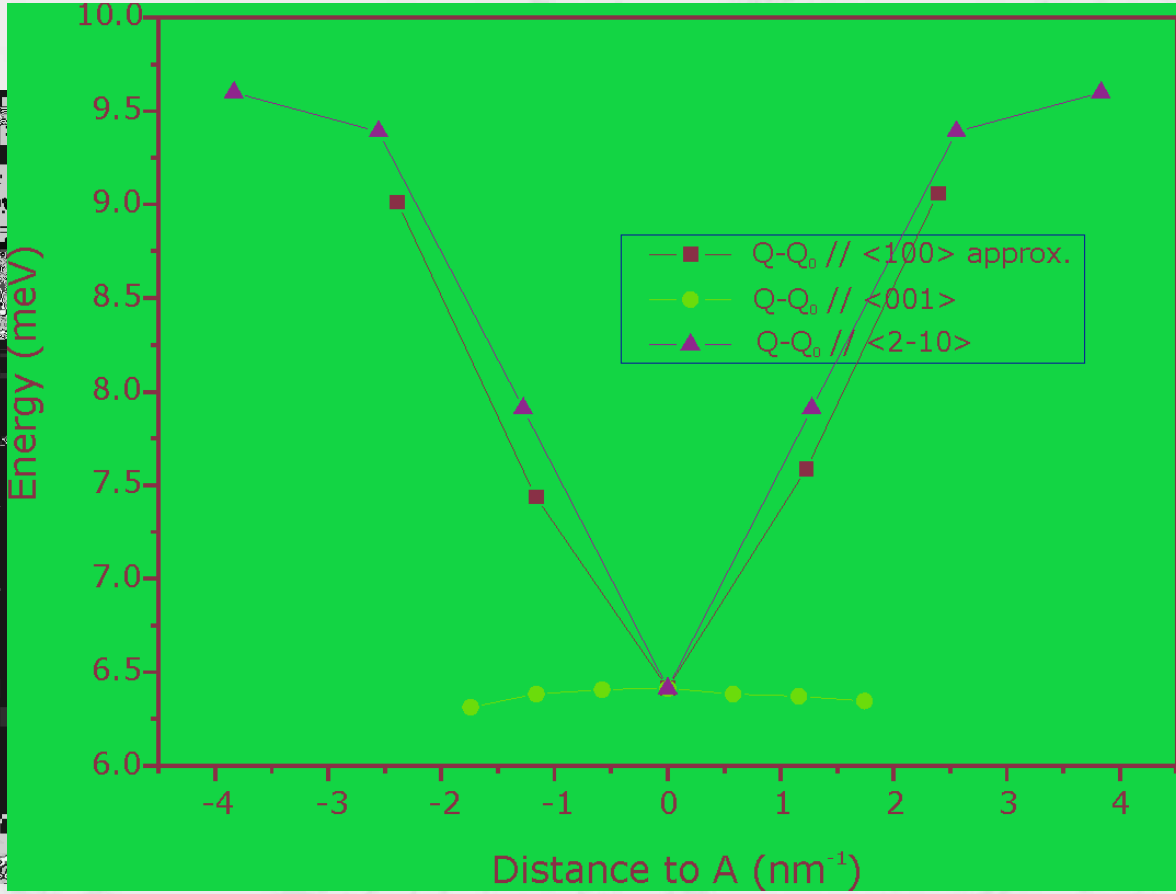

IXS: A is saddle point with energy of ~6.4 meV
CASTEP: minimum, nearly flat in c*, lower energy (~5.1 meV), does not fit with VDOS peak

Exploration of suspicious points and directions

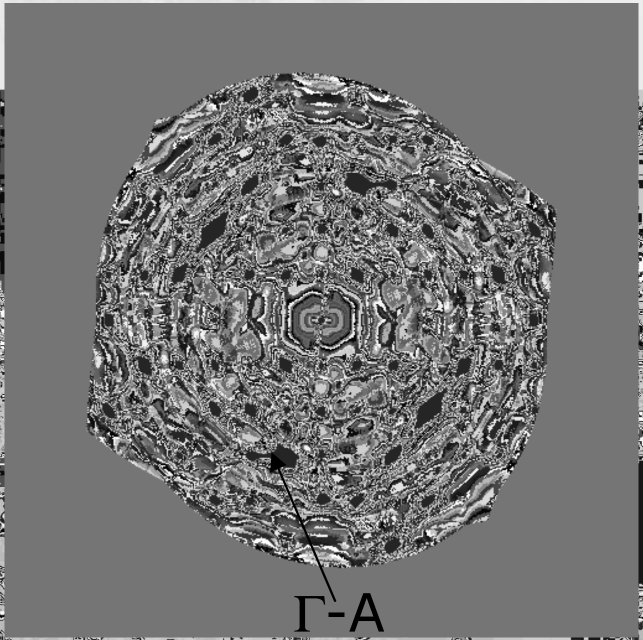

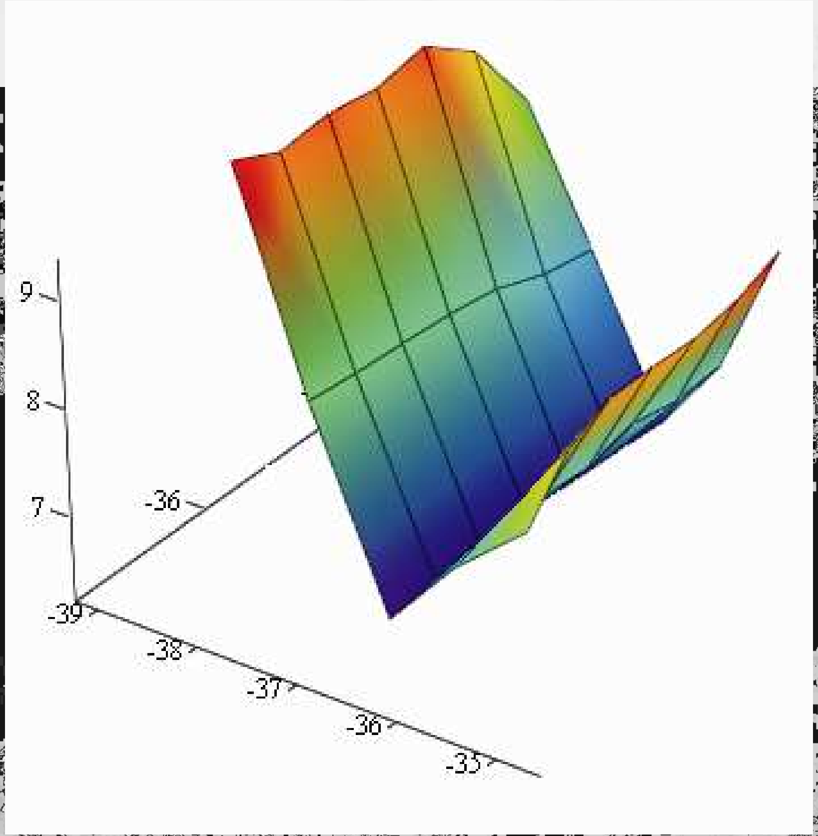

IXS: A is saddle point with energy of ~6.4 meV
CASTEP: minimum, nearly flat in c*, lower energy (~5.1 meV), does not fit with VDOS peak

Less trivial geometry for TA phonons observation

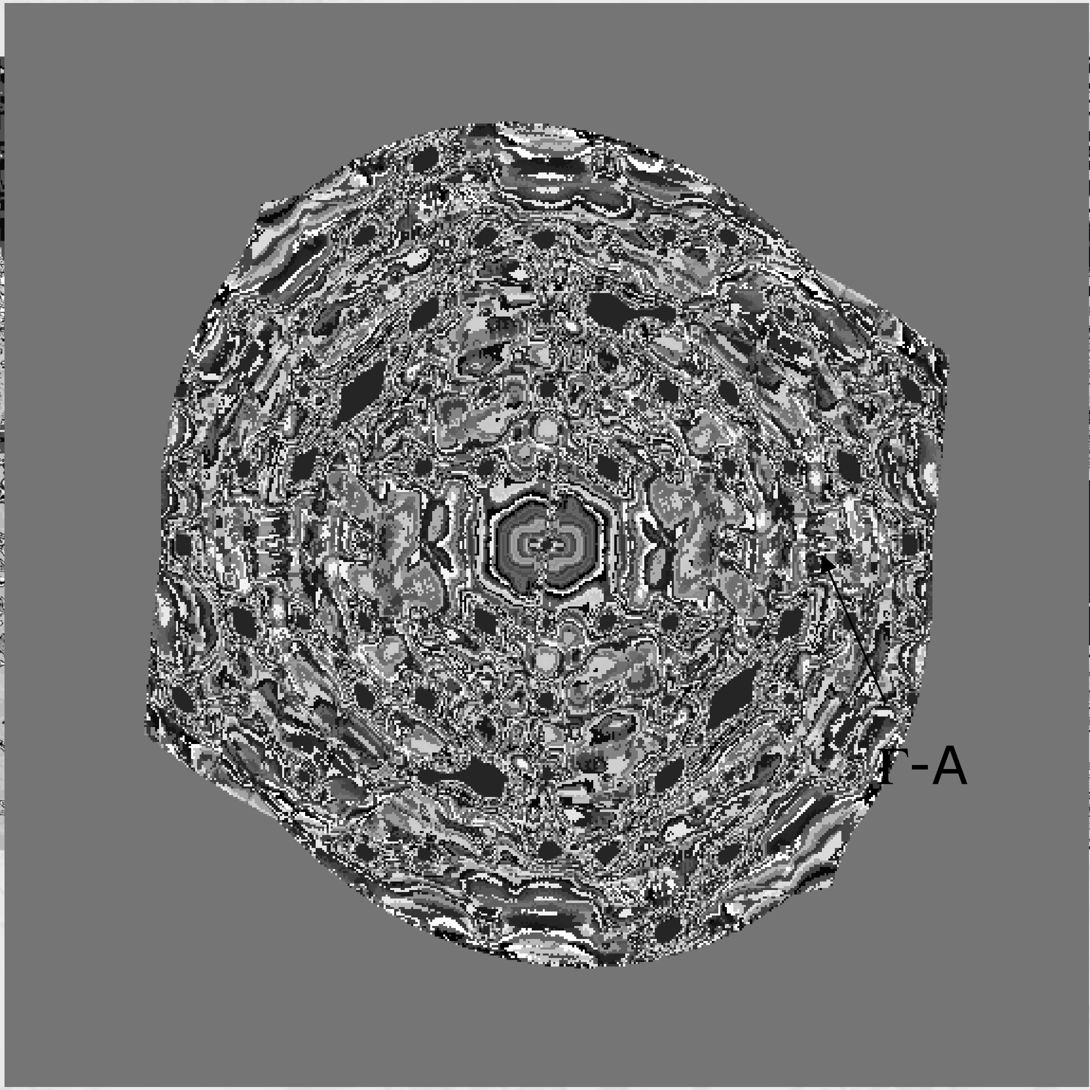

Less trivial geometry for TA phonons observation

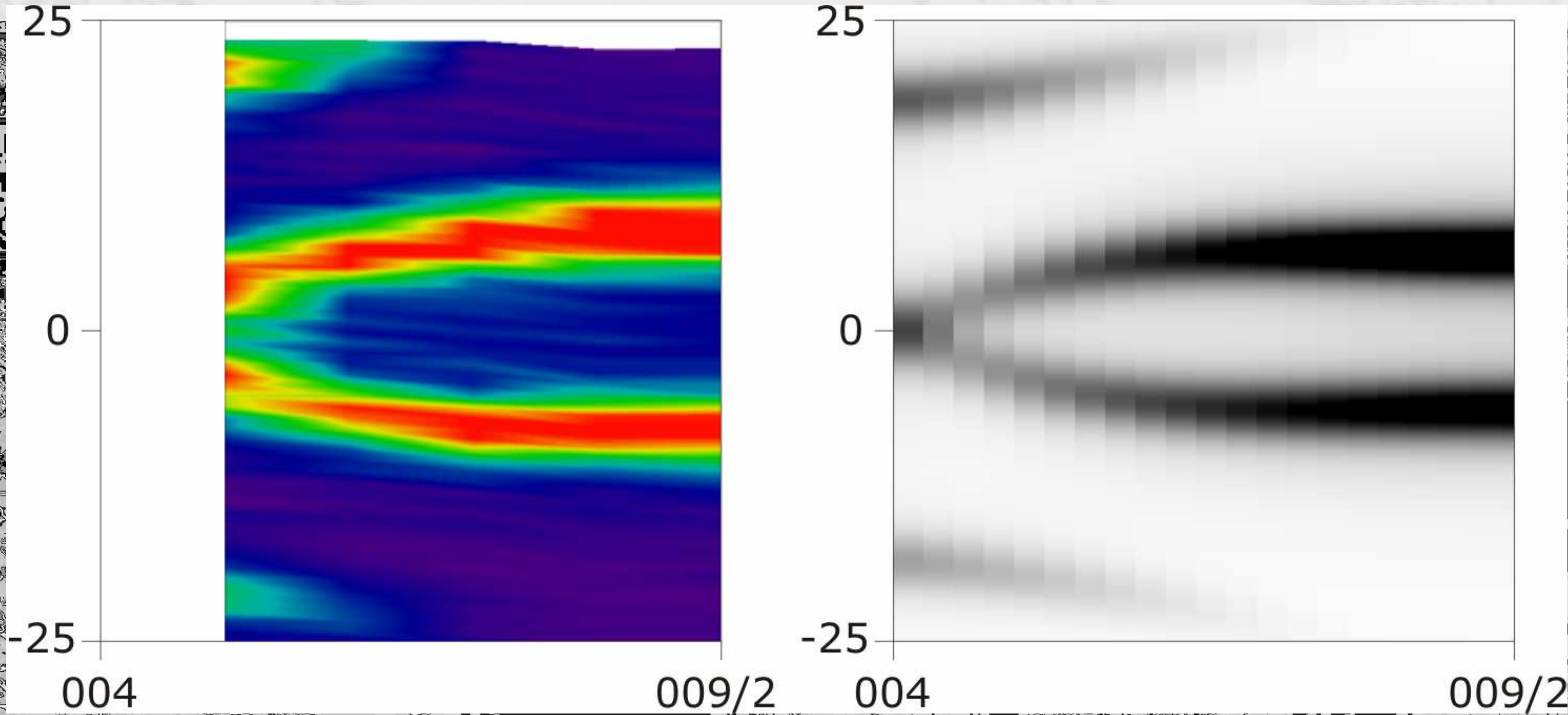

transverse acoustic phonons can be observed in purely longitudinal geometry

Exploration of suspicious points and directions

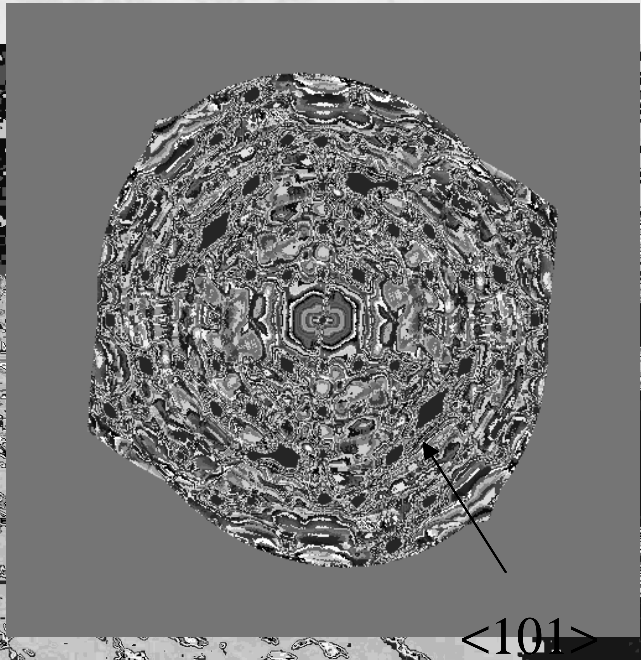

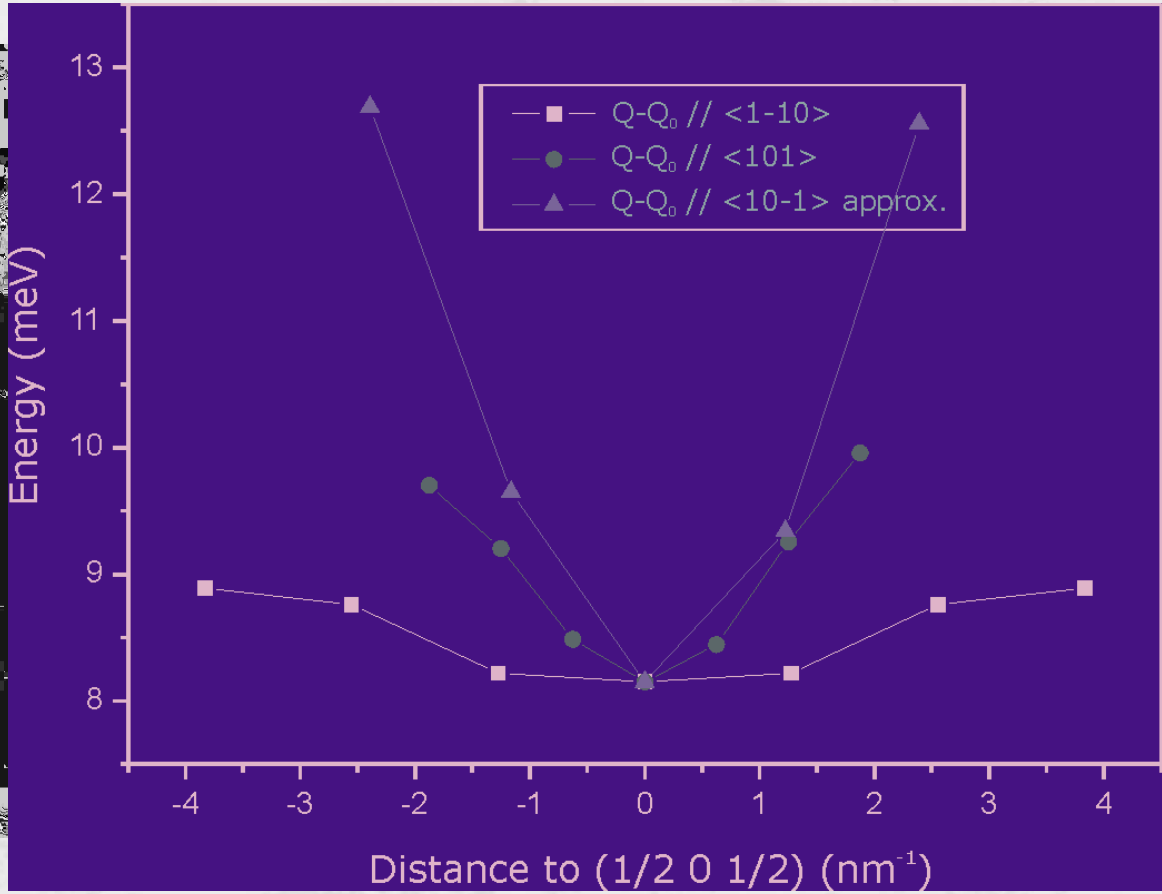

IXS: (1/2 0 1/2) is minimum with energy of ~8.2 meV
CASTEP: minimum

Exploration of suspicious points and directions

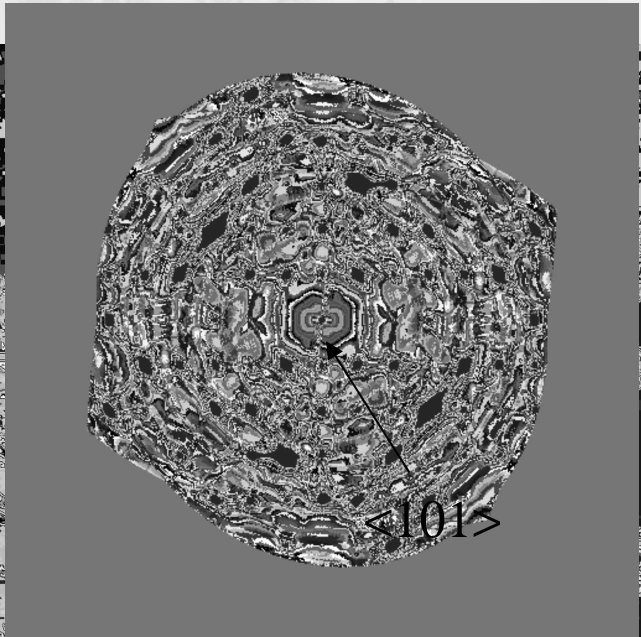

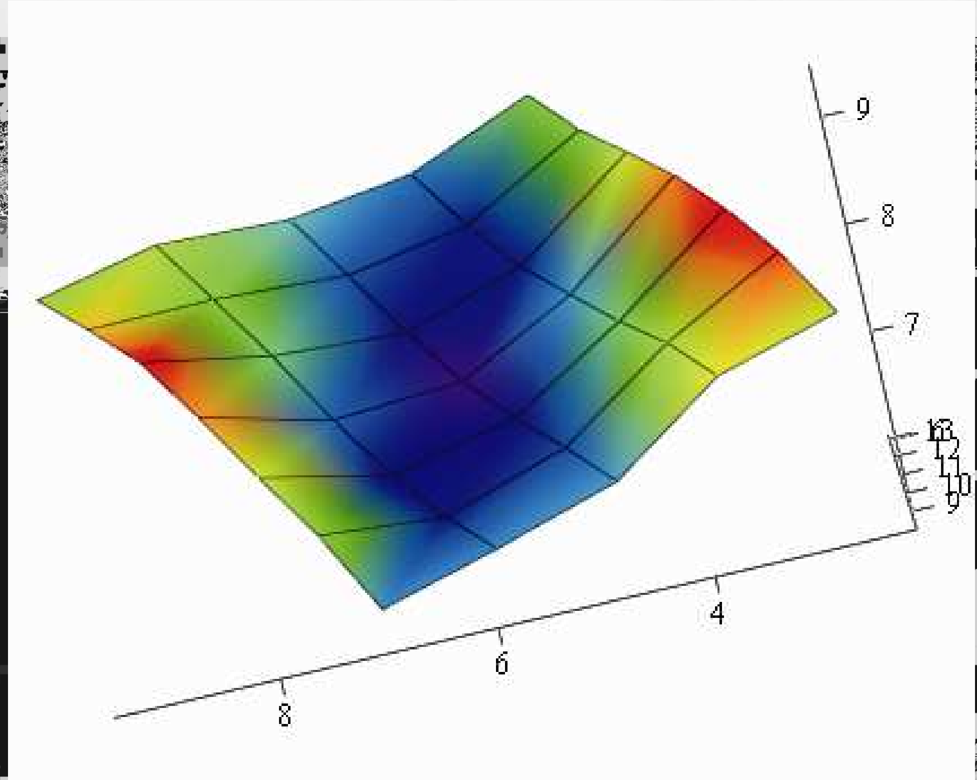

IXS: (1/2 0 1/2) is minimum with energy of ~8.2 meV
CASTEP: minimum

Exploration of suspicious points and directions

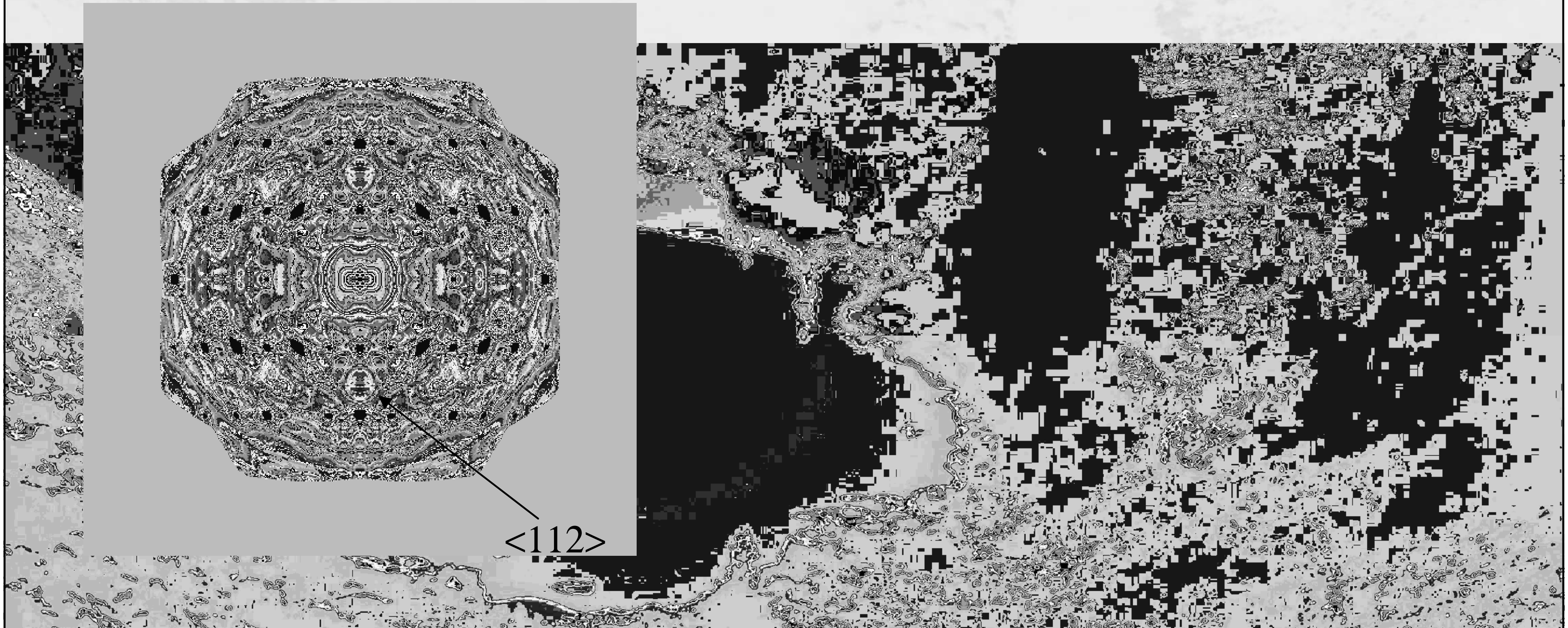

Exploration of suspicious points and directions

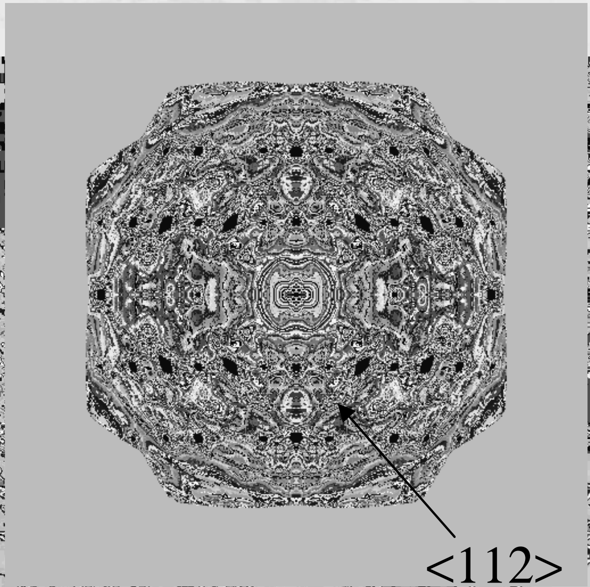

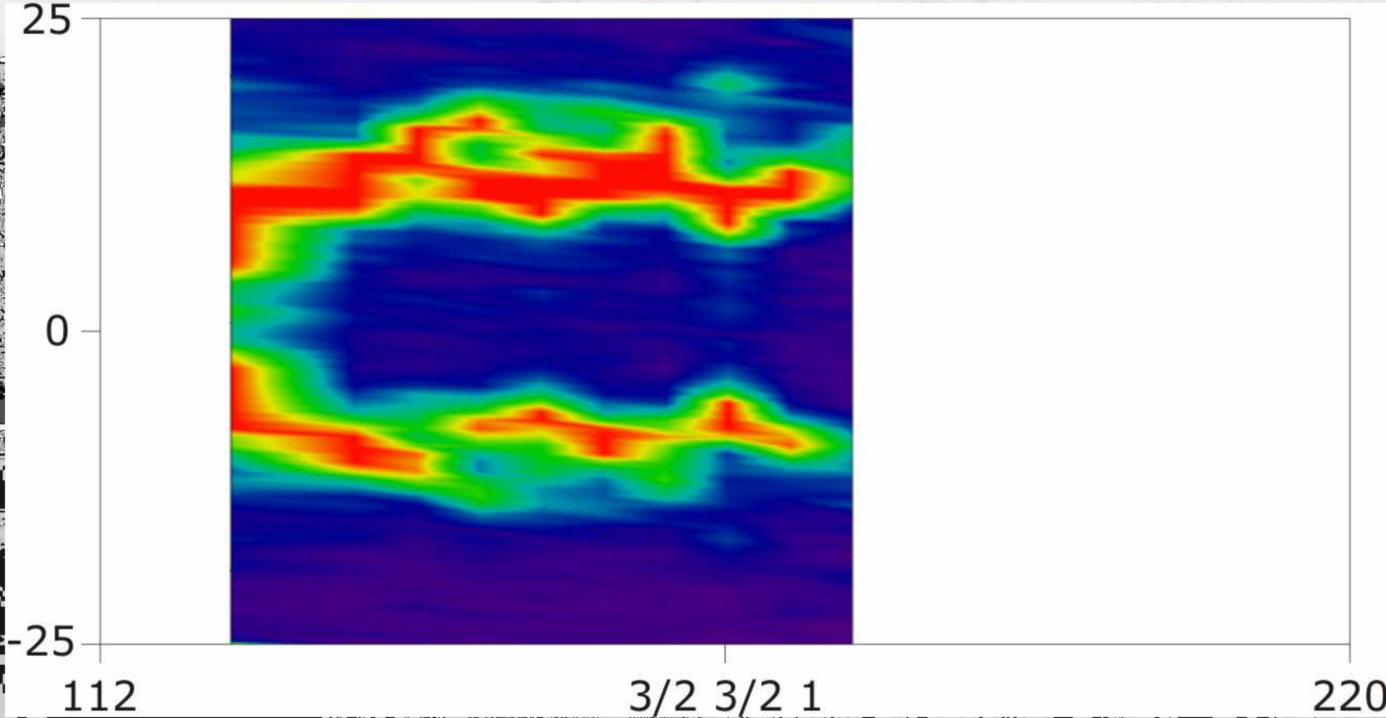

Exploration of suspicious points and directions

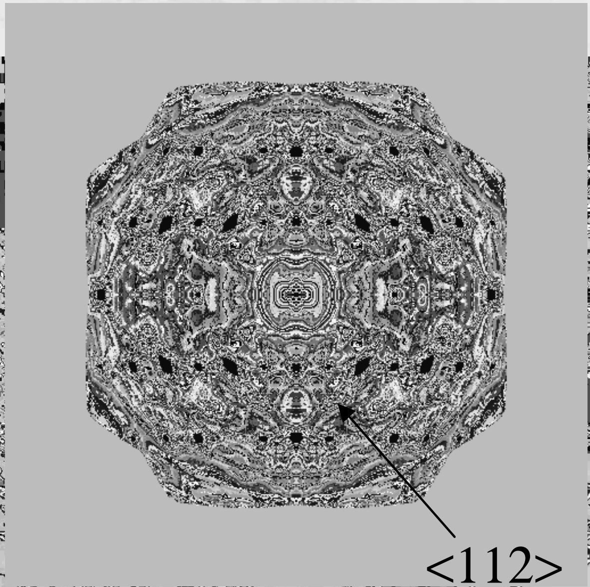

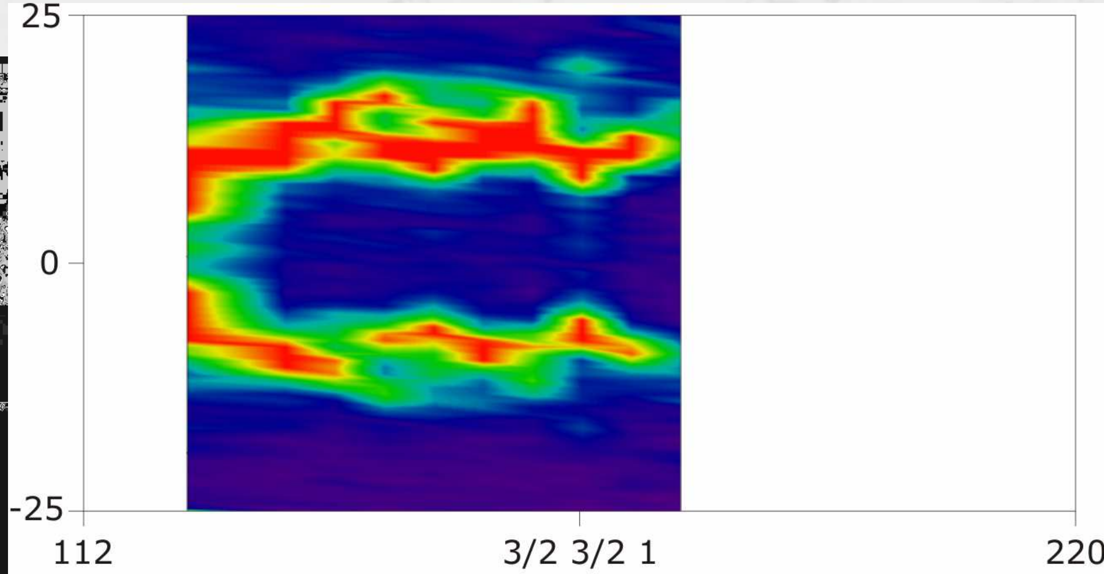

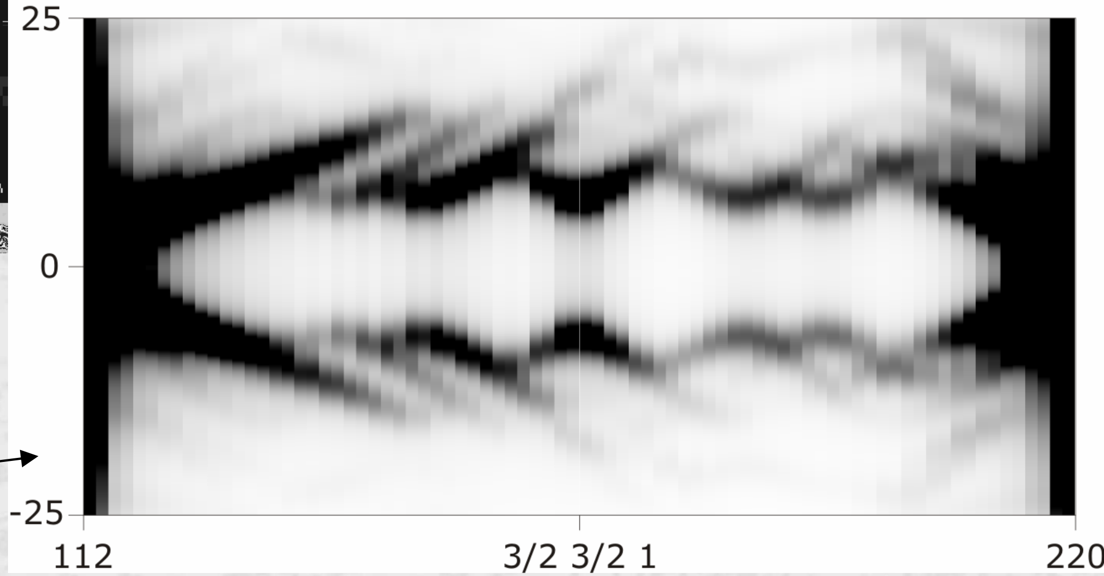

Q-search with given energy window: CASTEP

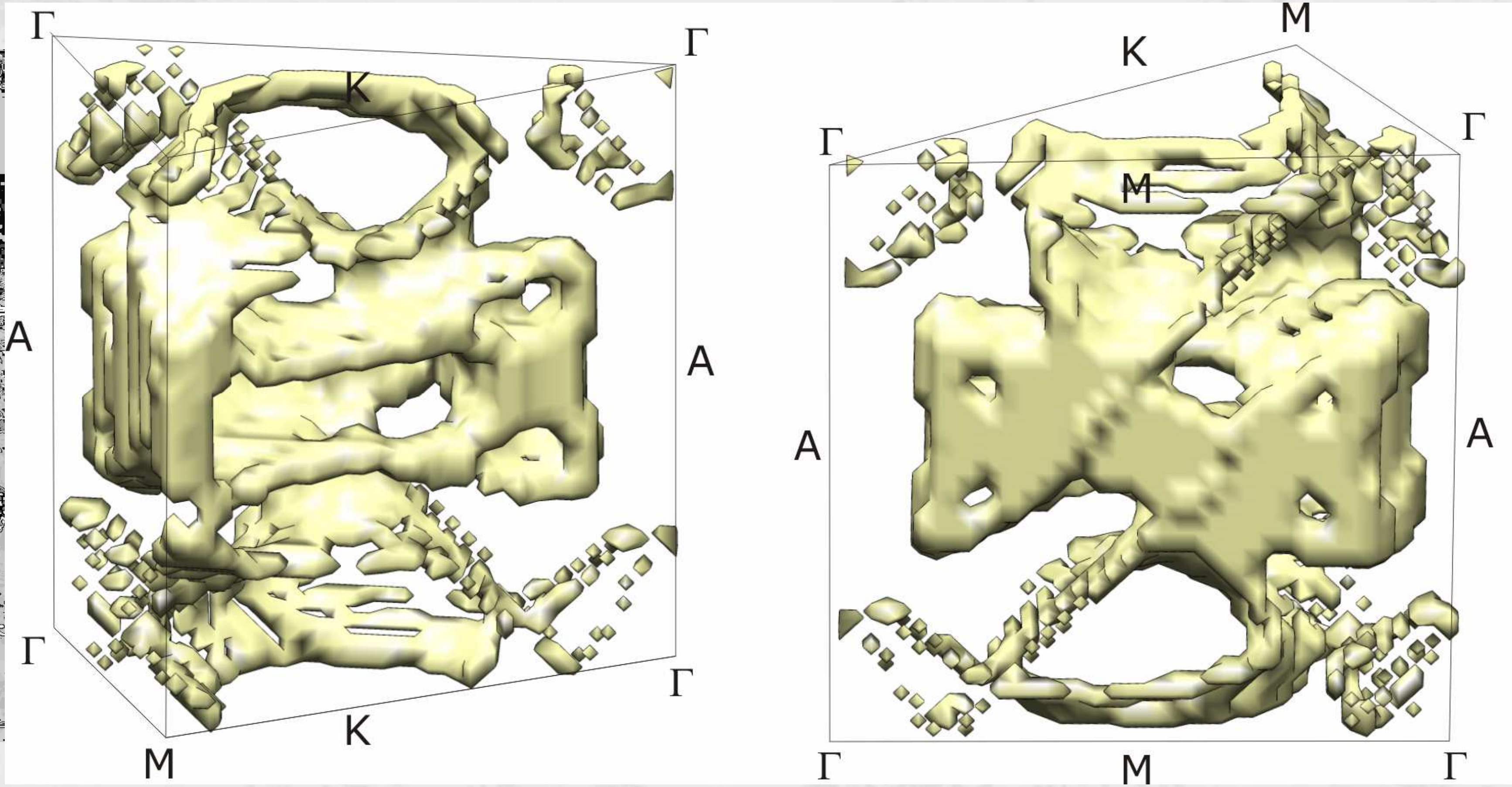

solids represent the q-volume where you have phonons with desired energy

promising area around ~(1/4 0 1/2)

Q-search with given energy window: CASTEP

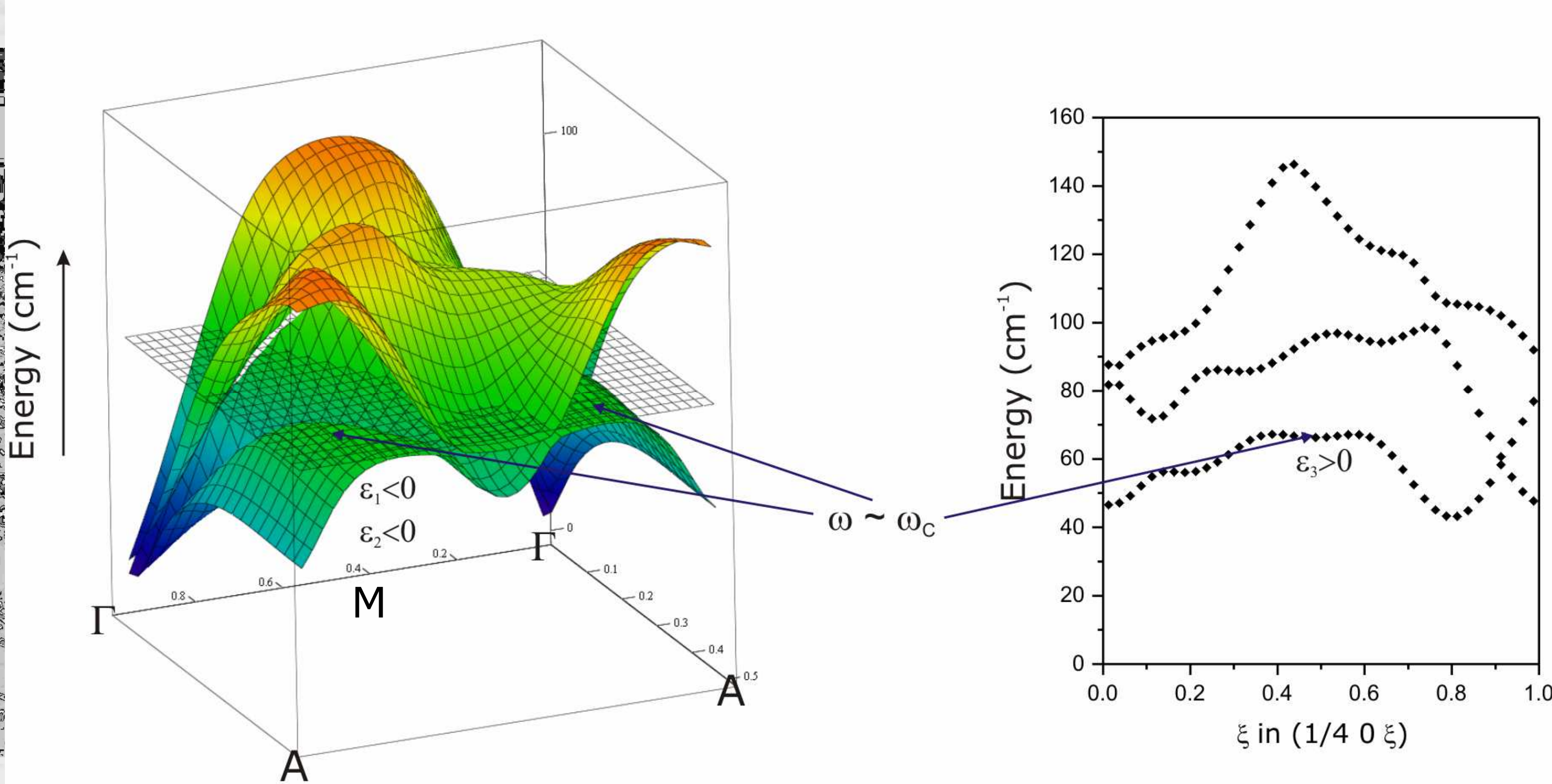

there is a saddle point close to (1/4 0 1/2) with the requested energy

IXS: singularity localized

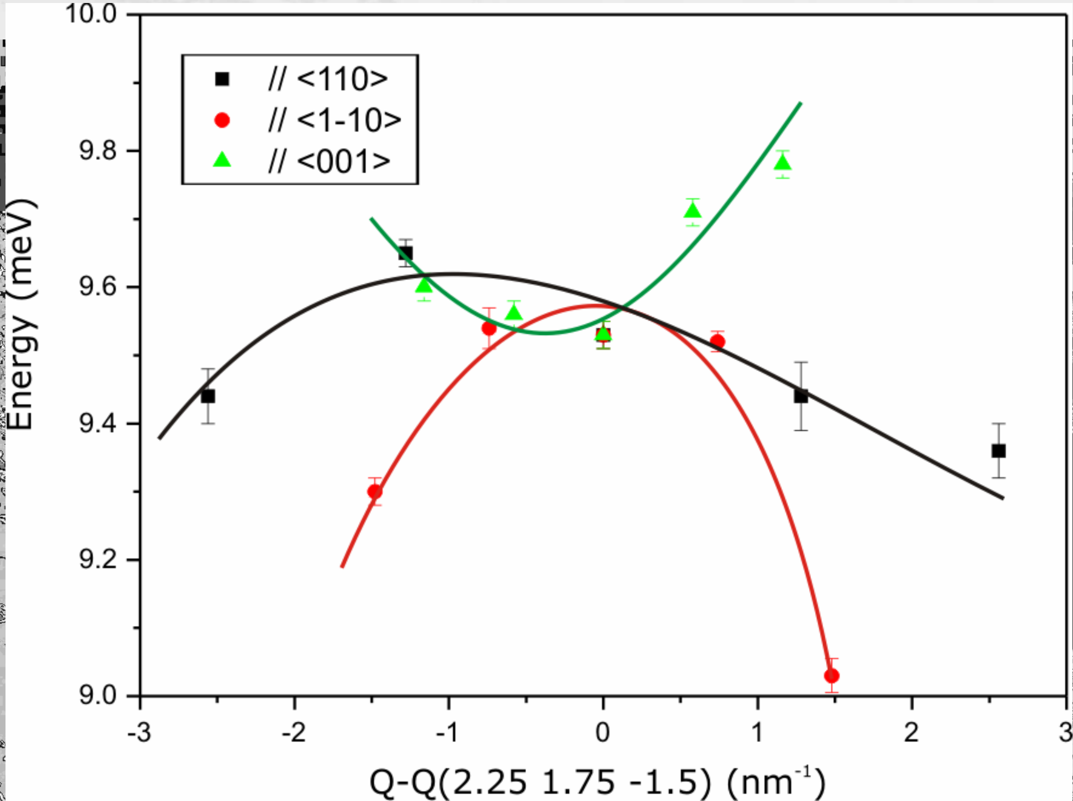

1st VDOS peak is associated with the proximity of (0.25 0 0.5)

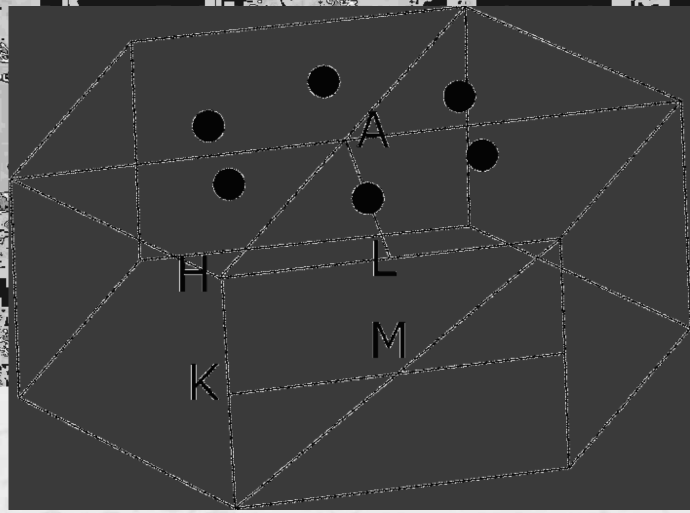

- intense TDS features are NOT necessarily soft branches
- soft branches are not necessarily associated with visible VDOS singularities
- calculations are highly desirable for the experiment planning and data interpretation

Electron-phonon coupling in zinc

VOLUME 2, NUMBER 9 PHYSICAL REVIEW LETTERS MAY 1, 1959

IMAGE OF THE FERMI SURFACE IN THE VIBRATION SPECTRUM OF A METAL*

W. Kohn
Department of Physics, Carnegie Institute of Technology, Pittsburgh, Pennsylvania
(Received April 6, 1959)

... we expect an abrupt change of the restoring force whenever $\vec{q}$ is such that, for some reciprocal lattice vector $\vec{K}_\nu$,

$$|\vec{q}+\vec{K}_\nu| = 2k_F. \quad (8)$$

On the surfaces in $\vec{q}$-space defined by (8), one finds the singularity ...

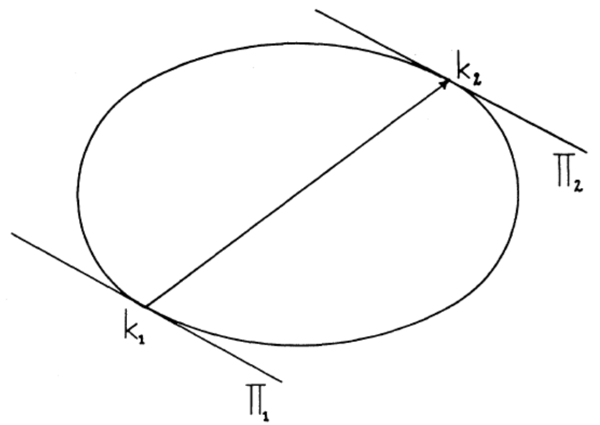

The magnitude of the effect may be quite large (very roughly of the order of percent), and its observation in lattice vibration spectra would give rather direct information about the shape of the Fermi surface.

Kohn anomaly in zinc

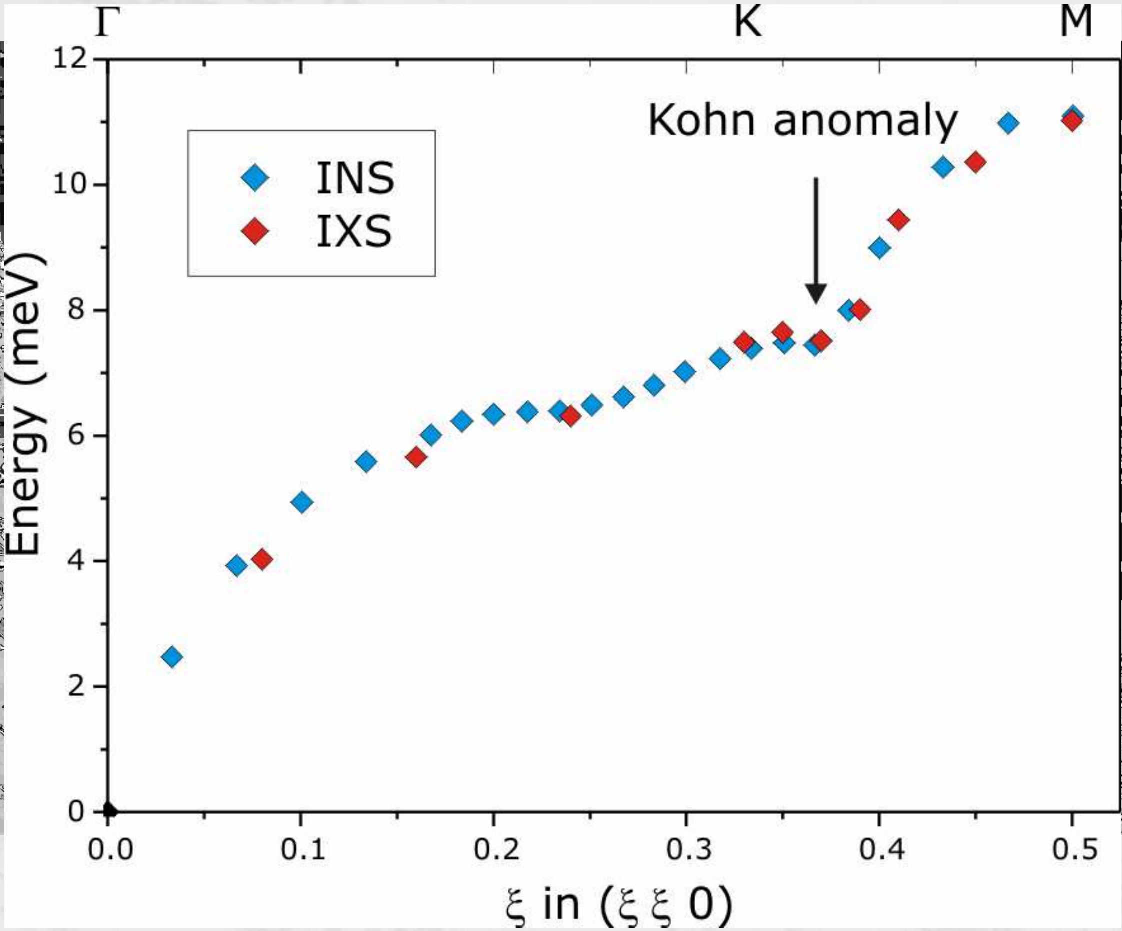

visible anomaly in Γ-K-M TA dispersion at $q = 2k_F$

Kohn anomaly in zinc

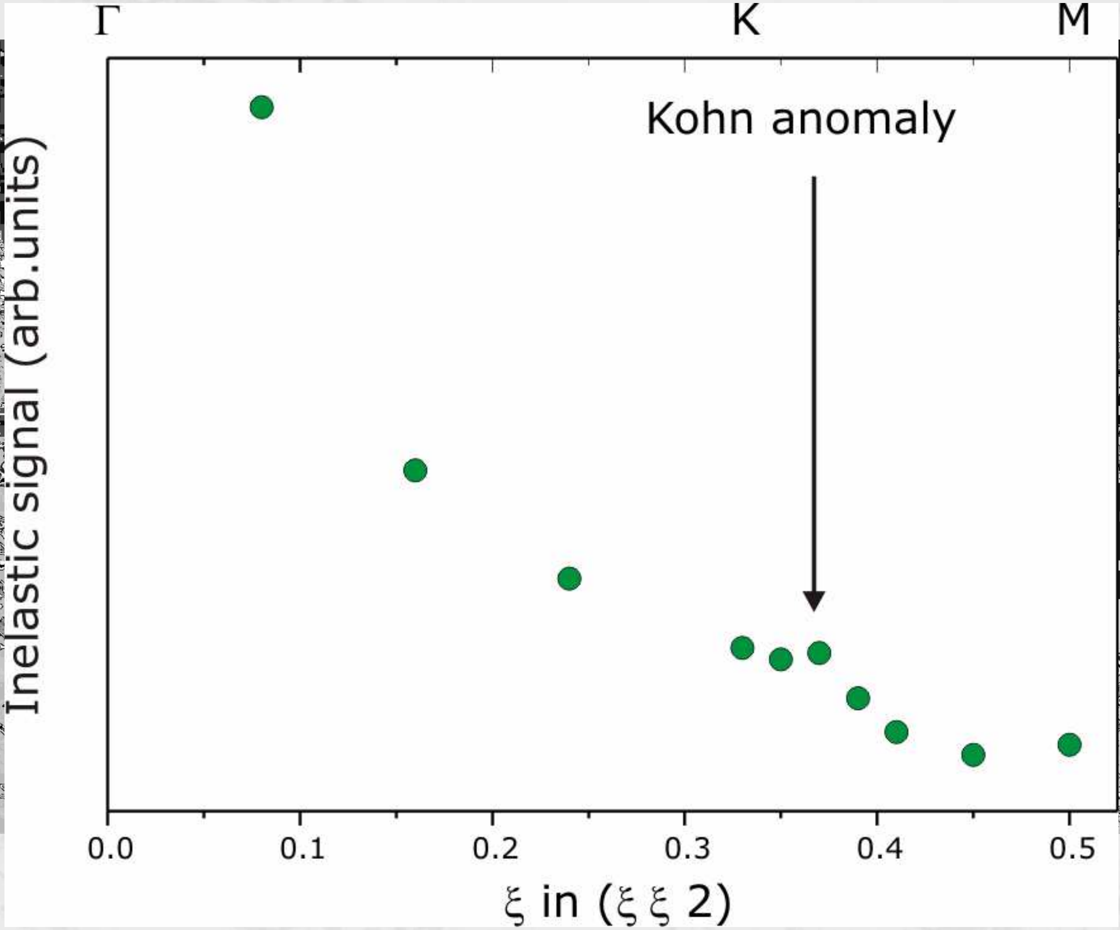

visible anomaly in Γ-K-M TA dispersion at $q = 2k_F$

pronounced intensity variation across the Kohn anomaly

Kohn surface visualization in zinc

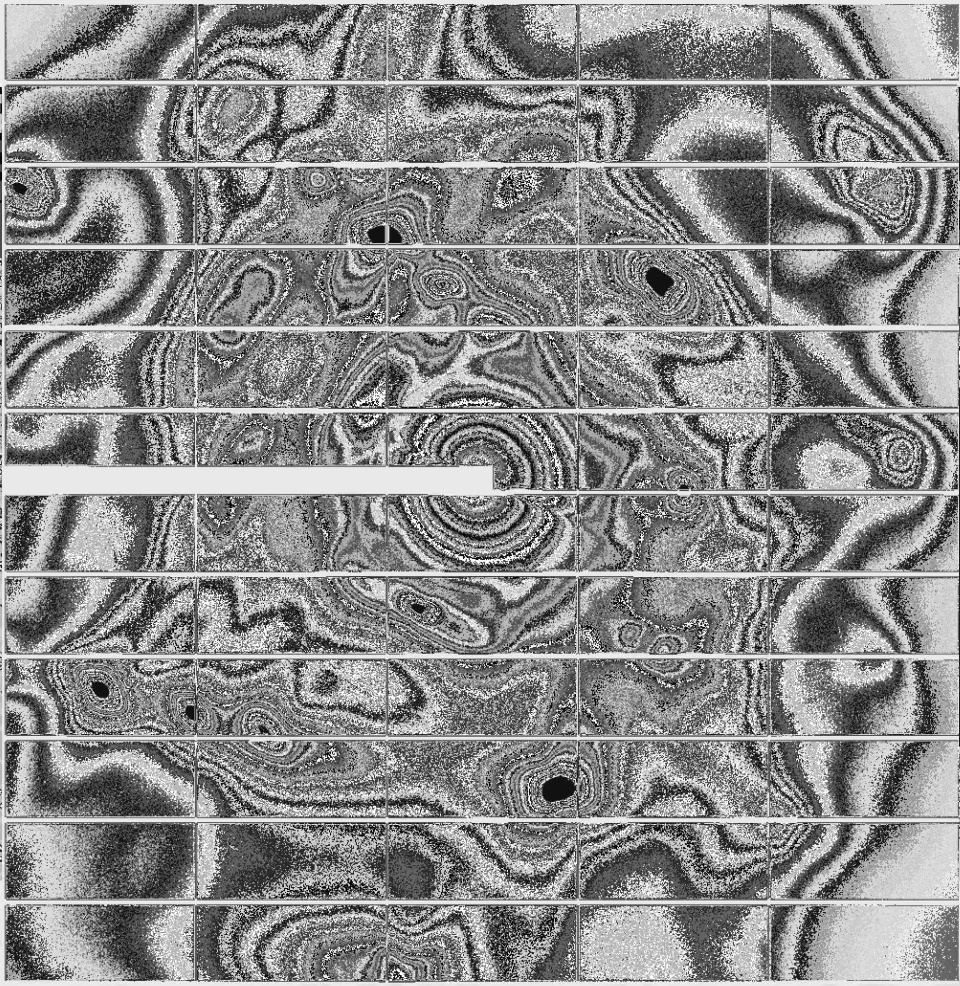

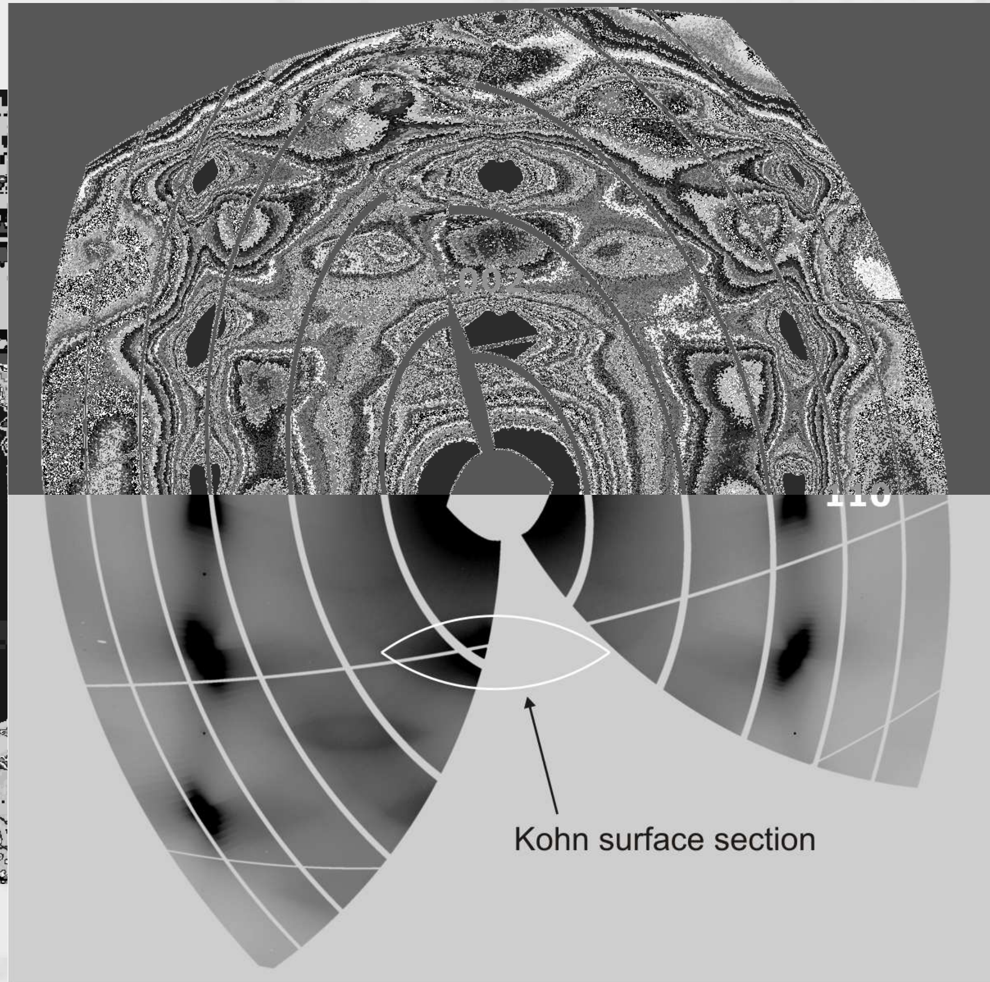

raw image

RS reconstruction with Crysalis software

PILATUS: strong suppression of fluorescence!

Kohn surface visualization in zinc

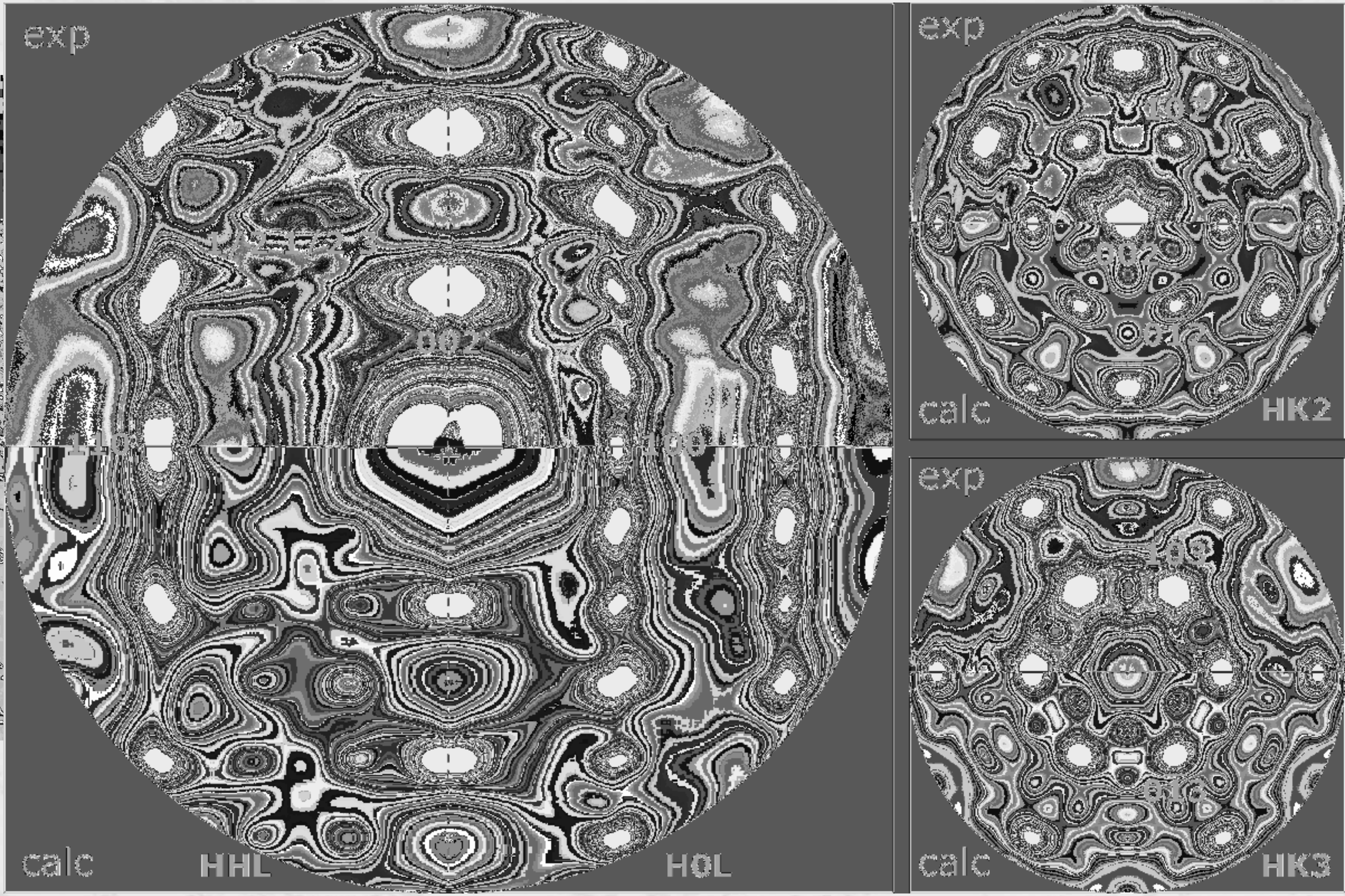

ab initio:
CASTEP
package

… and 3D TDS representation

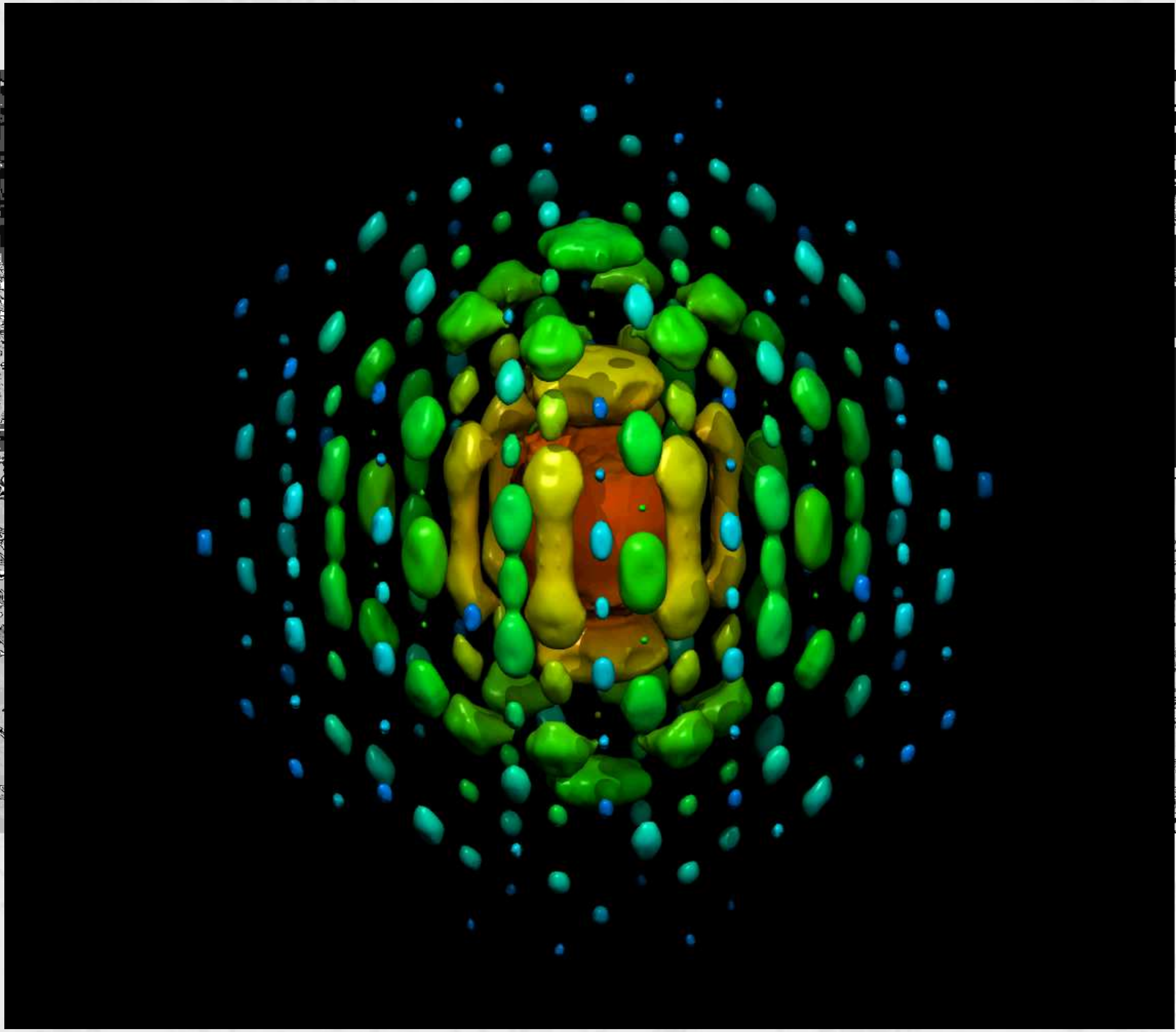

A. Bosak, M. Hoesch, M. Krisch,
D. Chernyshov, P. Pattison,
C. Schulze-Briese, B. Winkler,
V. Milman, K. Refson,
D. Antonangeli, and D. Farber
Phys. Rev. Lett. **103**, 076403
(2009)

elastic contribution can be neglected (proven by IXS)

… and 3D TDS representation

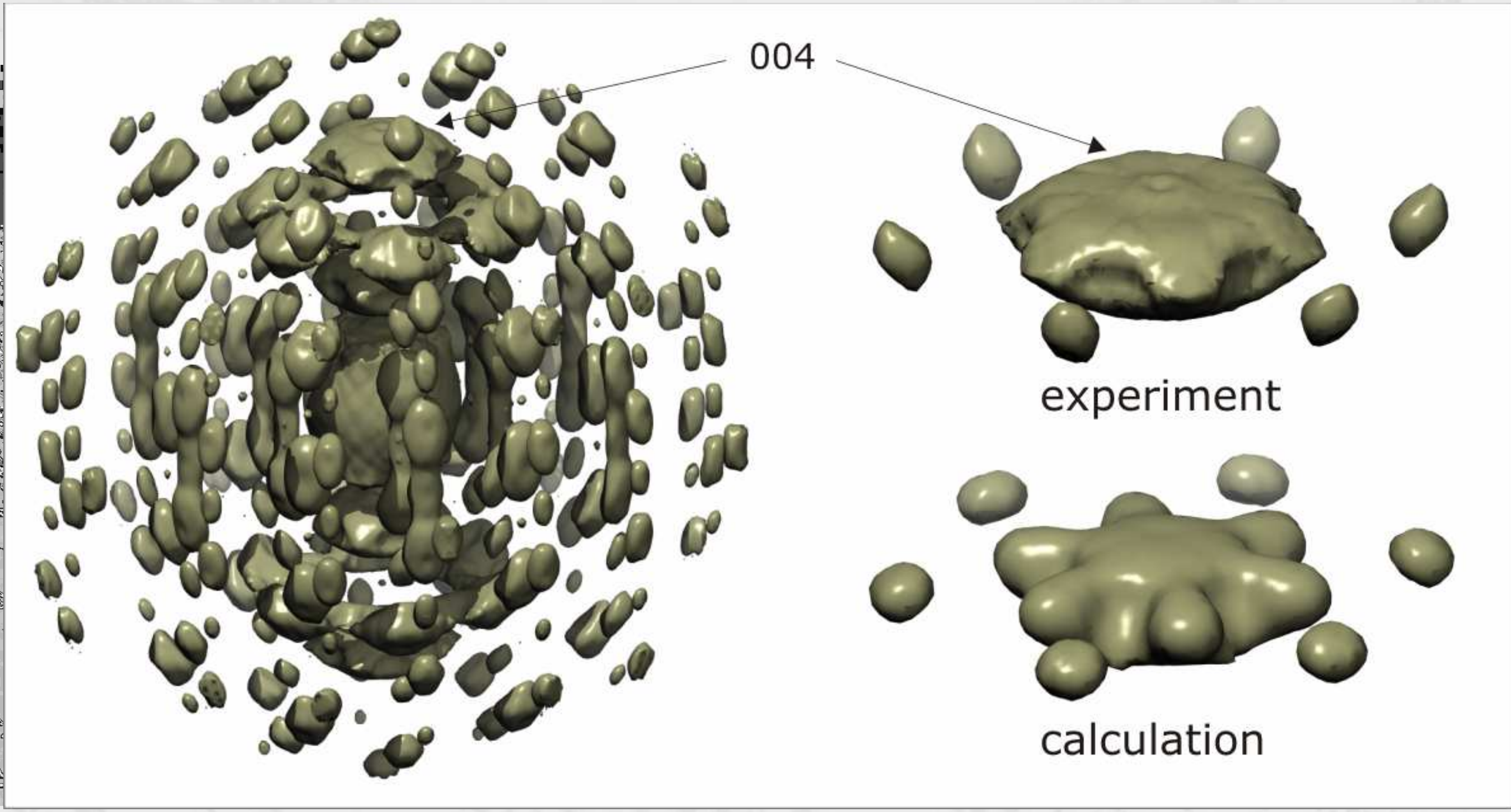

"lens" curvature => $q/2 \approx k_F \approx 1.57$ Å^{-1}
free electrons model => $k_F \approx 1.573$ Å^{-1}

elastic contribution can be neglected (proven by IXS)

… and 3D TDS representation

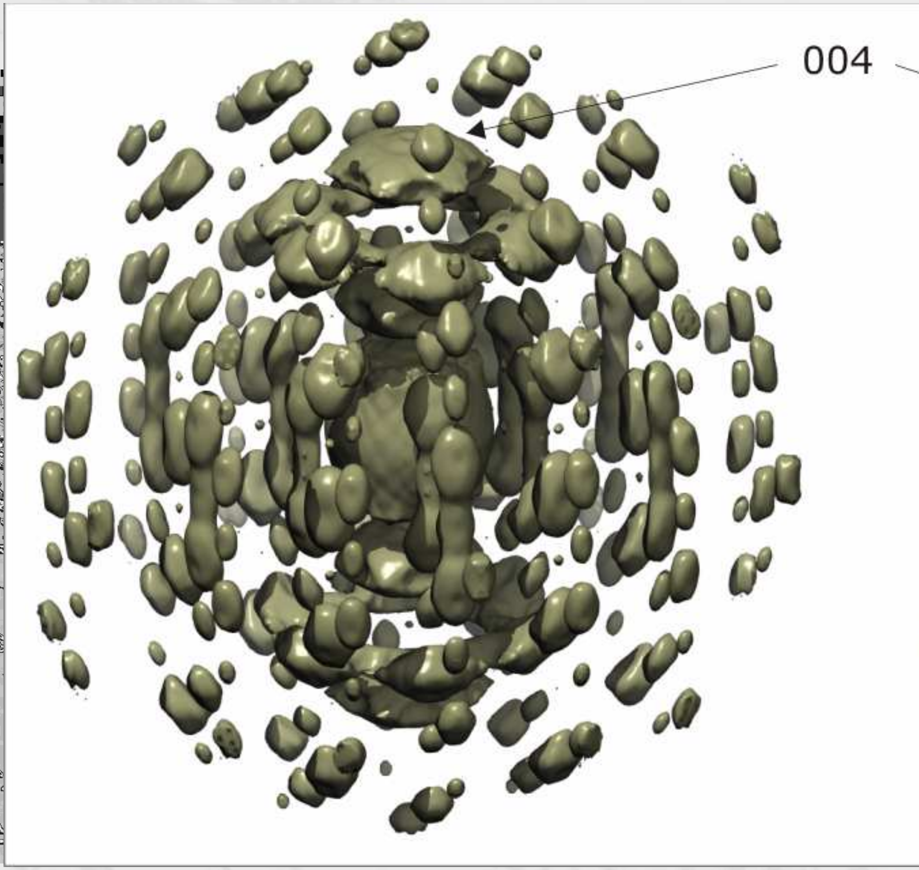

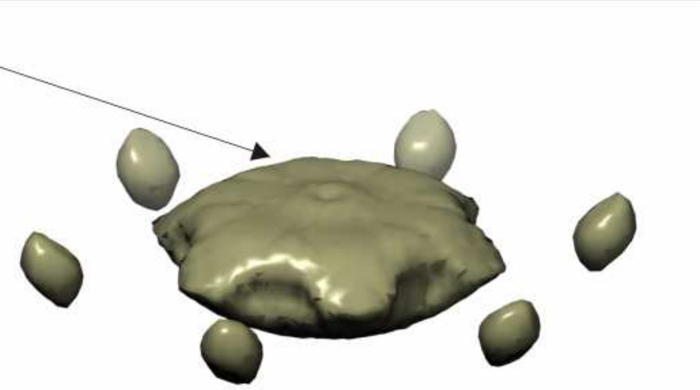

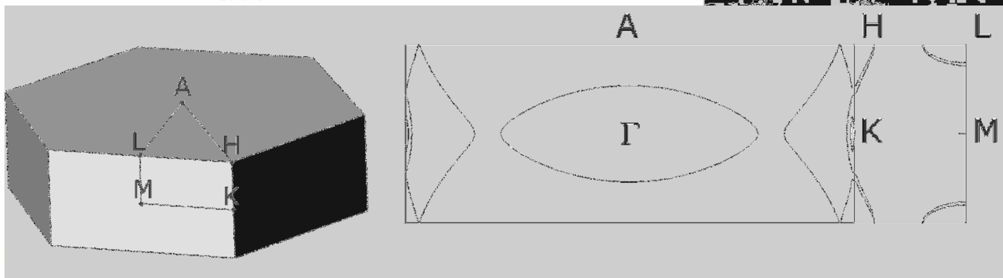

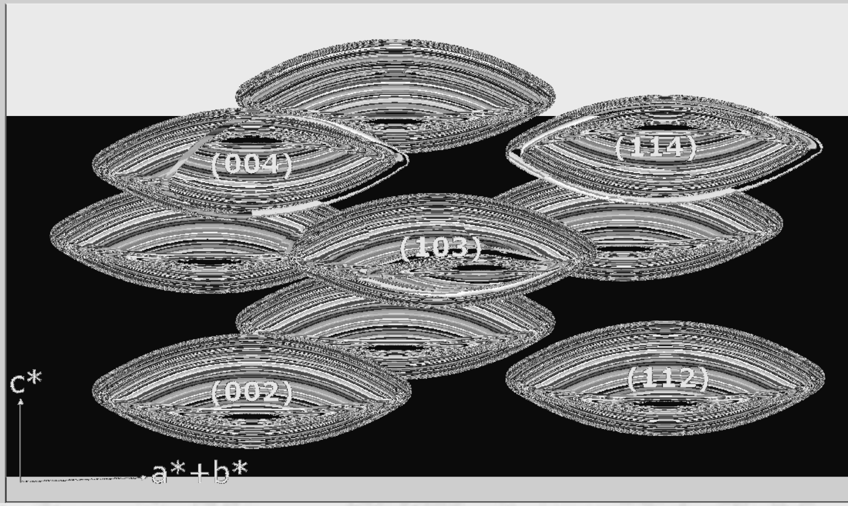

A. Bosak, M. Hoesch, M. Krisch, D. Chernyshov, P. Pattison, C. Schulze-Briese, B. Winkler, V. Milman, K. Refson, D. Antonangeli, and D. Farber, Phys. Rev. Lett. ***103****, 076403 (2009)*

Magnetite

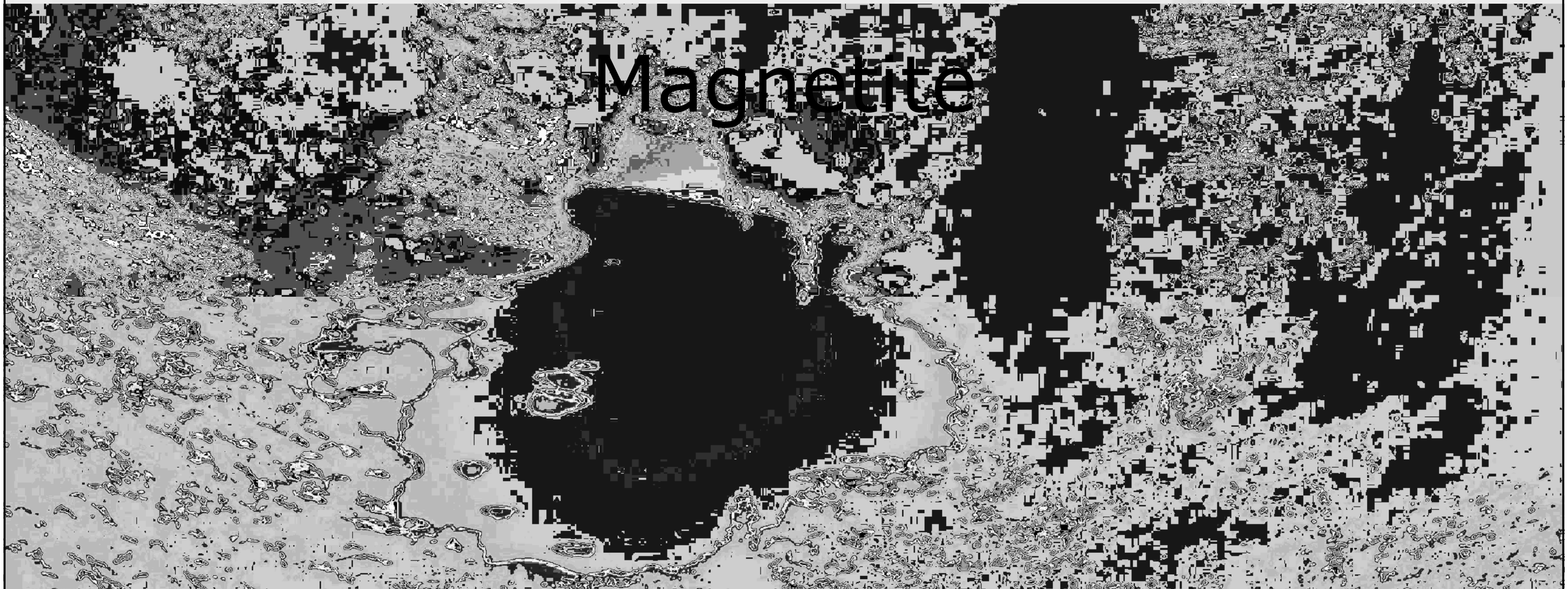

A. Bosak, P. Piekartz, M. Hoesch, D. Chernyshov, C. Schulze-Briese

The oldest known magnetic material

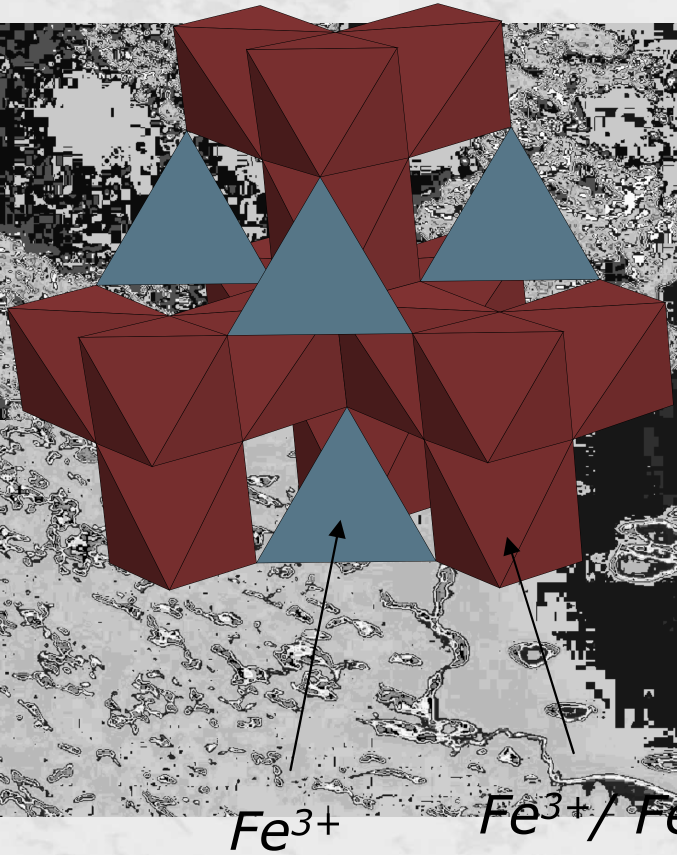

discovery: about 4,000 years ago (legend)

structure: 1915 (Bragg)

Verwey transition below 120 K (1936):

an electron-ordering transition occurring in a mixed-valent system that results in an ordering of formal valence states in the low-temperature phase

2010: structure of low-temperature phase is still unknown

High-temperature phase: neutron diffuse scattering

K. Siratori, Y. Ishii, Y. Morii, S. Funahashi, S. Todo, and A.Yanase
J. Phys. Soc. Jpn. 67, 2818 (1998)

triple-axis neutron spectrometer

125 K

150 s/point

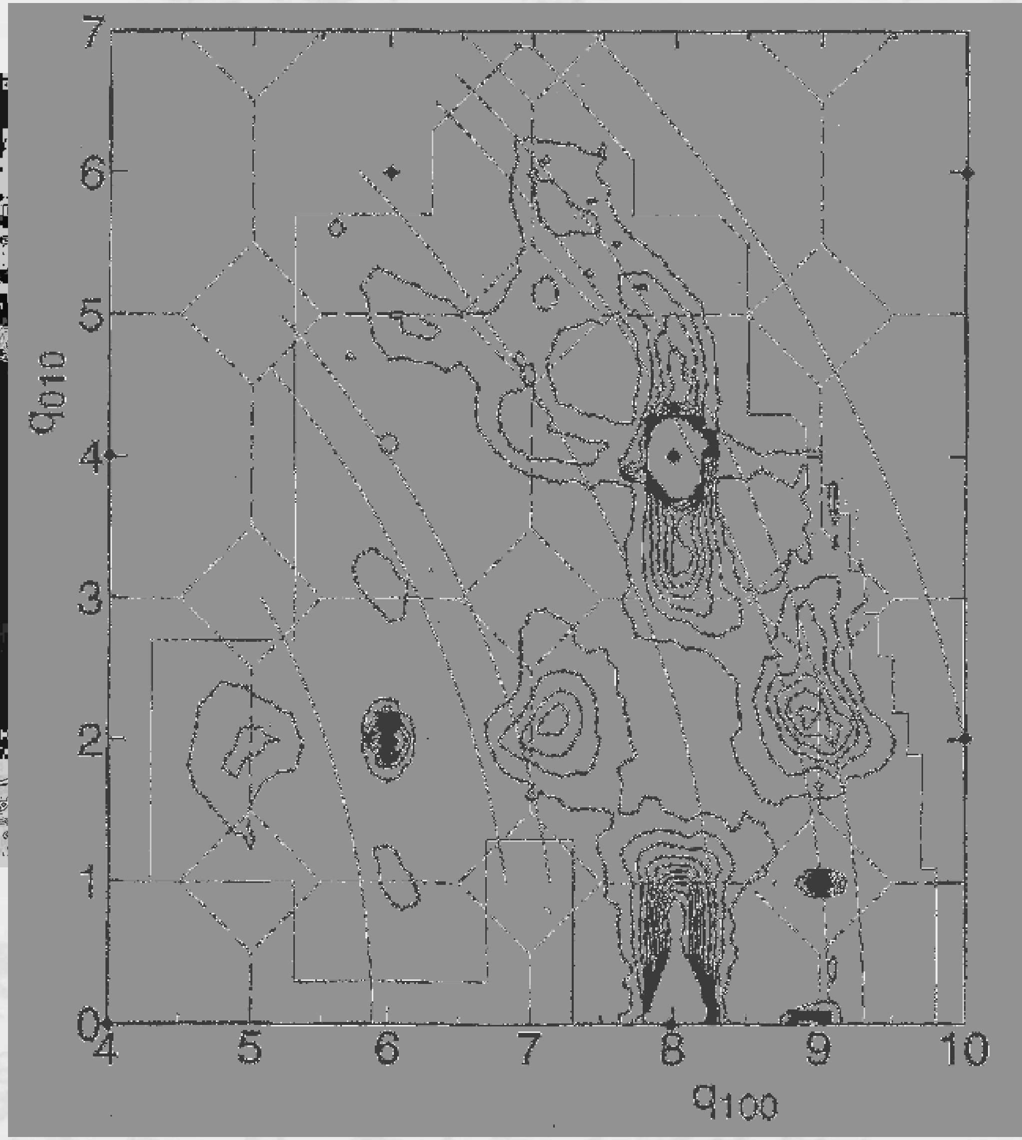

large polarons of specific structure

X-ray diffuse scattering

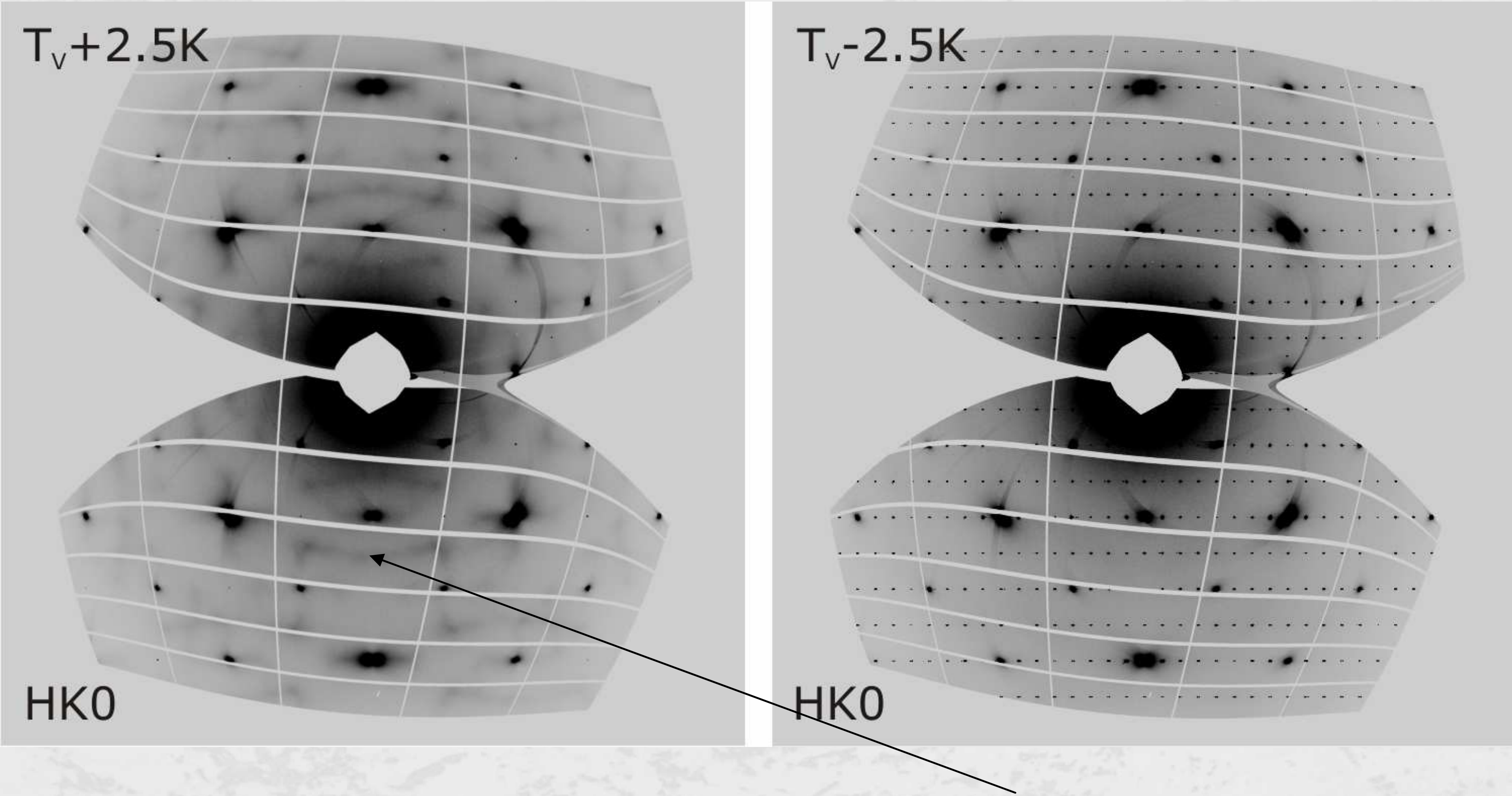

all the features observed with neutrons are visible + some additional

diffuse features fully disappear below the transition (except for TDS)

X-ray diffuse scattering

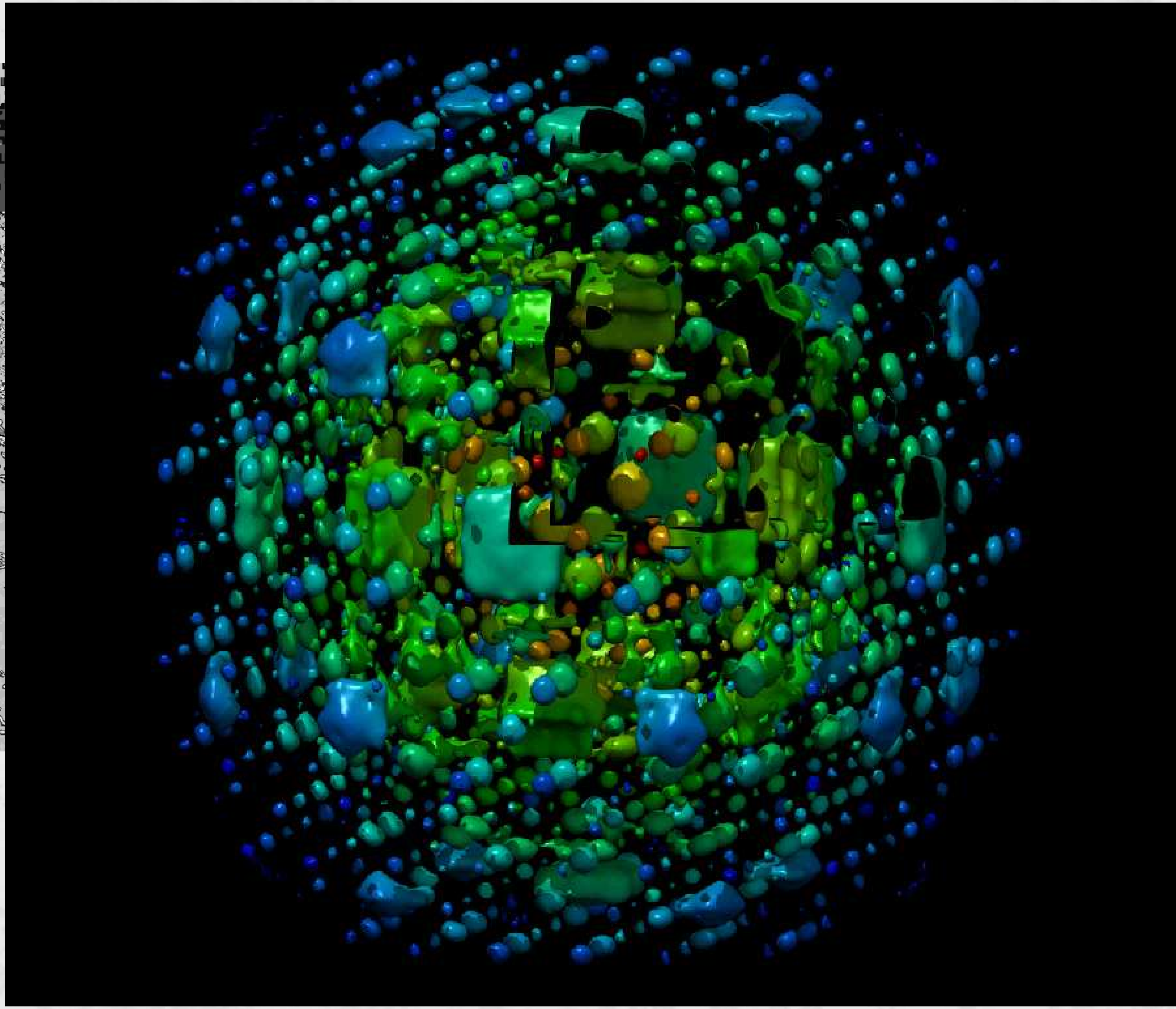

X-ray diffuse scattering

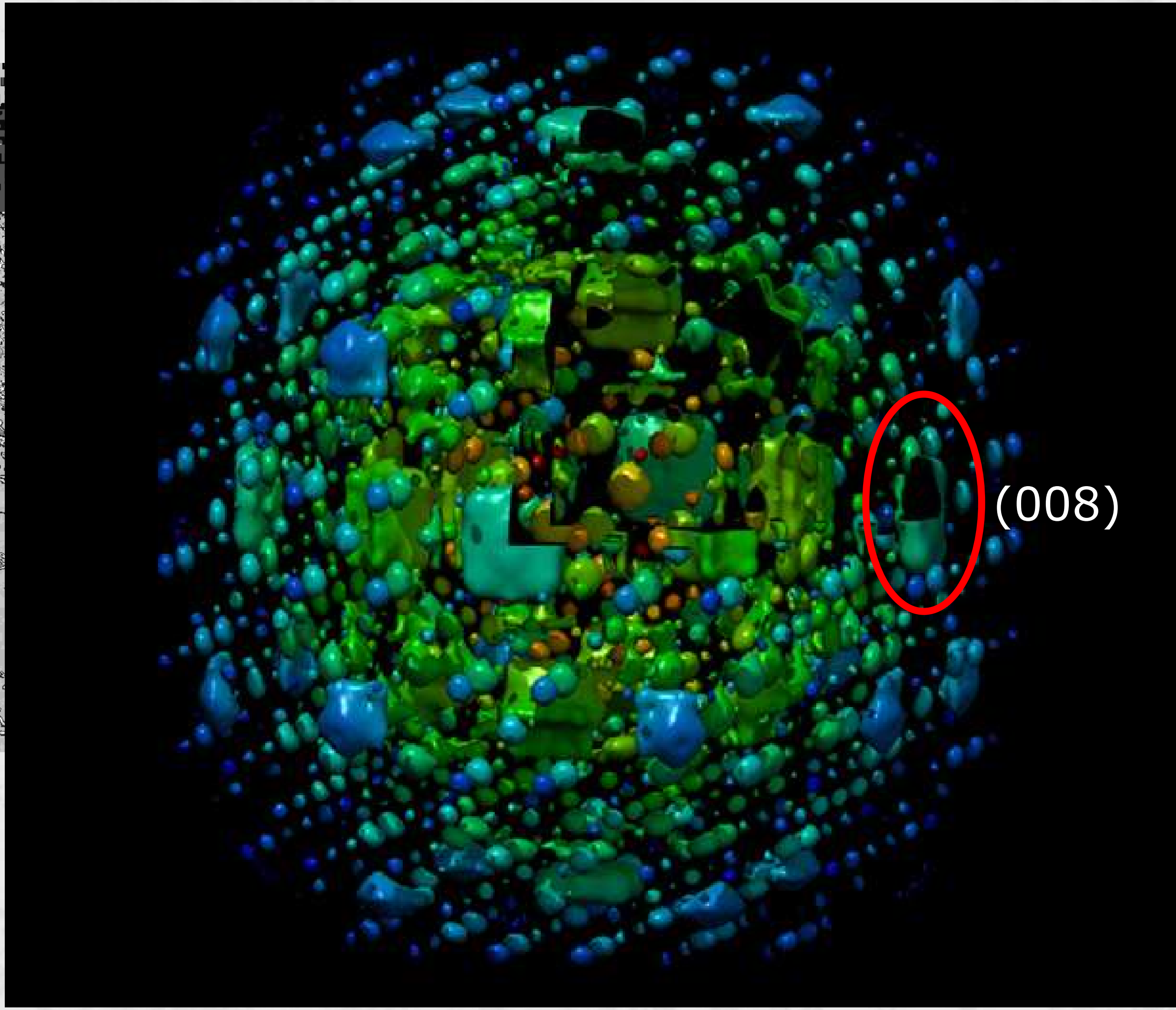

X-ray diffuse scattering

X-ray diffuse scattering

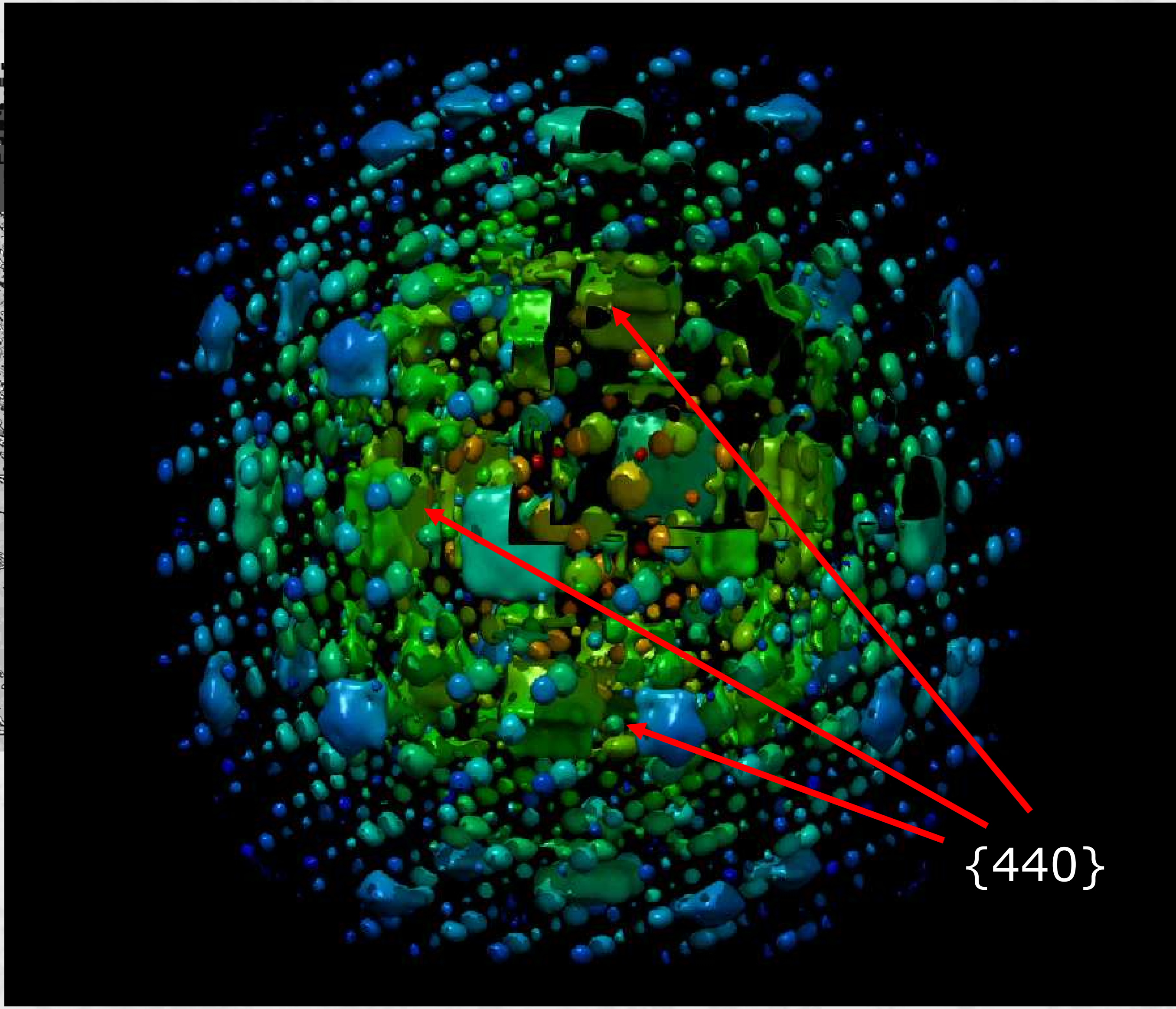

X-ray diffuse scattering

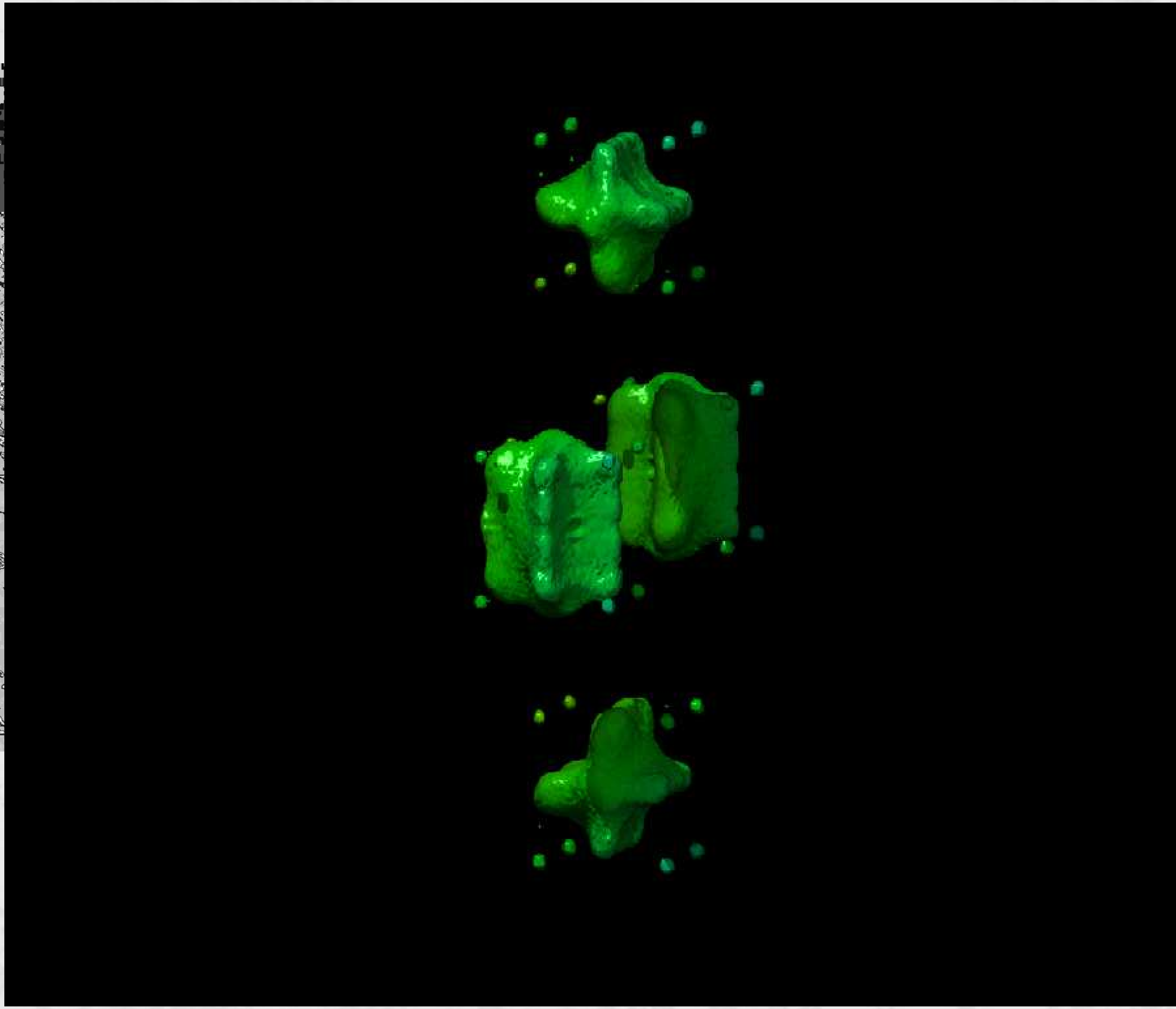

X-ray diffuse scattering

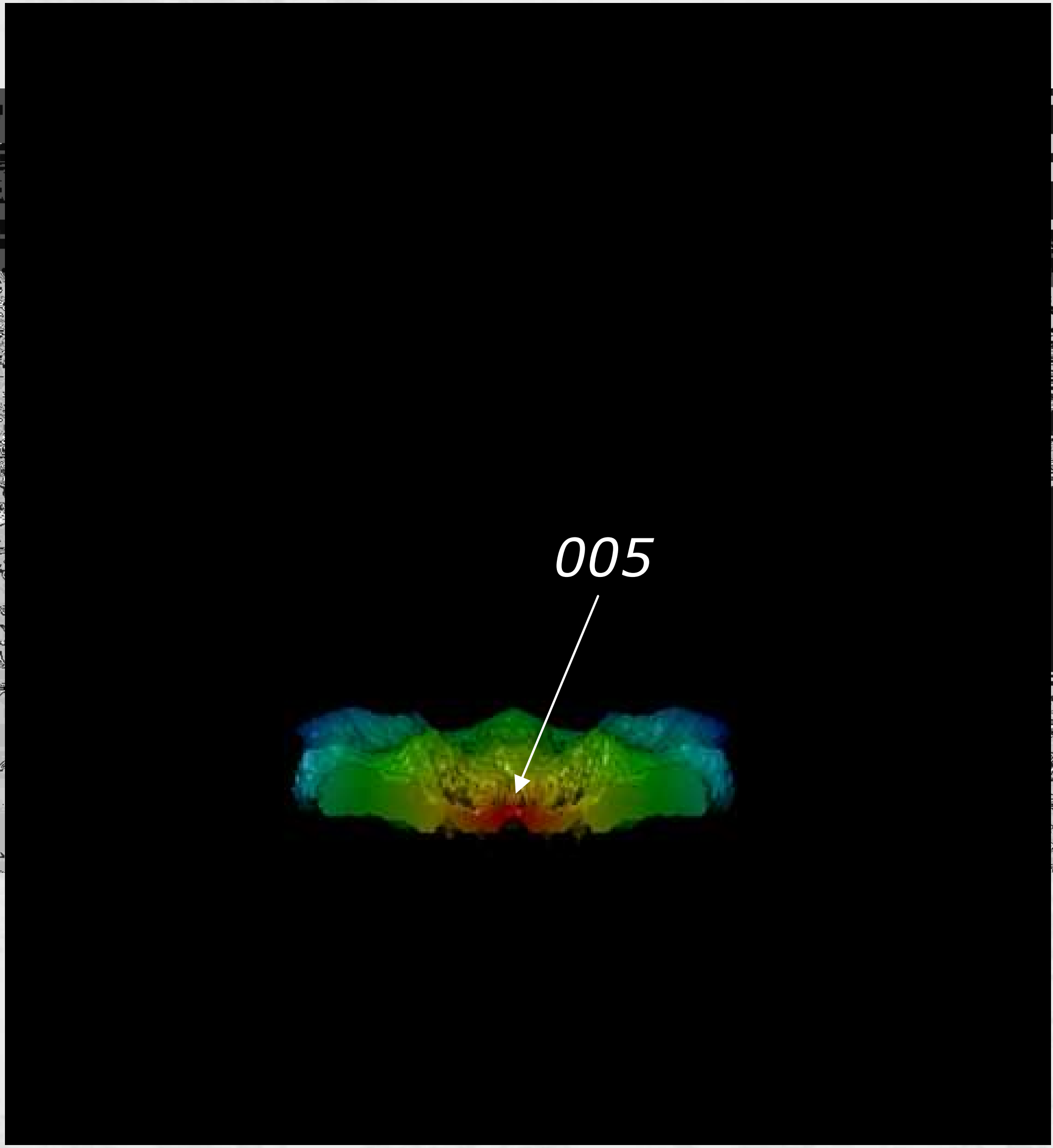

X-ray diffuse scattering

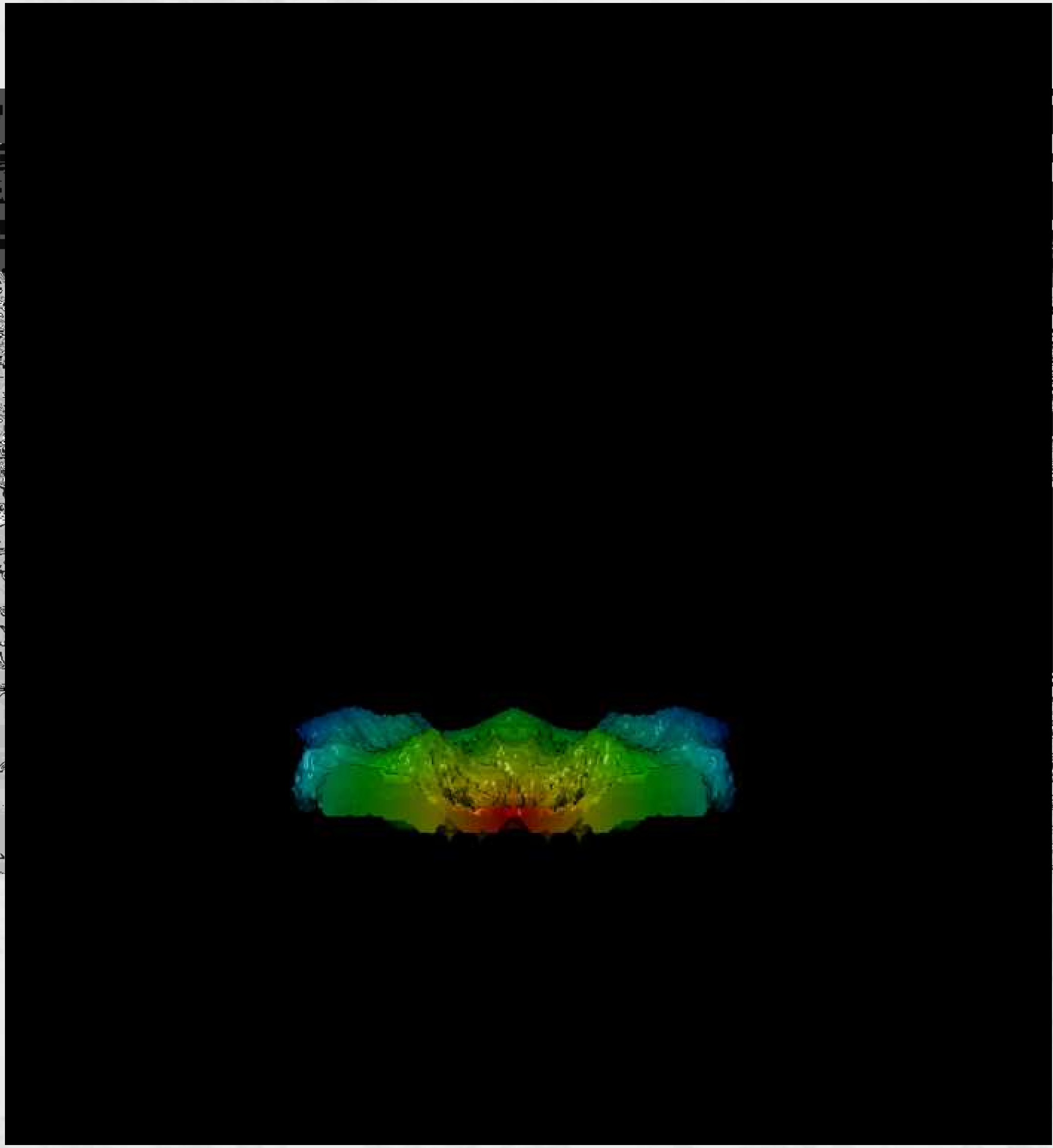

Source of diffuse scattering

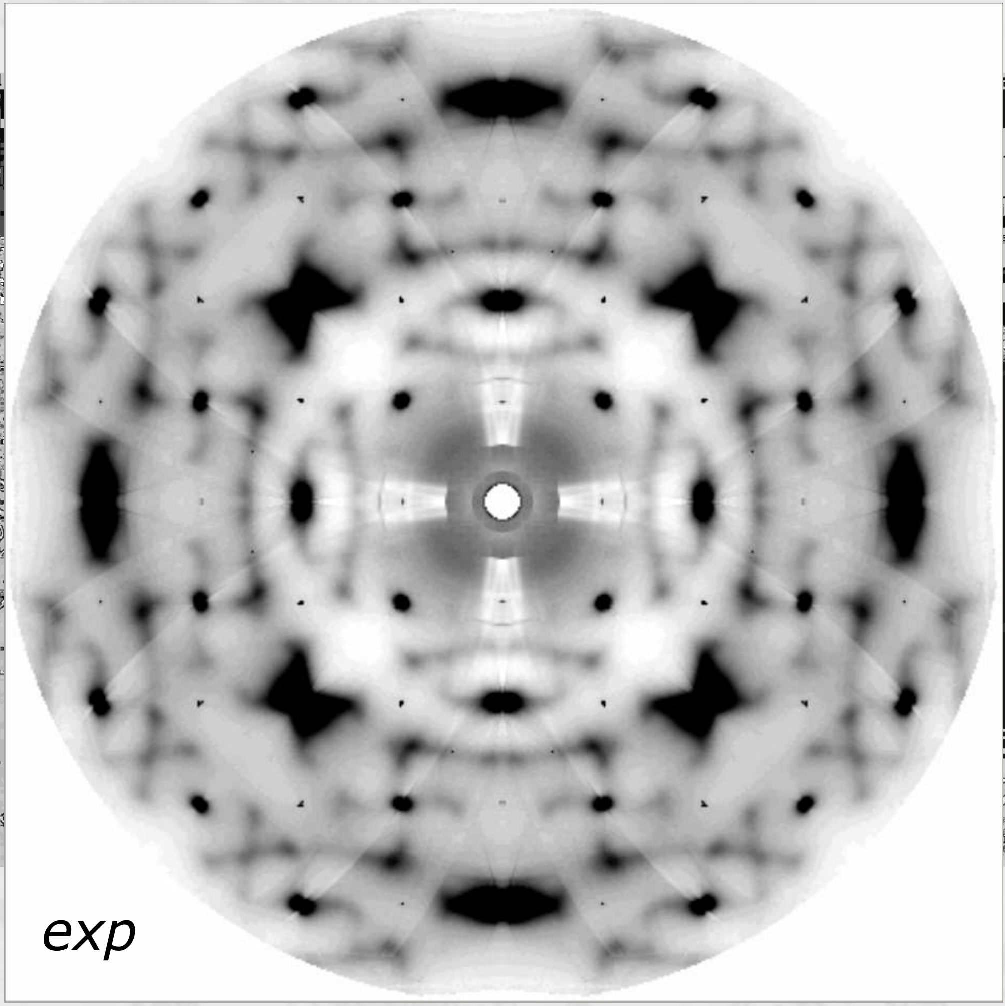

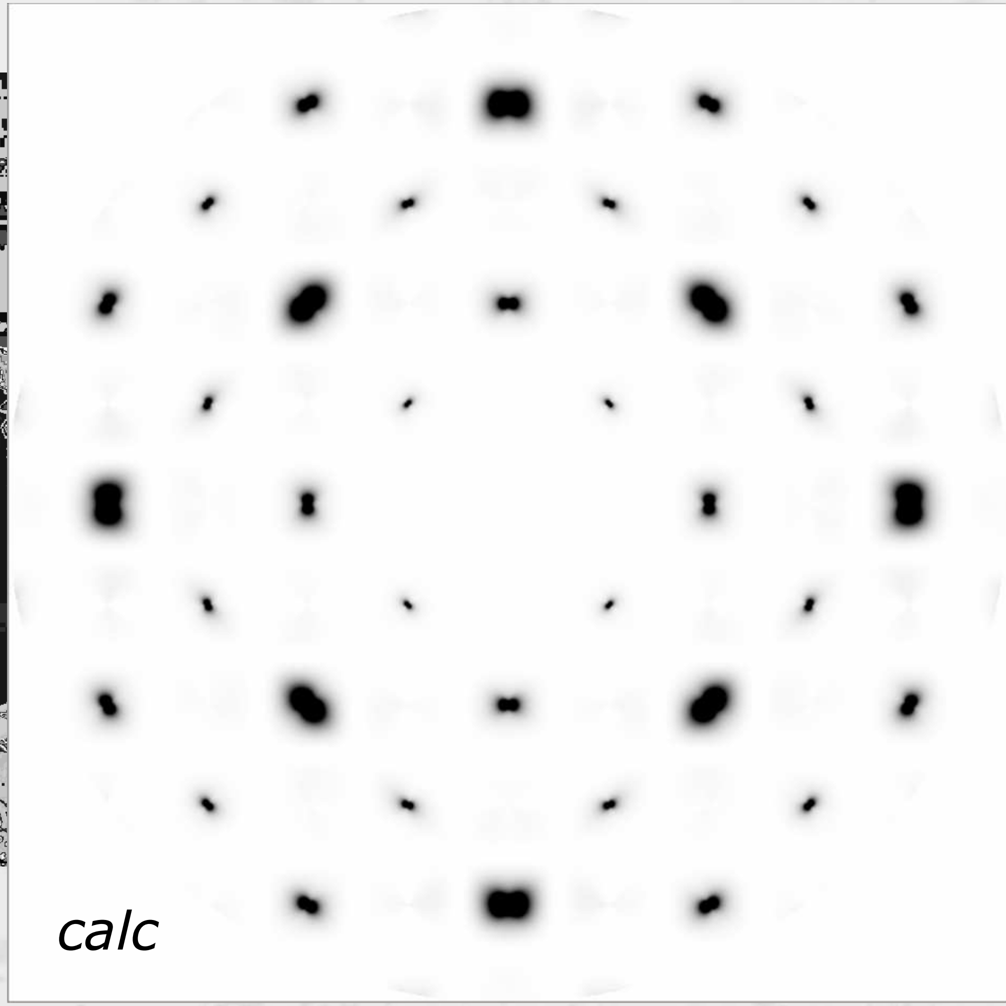

TDS from elastic moduli

Source of diffuse scattering

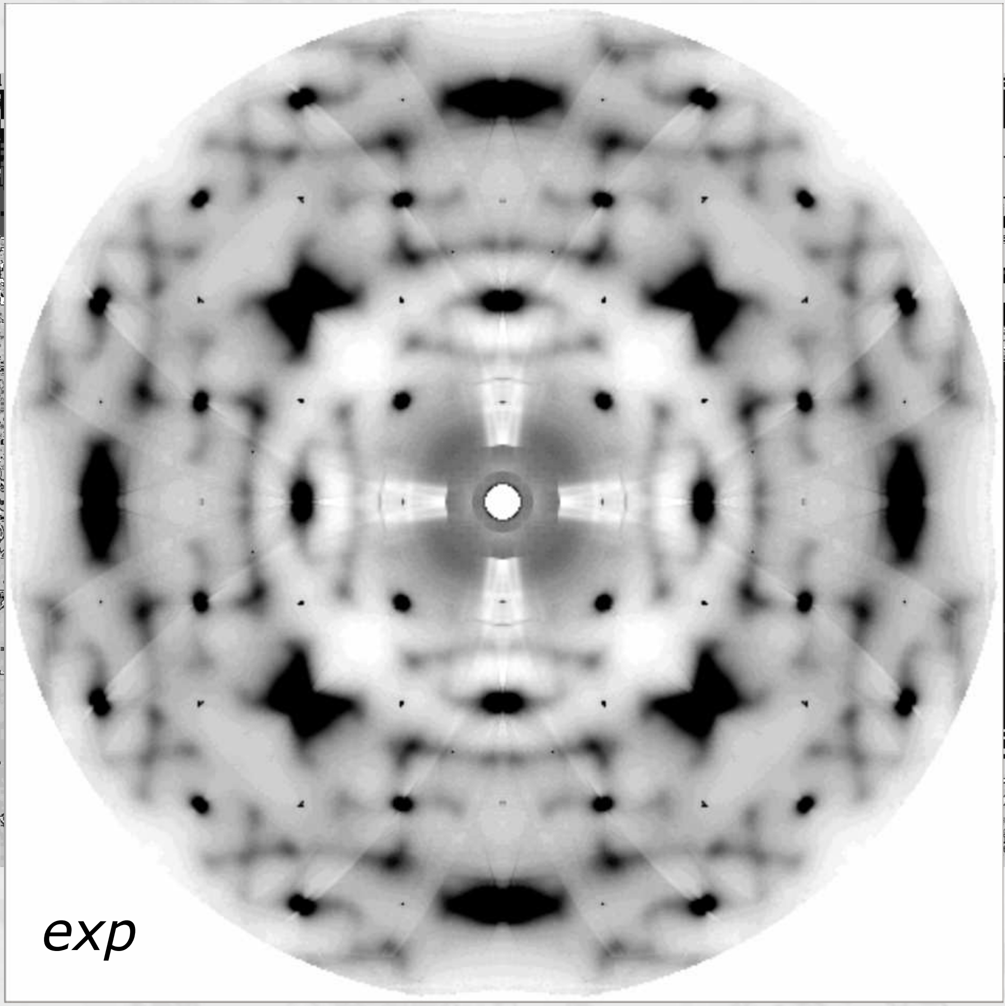

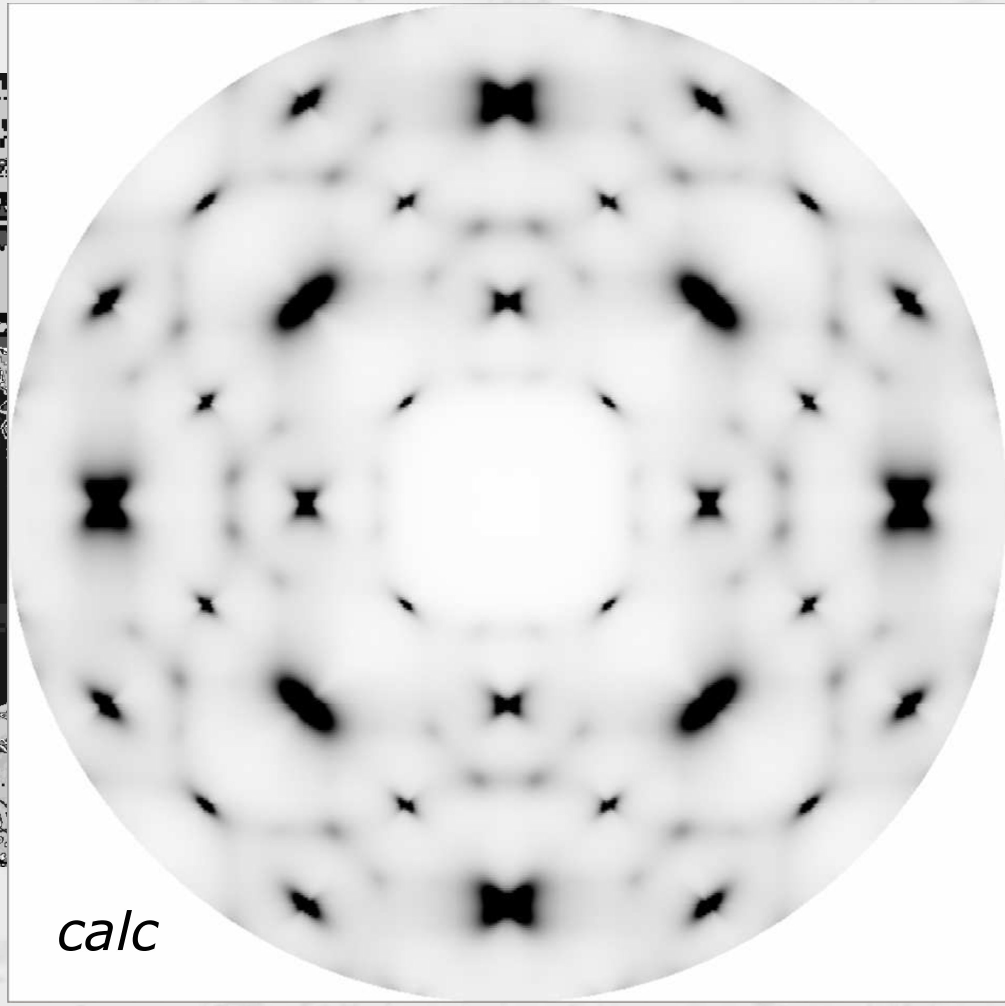

TDS from WIEN2K + Phonons

IXS experiment

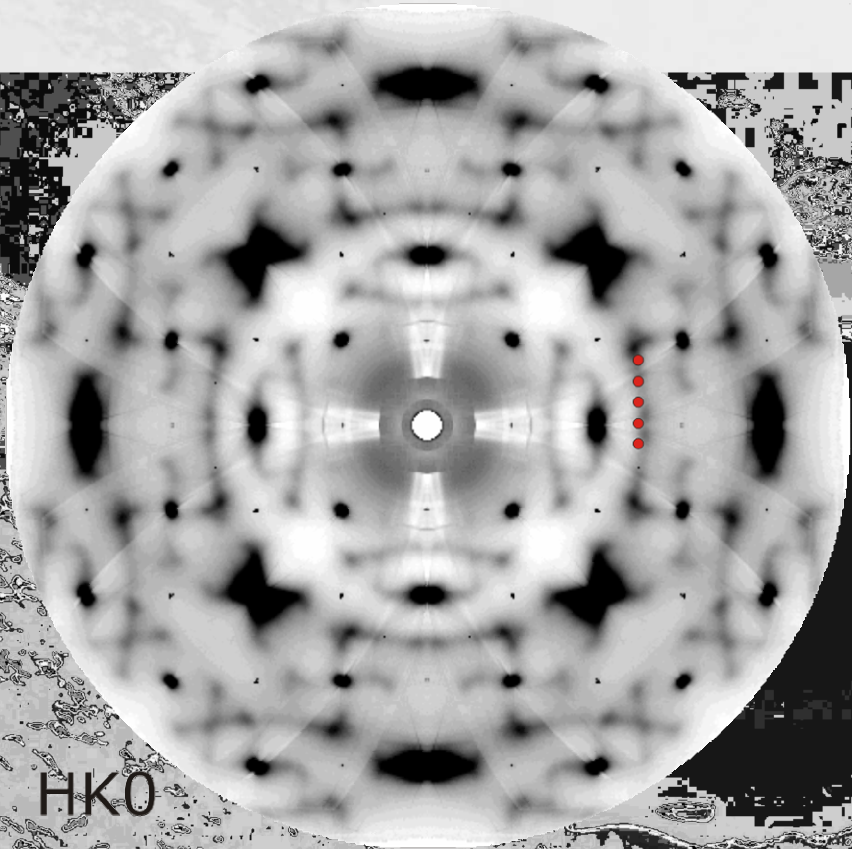

IXS experiment

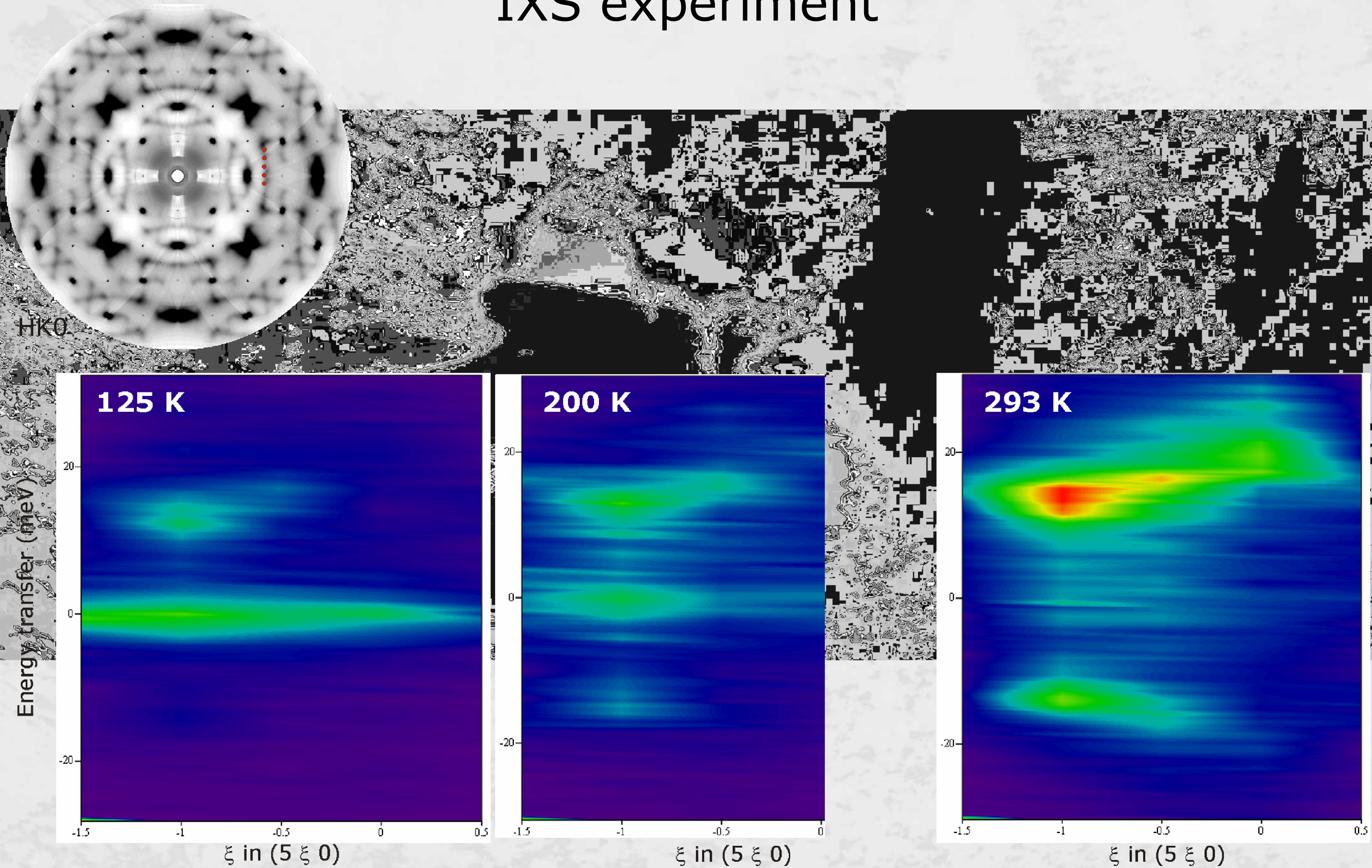

IXS experiment

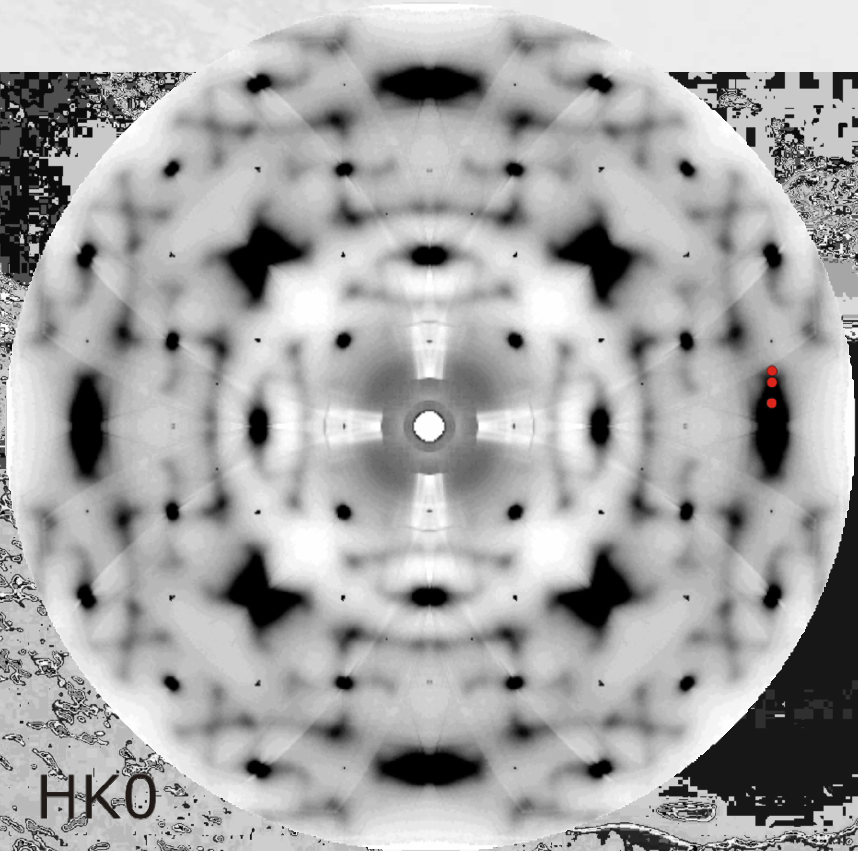

IXS experiment

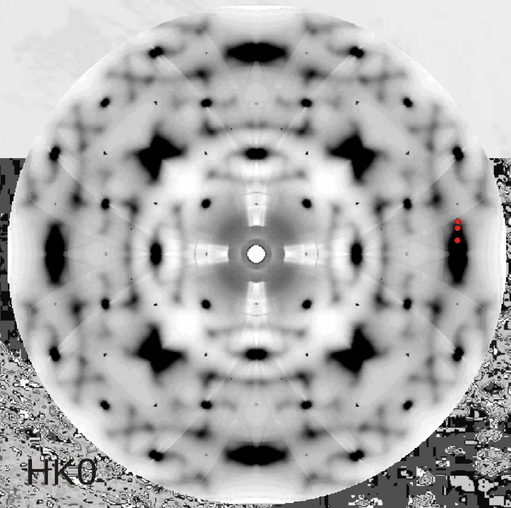

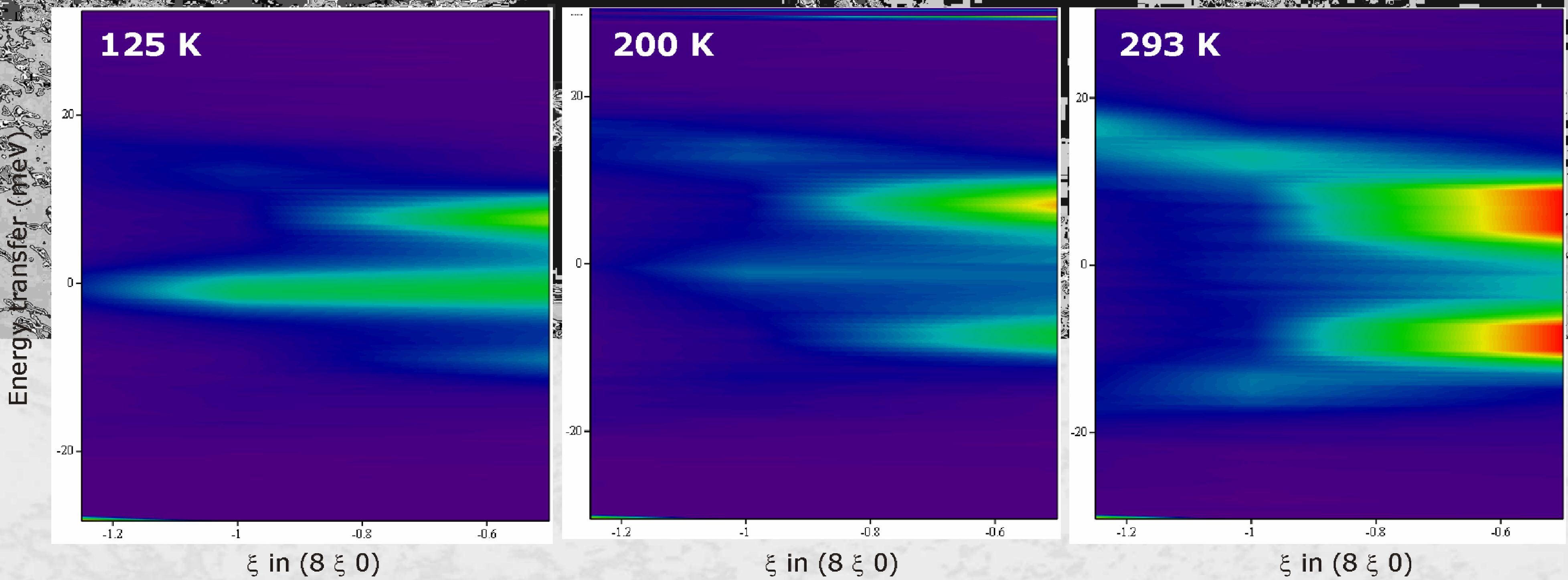

Fermi surface?

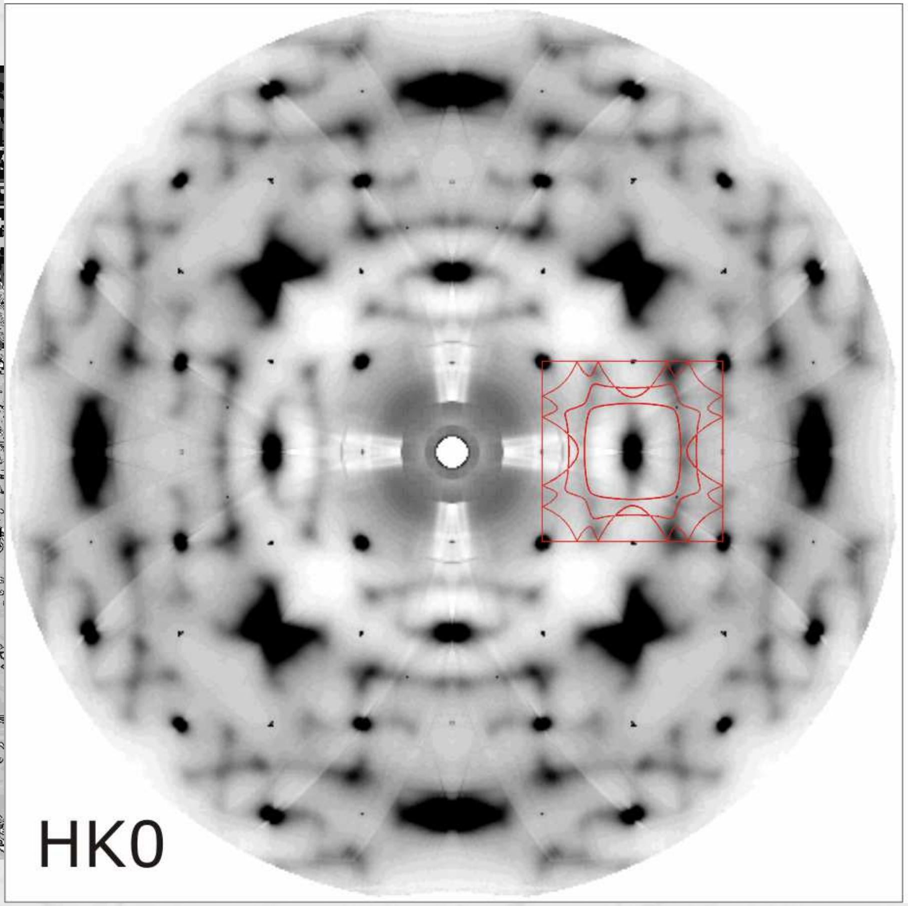

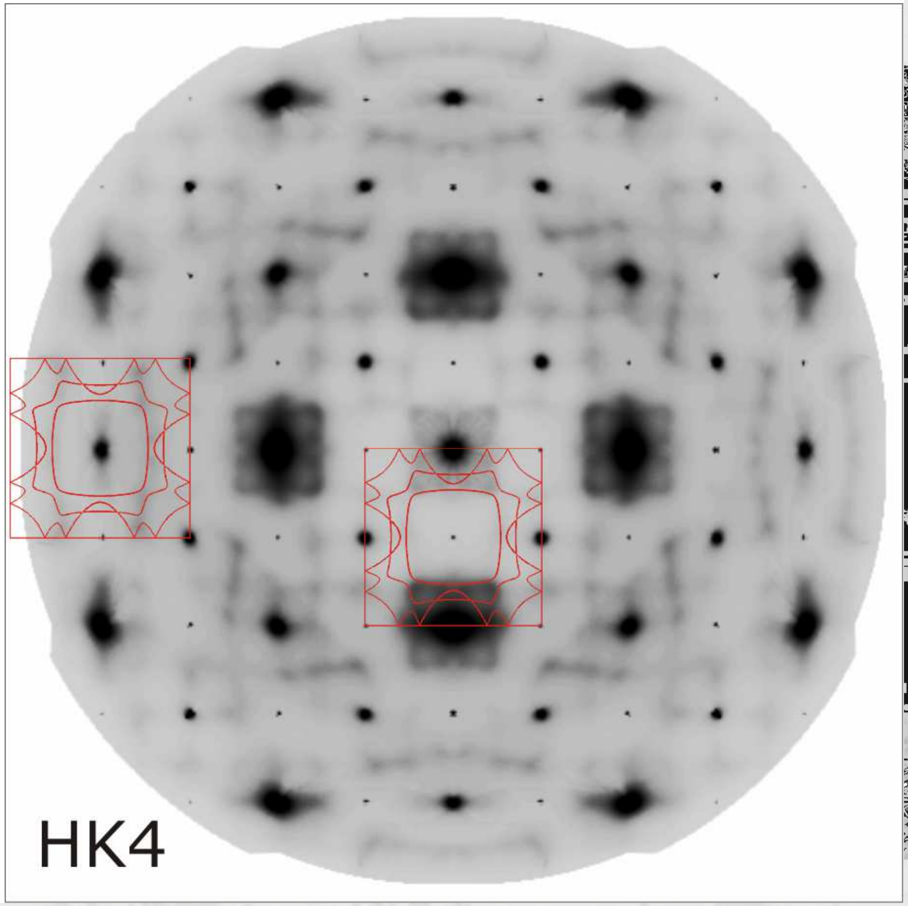

nesting of Fermi surface => discontinuity of interaction potential => signature in charge movement

A. Bosak, P. Piekartz, M. Hoesch, D. Chernyshov, C. Schulze-Briese, in preparation

Correlated disorder in Prussian Blue

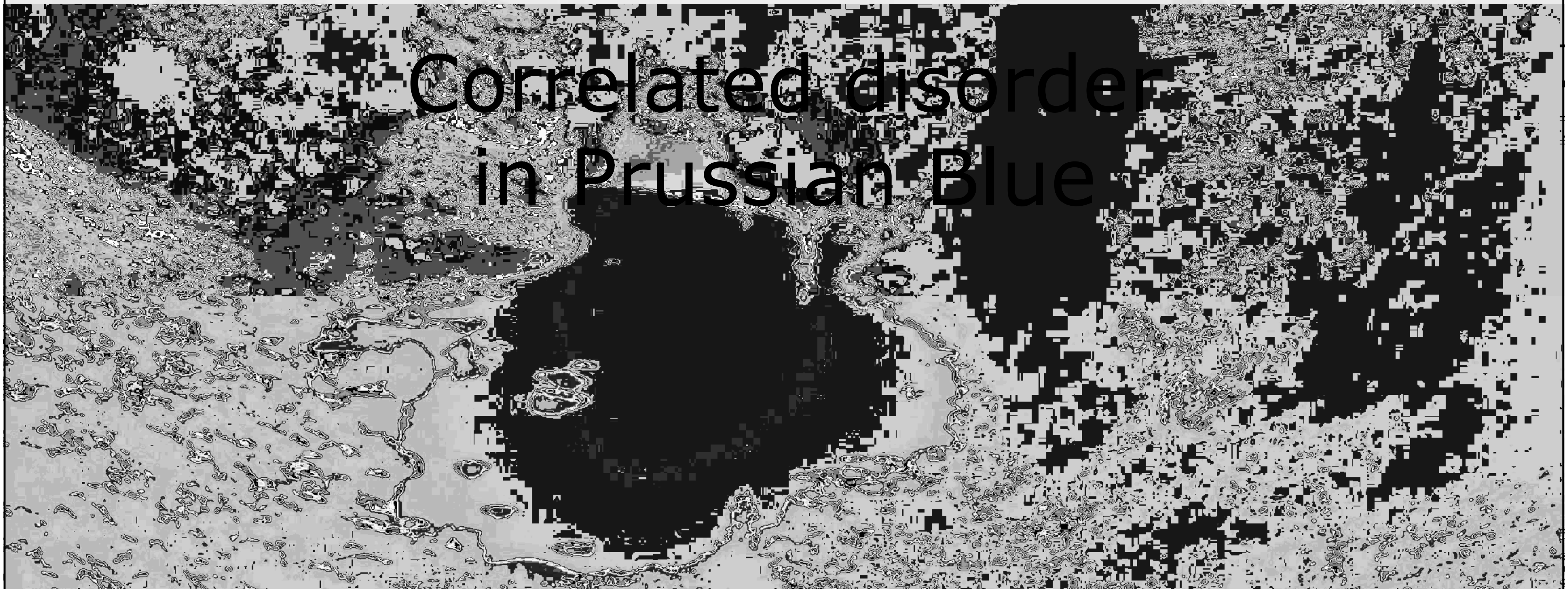

A. Bosak, D. Chernyshov, *Phase Transitions (2010)*

Diffuse scattering in Prussian Blue analog

Crystalline, Mixed-Valence Manganese Analogue of Prussian Blue: Magnetic, Spectroscopic, X-ray and Neutron Diffraction Studies

Patrick Franz,[†] Christina Ambrus,[†] Andreas Hauser,[‡] Dmitry Chernyshov,[1,§] Marc Hostettler,[†] Jürg Hauser,[†] Lukas Keller,[||] Karl Krämer,[†] Helen Stoeckli-Evans,[#] Philip Pattison,[⊥] Hans-Beat Bürgi,[†] and Silvio Decurtins[†,*]

Contribution from the Departement für Chemie und Biochemie und Laboratorium für Kristallographie, Universität Bern, Freiestrasse 3, CH-3012 Bern, Switzerland

J. AM. CHEM. SOC. 2004, 126, 16472–16477

$Mn(II)[Mn(III)(CN)_6]_{2/3}\cdot(6H_2O)_{1/3}\cdot yH_2O$

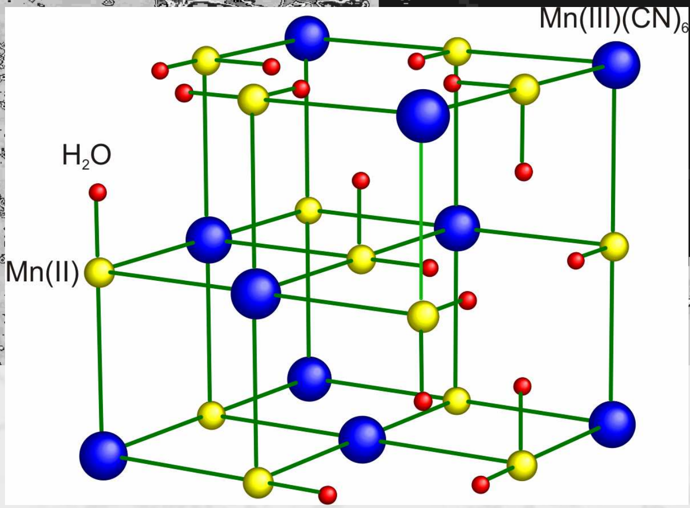

2D

1D

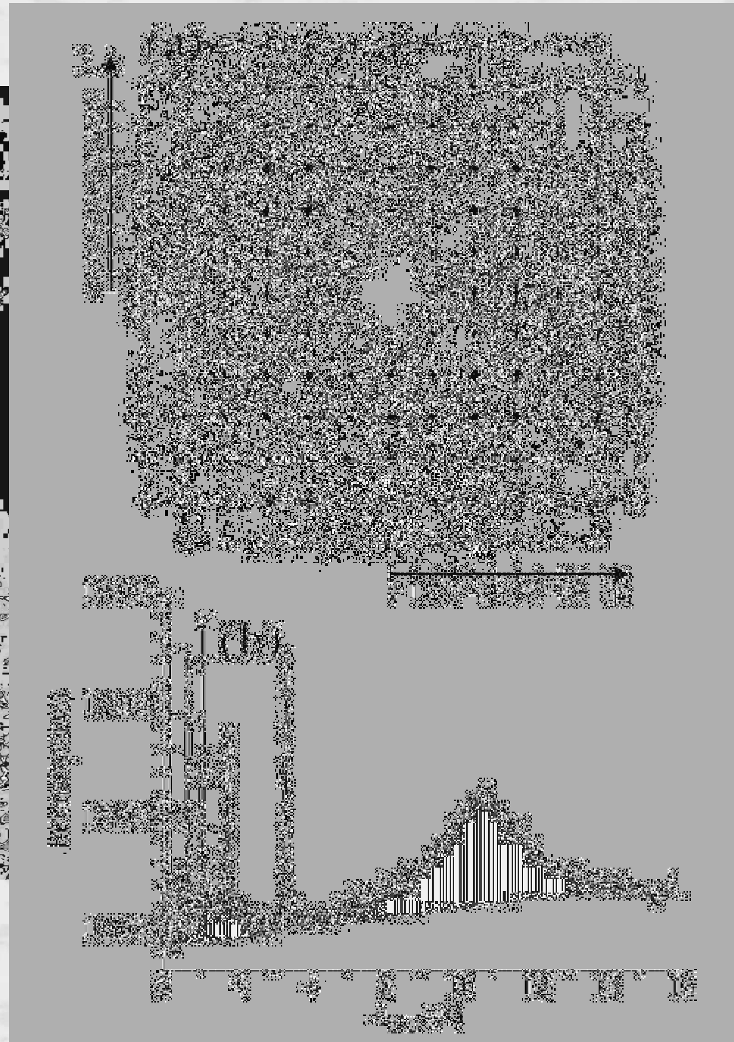

Figure 8. (a) Diffuse scattering of 1 obtained from a) single-crystal X-ray diffraction (H0L-layer, $T = 293$ K), (b) neutron powder diffraction (153 K). The gray areas in the powder diagram indicate diffuse contributions and correspond to the blurred features seen in a).

Swiss Norwegian Beam Lines / MAR Image Plate
SLS / PILATUS 6M

Diffuse scattering in Prussian Blue analog

replacement of $[Mn(CN)_6)]$ by $[6H_2O]$

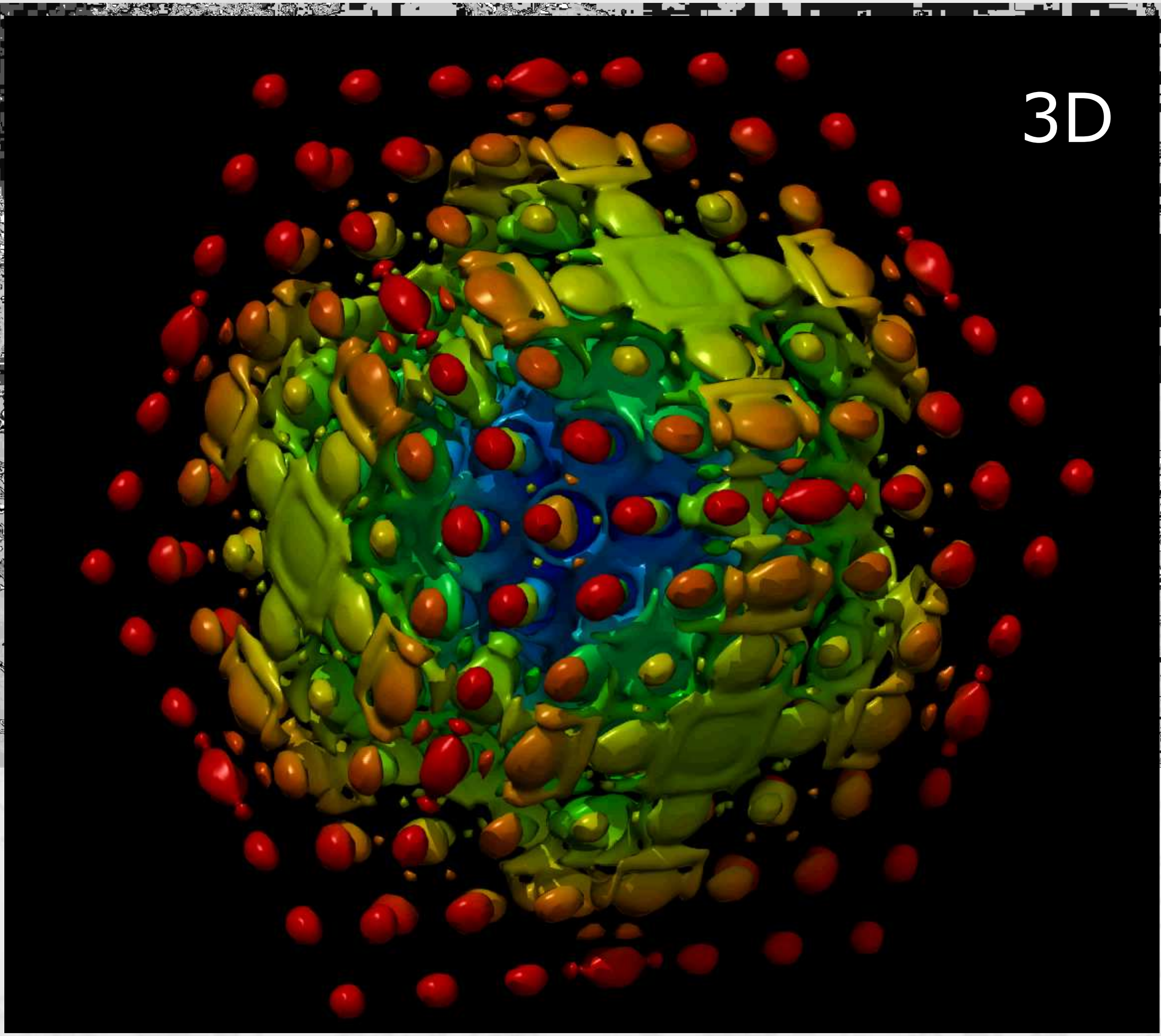

Diffuse scattering in Prussian Blue analog

replacement of $[Mn(CN)_6)]$ by $[6H_2O]$

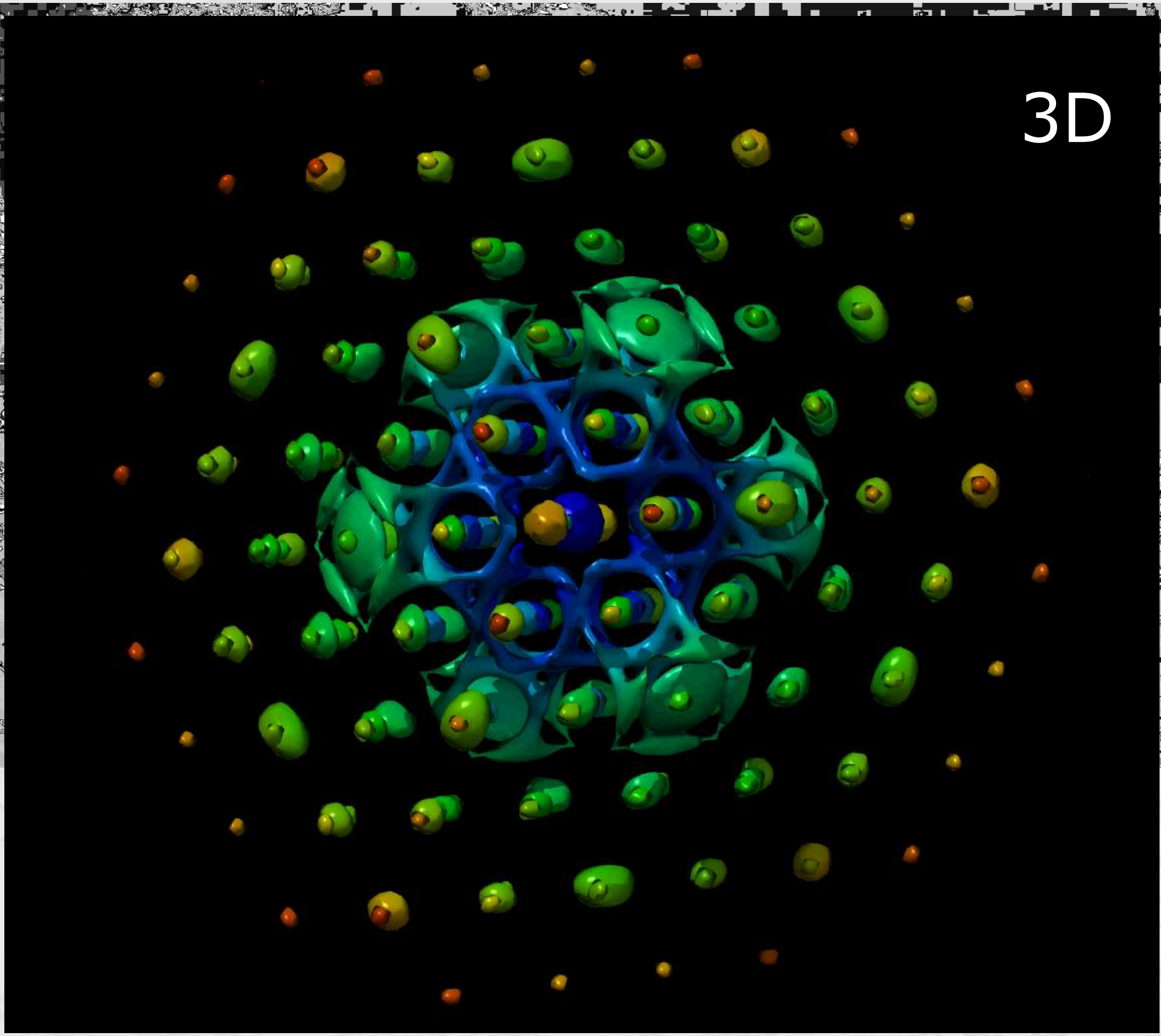

Elastic or inelastic?

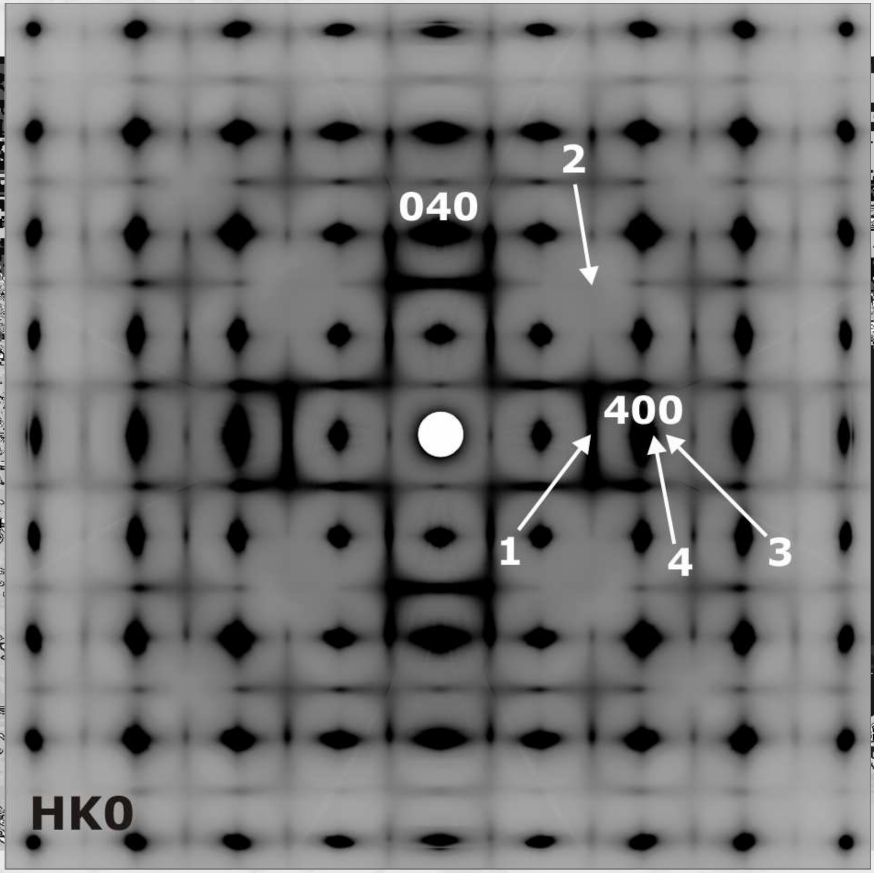

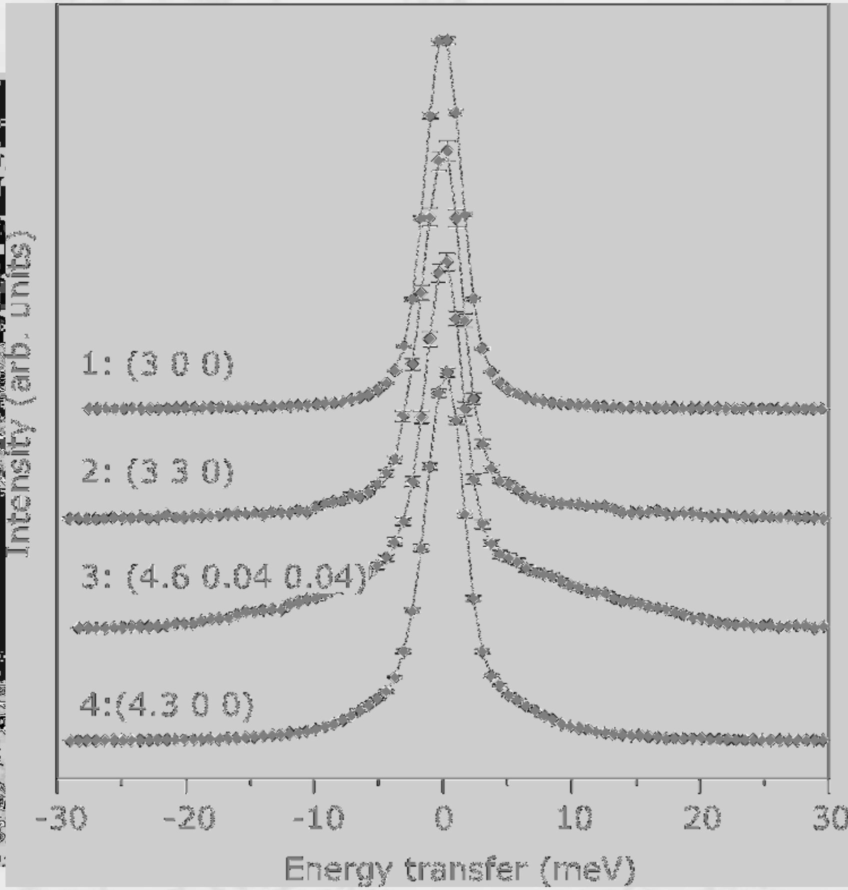

diffuse scattering is essentially (quasi)elastic and related to the disorder

Elastic or inelastic?

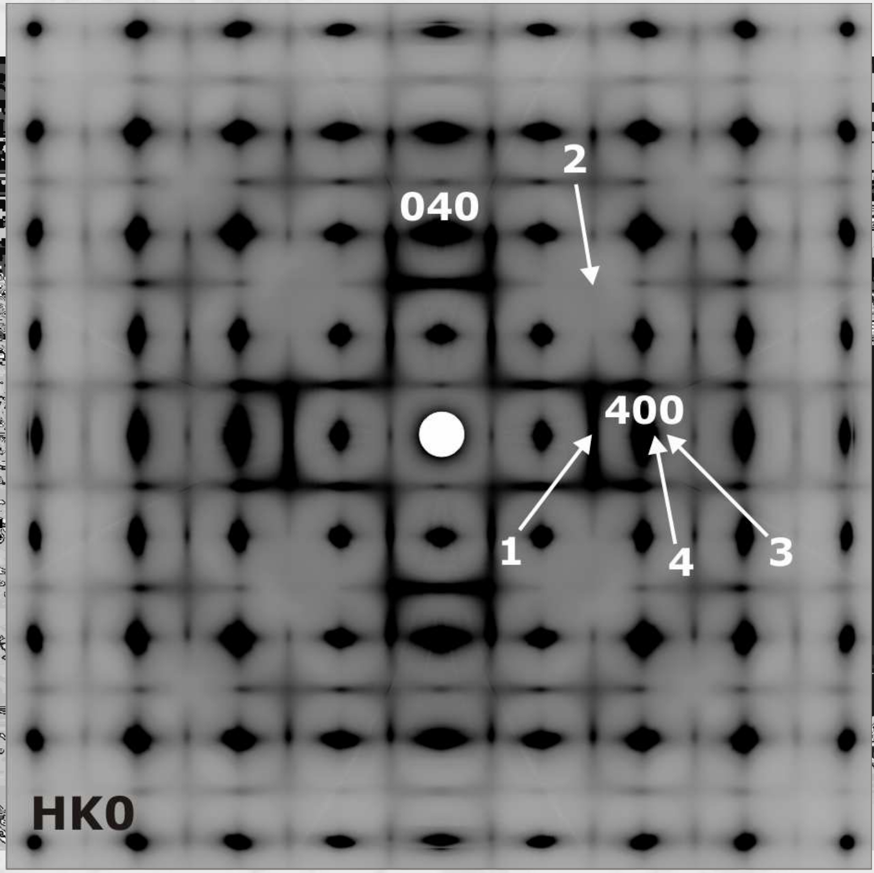

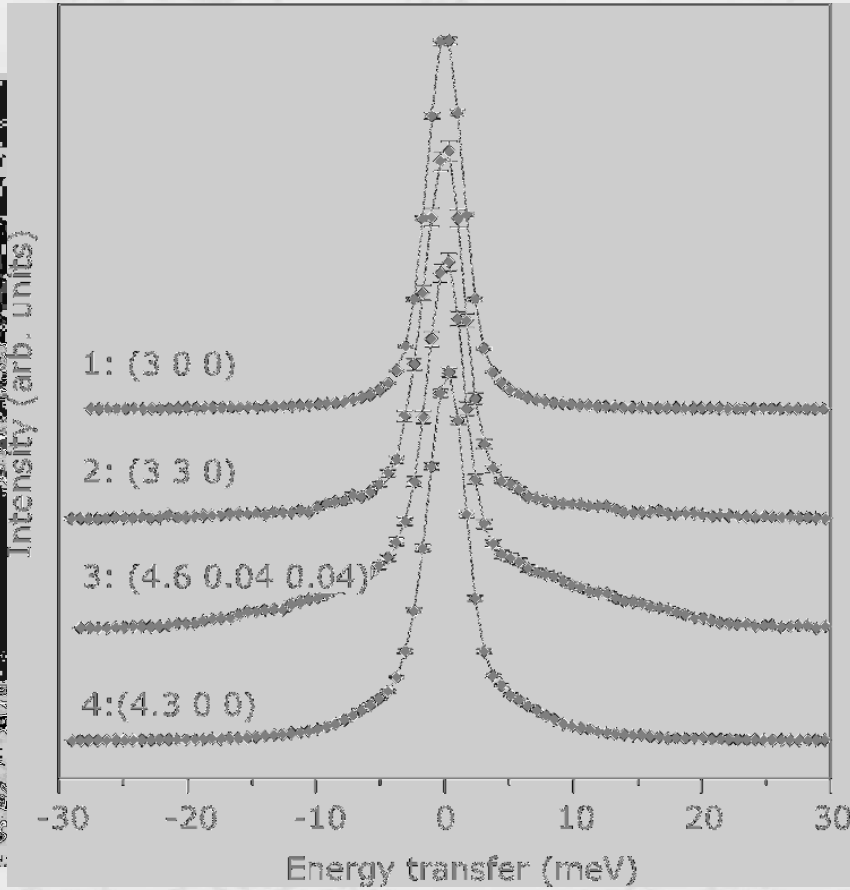

diffuse scattering is essentially (quasi)elastic and related to the disorder

Simple parametrization

$$\left\langle \left|c_{\mathbf{q}}\right|^2 \right\rangle \approx p(\mathbf{q}) \otimes \sum_{\alpha,\beta,\gamma} \sum_{n_\alpha,n_\beta,n_\gamma=-\infty}^{\infty} \left(\delta(q_\alpha + 2n_\alpha)\cdot\left(\delta(q_\beta + 2n_\beta + 1) + \delta(q_\gamma + 2n_\gamma + 1)\right)\right)$$

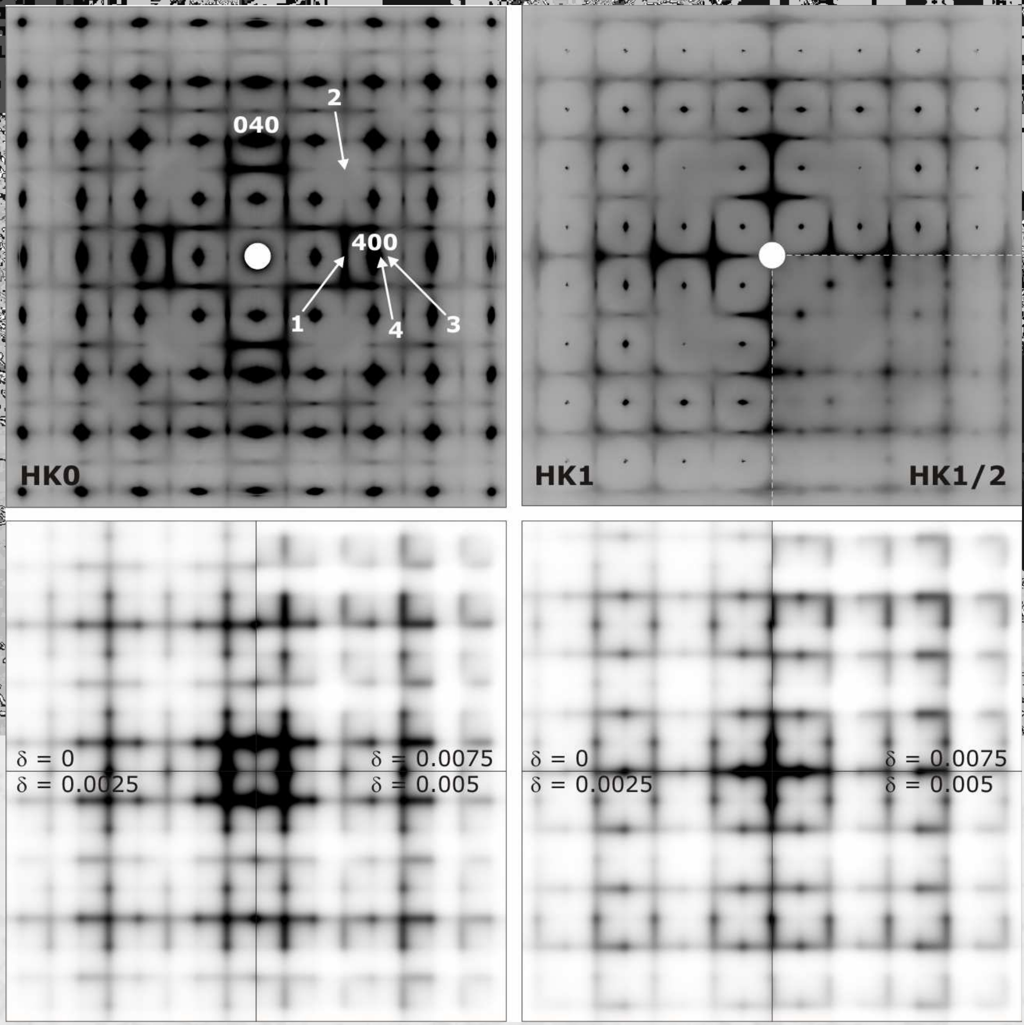

$$I_{DIF} = N\left\langle \left|c_{\mathbf{q}}\right|^2 \right\rangle \left(f_{\mathbf{q}}^A - f_{\mathbf{q}}^B\right)^2$$

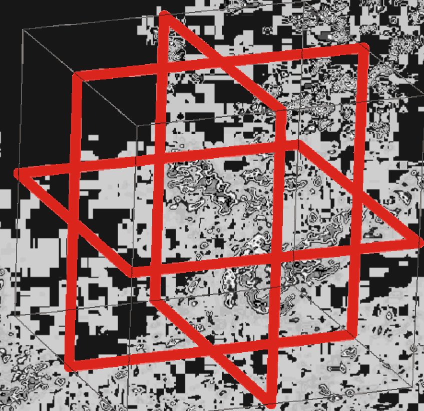

three families of intersecting rods

displacements are not taken into account => perfect fit is not possible

Autocorrelator

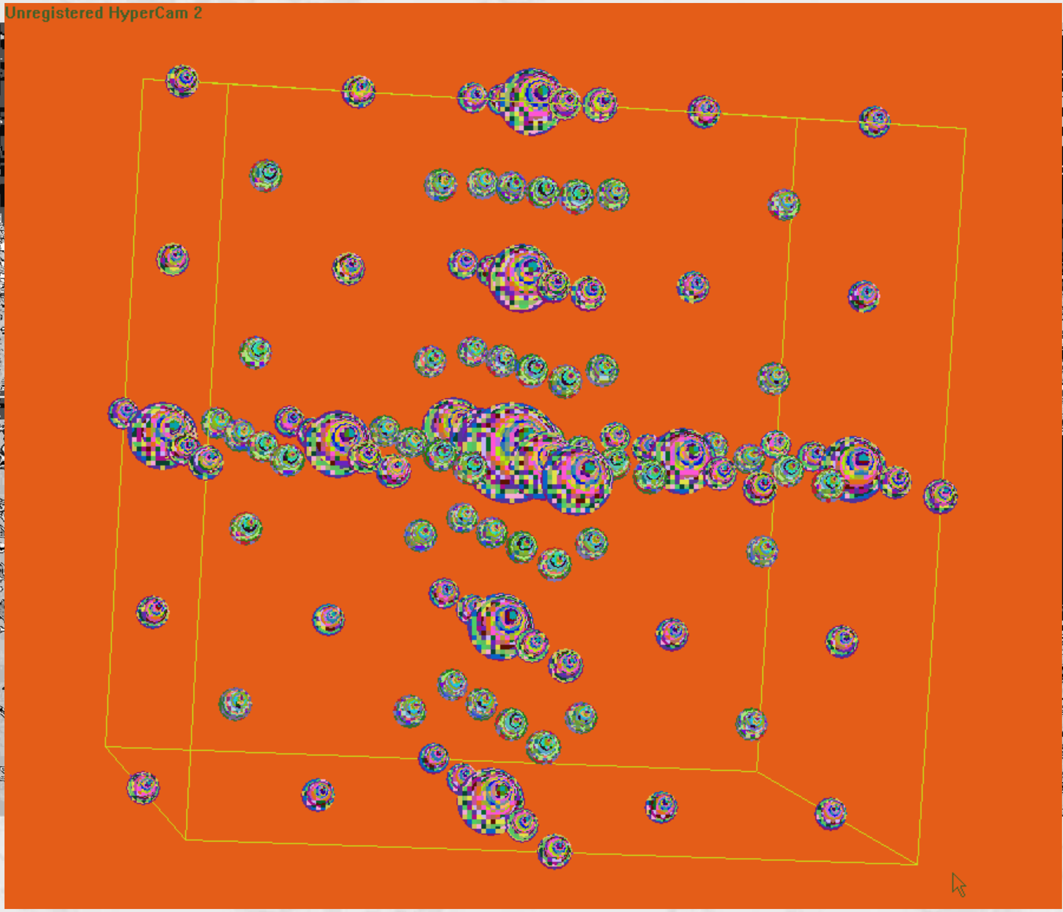

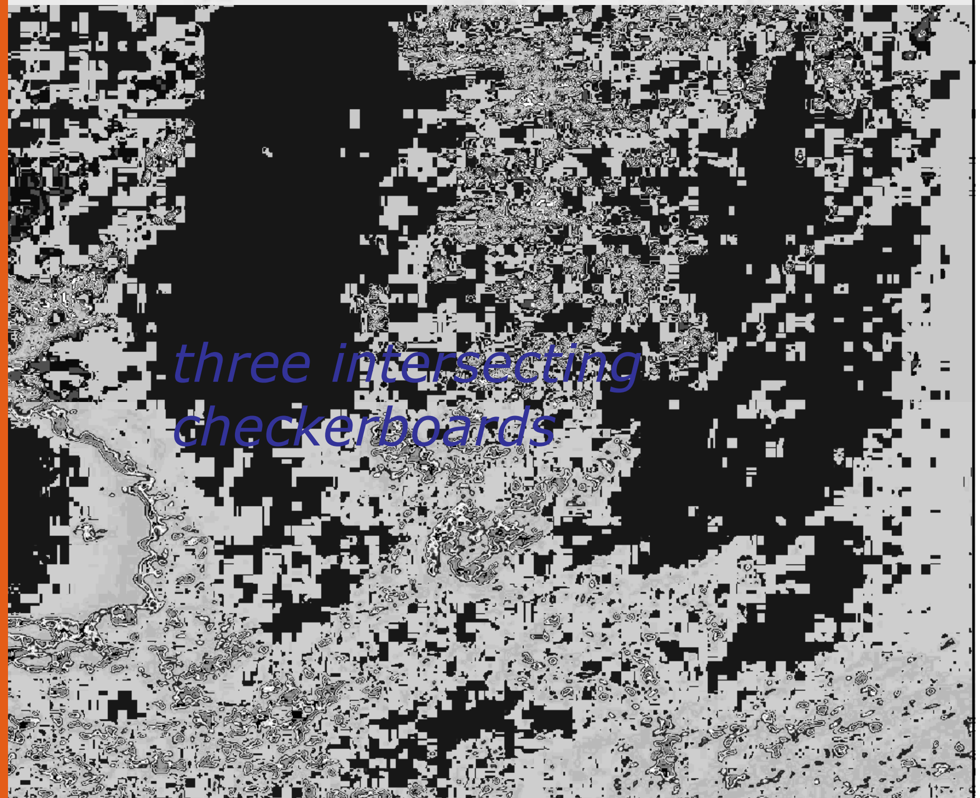

Autocorrelator

$$G(\mathbf{r}) = A' \cdot P(\mathbf{r}) \cdot \sum_{\alpha,\beta,\gamma} \sum_{n_\alpha, n_\beta, n_\gamma = -\infty}^{\infty} \left(\delta(r_\alpha) \cdot \left(\delta(r_\beta + n_\beta)\delta(r_\gamma + n_\gamma) - \delta(r_\beta + n_\beta + 1/2)\delta(r_\gamma + n_\gamma + 1/2) \right) \right)$$

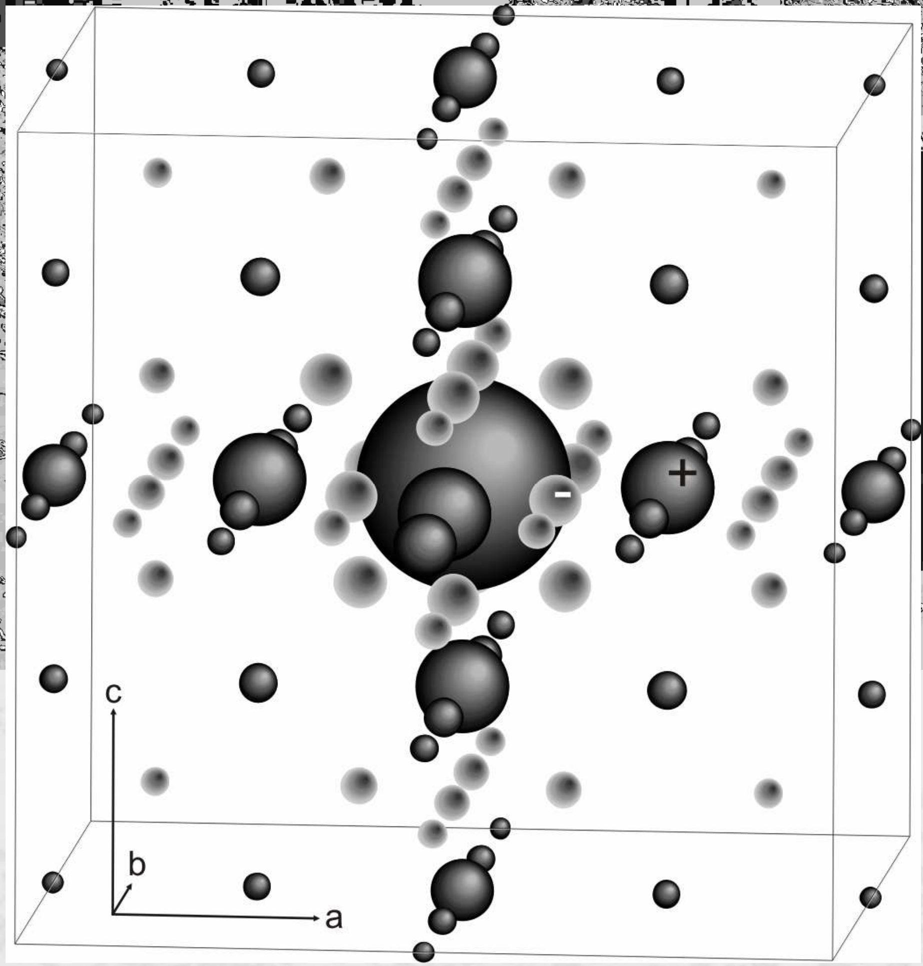

$P(\mathbf{r})$ – decay function, responsible for finite rod thickness

three intersecting checkerboards

Real space implementation

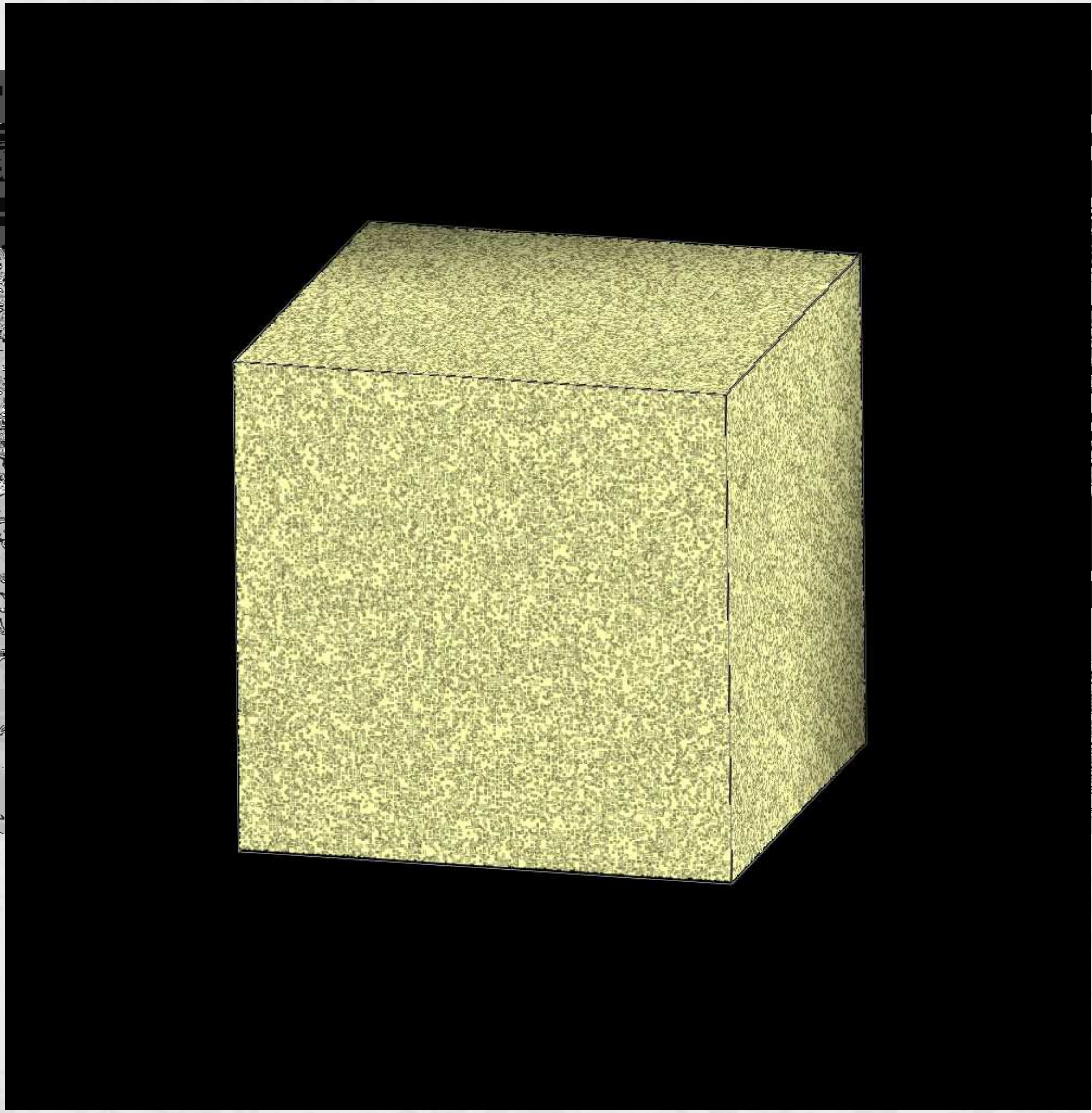

Real space implementation

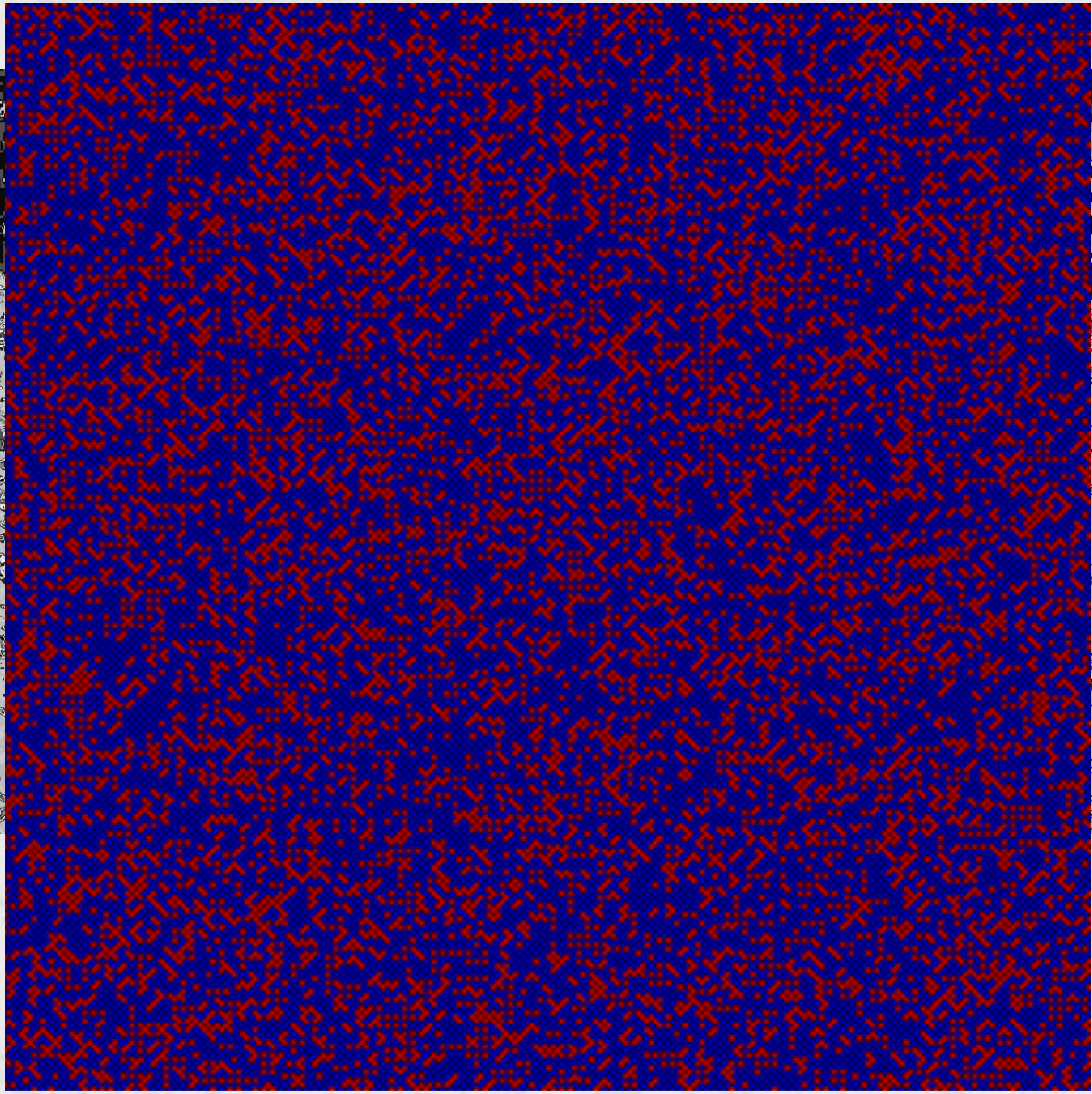

Real space implementation

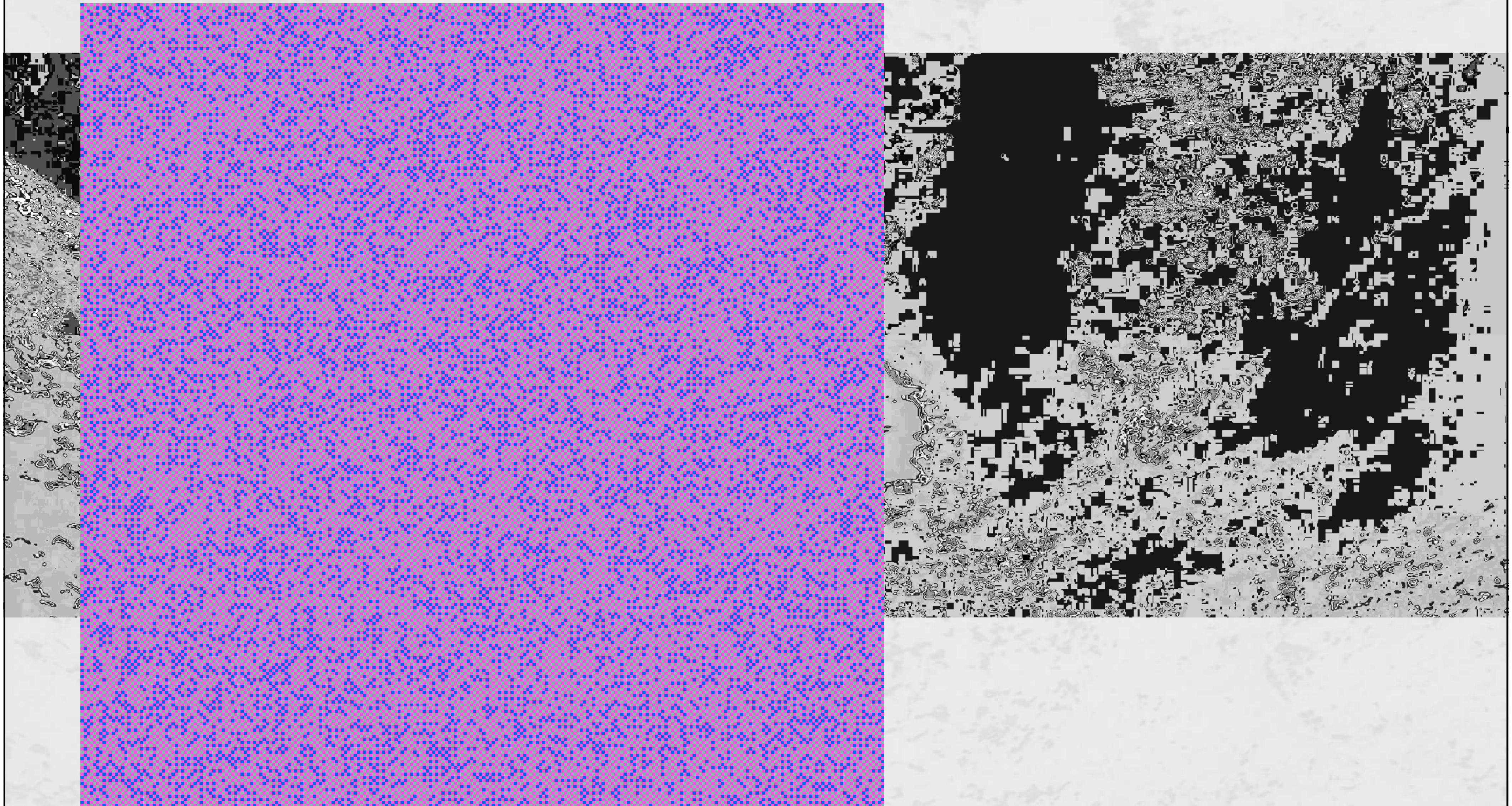

…and back to the reciprocal space

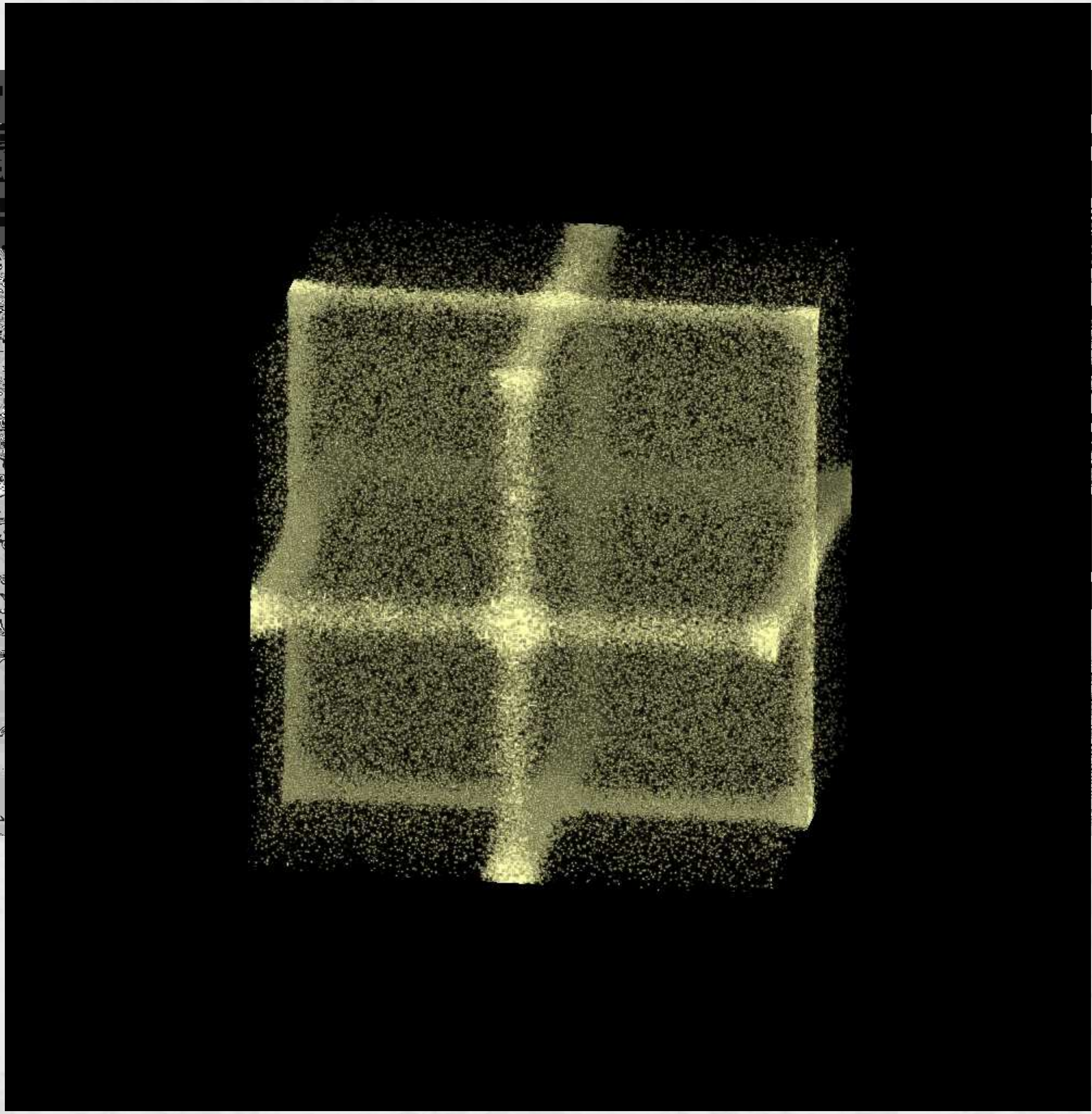

is it general for Prussian Blue analogs?

is calculating multi-site correlations useful?

to which physical properties we can access?

$BaMg_{1/3}Ta_{2/3}O_3$

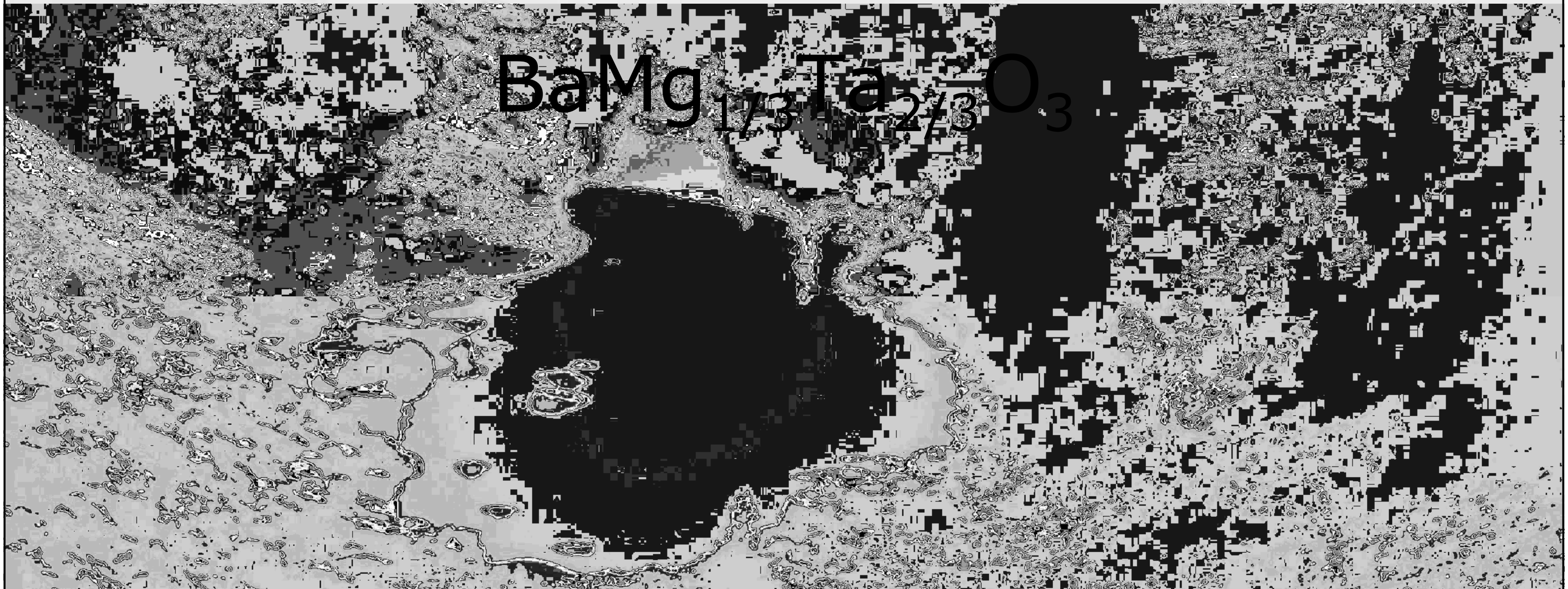

Relaxor-related system

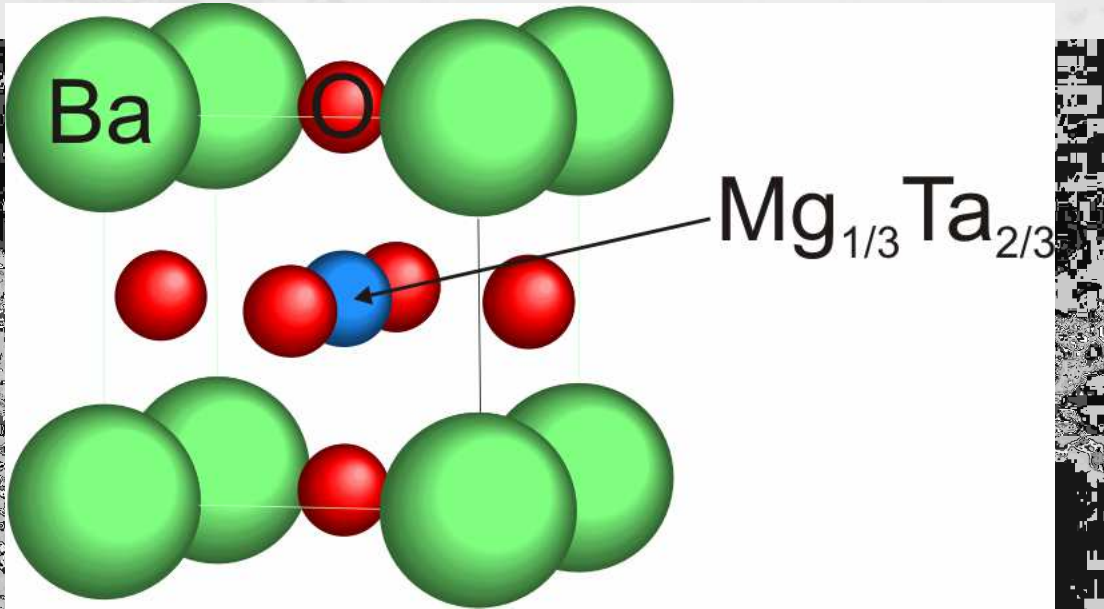

stoichiometry as in PMT ($PbMg_{1/3}Ta_{2/3}O_3$) but no relaxor properties

interesting diffuse scattering!

first observed at SNBL@ESRF circa 2005
S. Gvasaliya, S. Lushnikov, D. Chernyshov

X-ray diffuse scattering

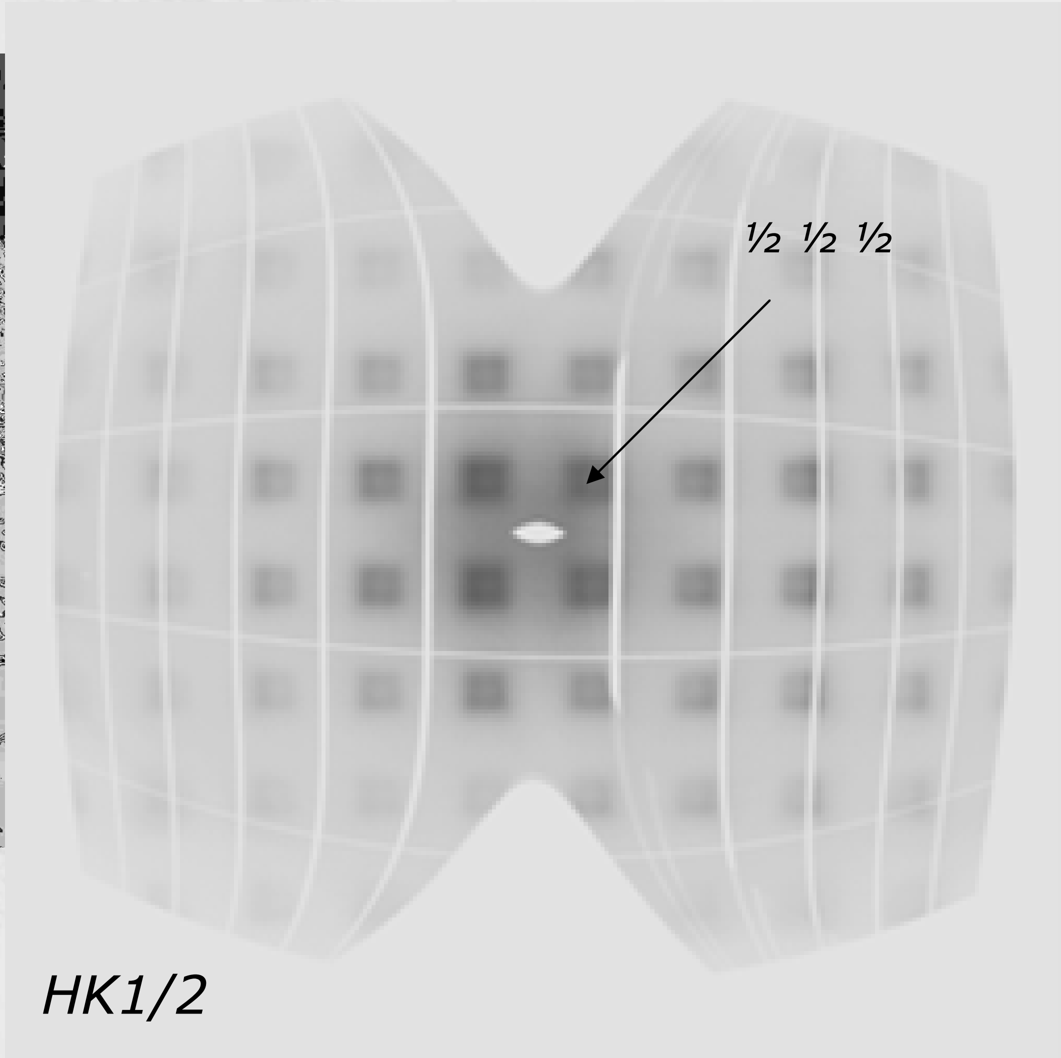

set of cubes centered at (H+1/2 K+1/2 L+1/2)

local minimum of intensity in center

X-ray diffuse scattering

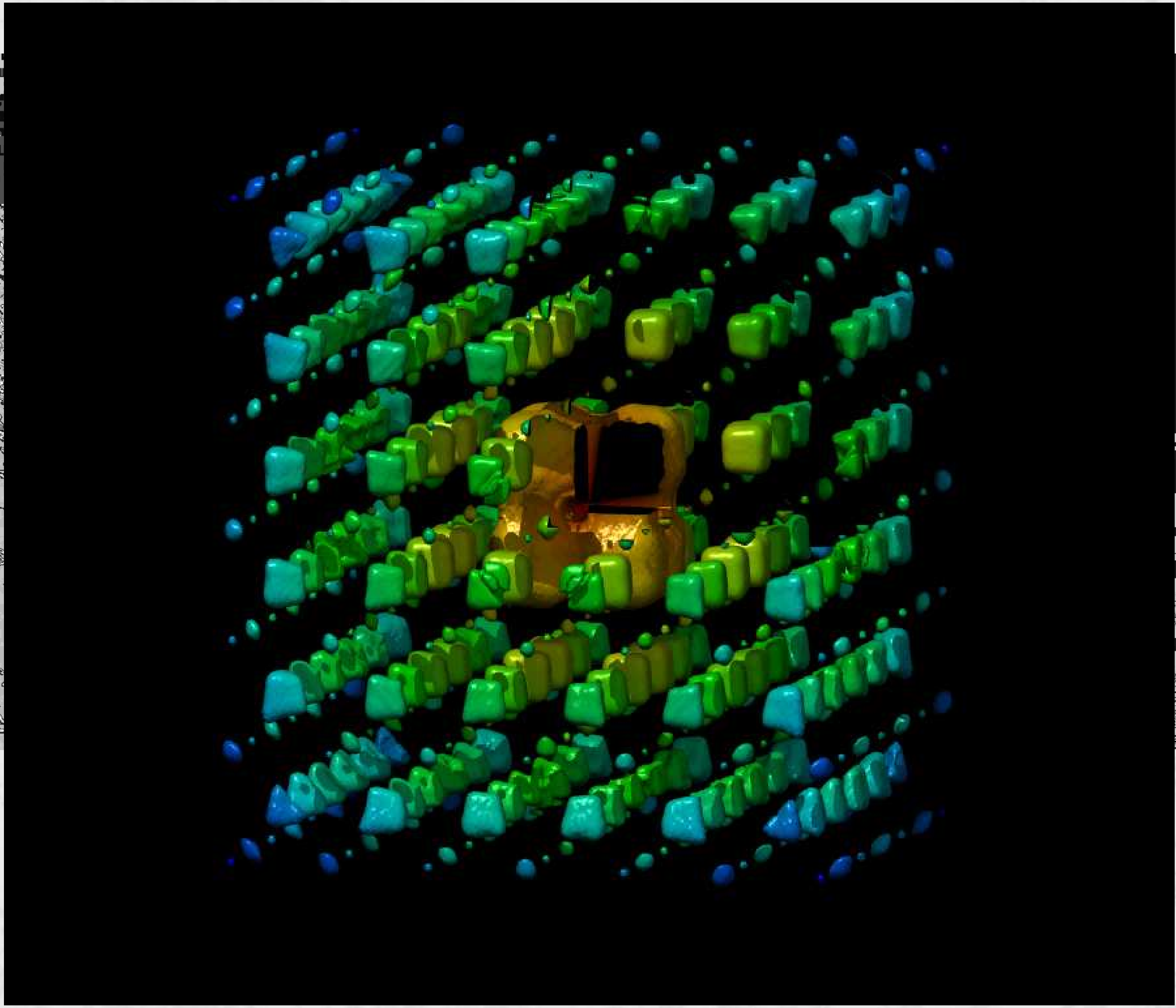

$I(\mathbf{Q})/\left(f_{Mg}(Q)-f_{Ta}(Q)\right)^2$

normalized intensity is nearly the same for all cubes => diffuse pattern relates to Ta/Mg correlations only

Simple parametrization

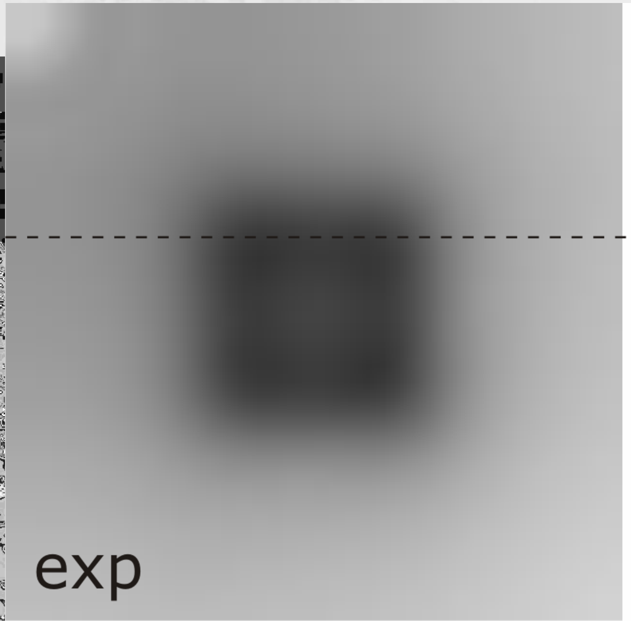

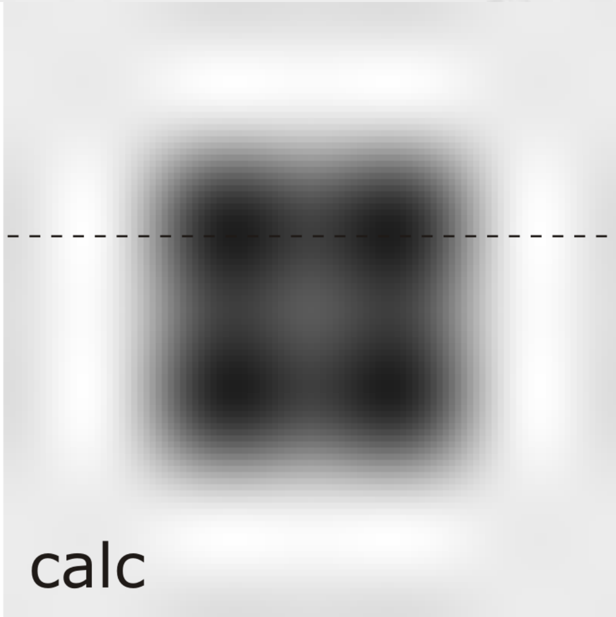

cube

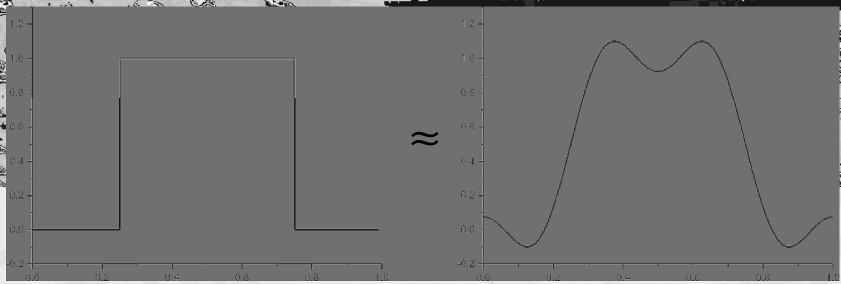

2 terms of Fourier series retained

$$I(\mathbf{q}) = A \cdot \prod_{\alpha=1}^{3} \left(1 - \frac{4}{\pi}\cos(2\pi q_\alpha) + \frac{4}{3\pi}\cos(6\pi q_\alpha) \right)$$

Autocorrelator

$$G(\mathbf{r}) = A' \prod_{\alpha=1}^{3}\left(\delta(r_\alpha) - \frac{2}{\pi}\left(\delta(r_\alpha + a) + \delta(r_\alpha - a)\right) + \frac{2}{3\pi}\left(\delta(r_\alpha + 3a) + \delta(r_\alpha - 3a)\right)\right)$$

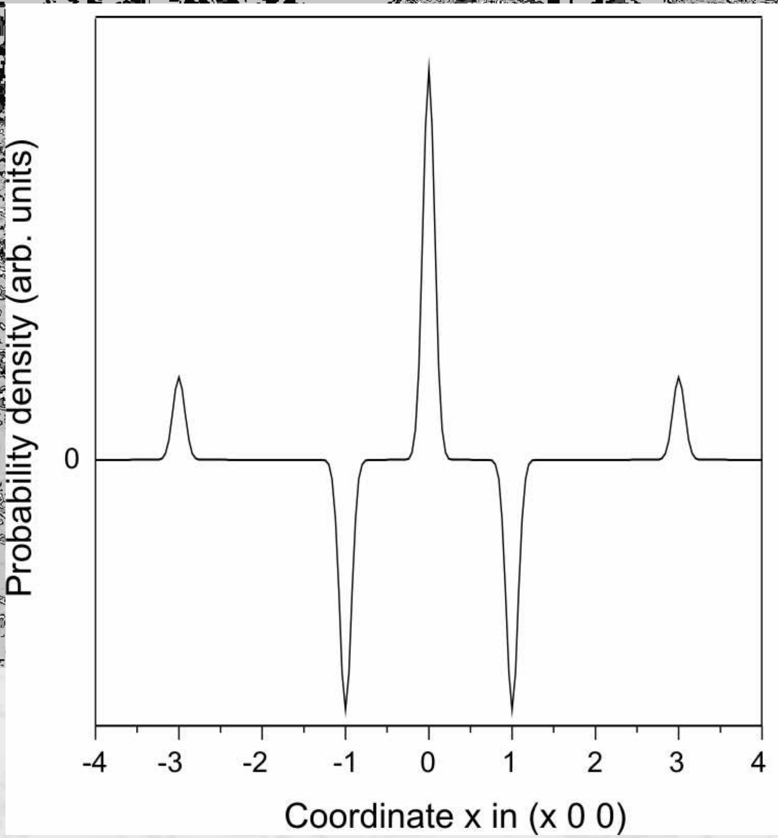

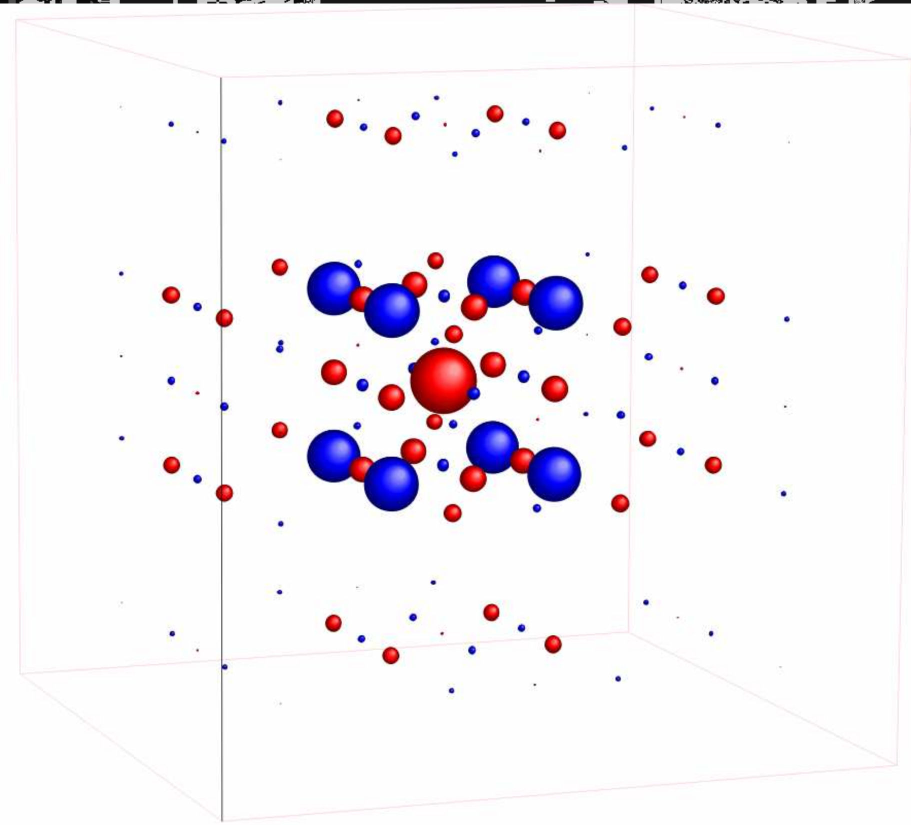

Real space implementation

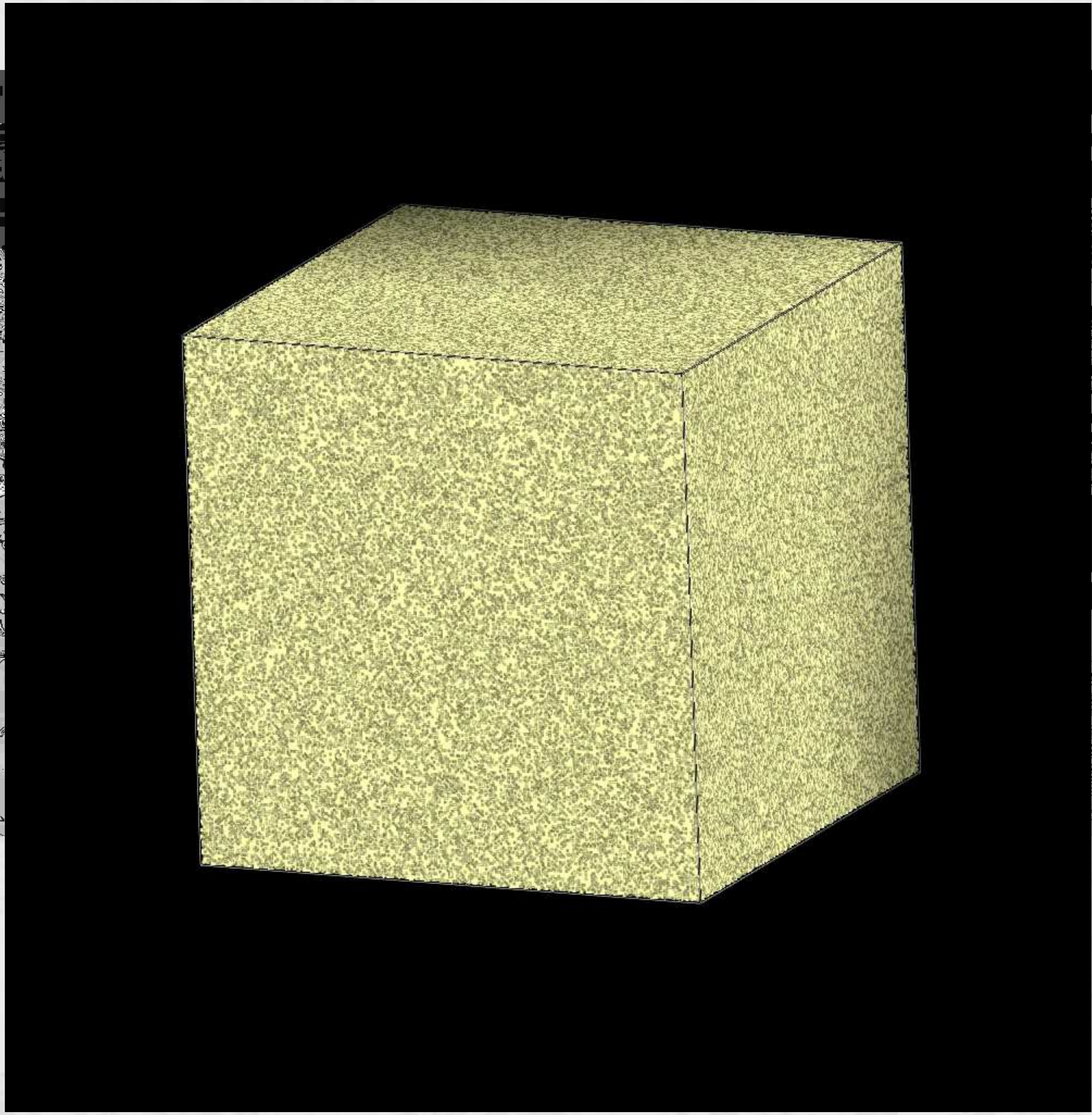

…and back to the reciprocal space

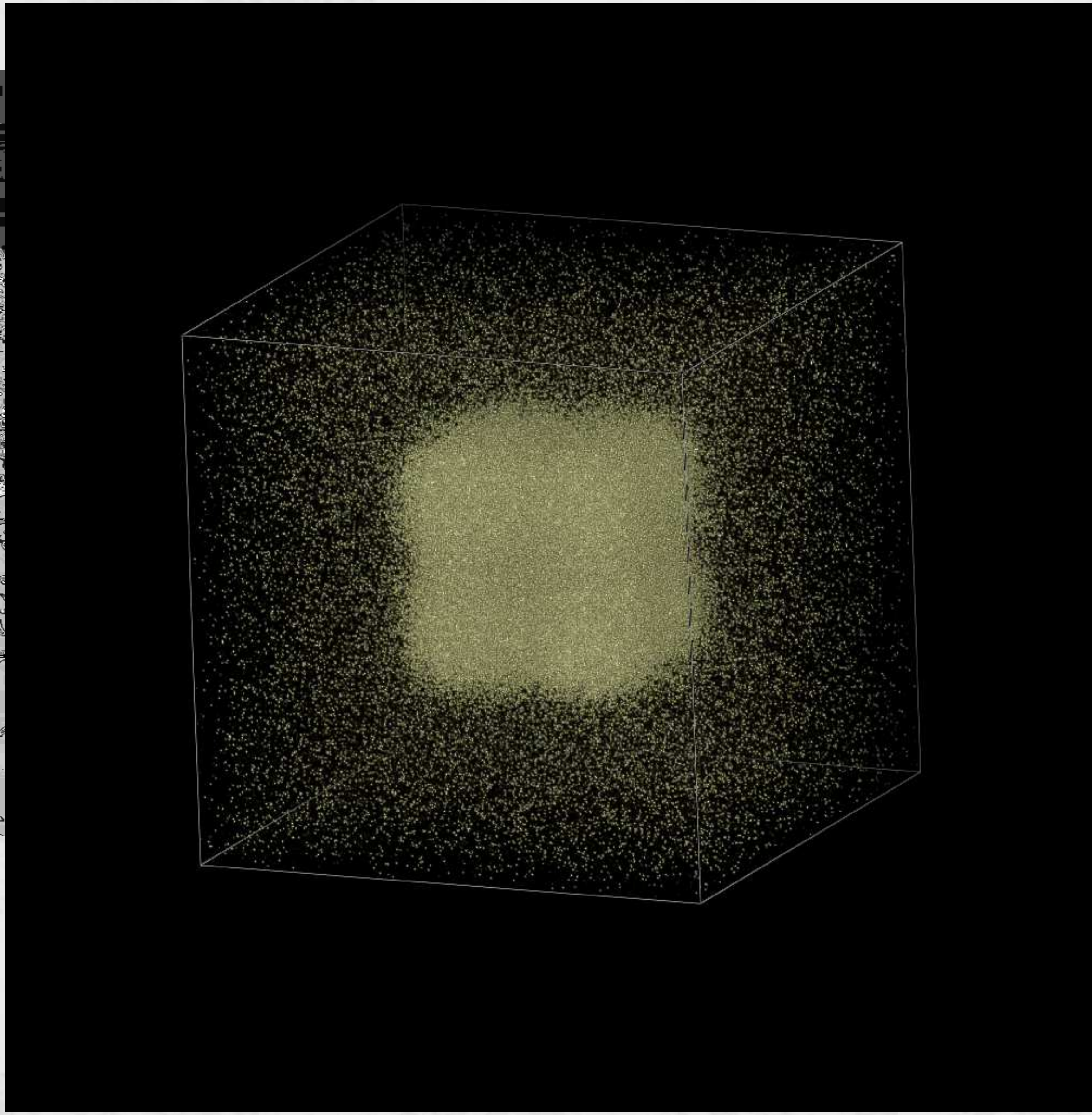

Displacements

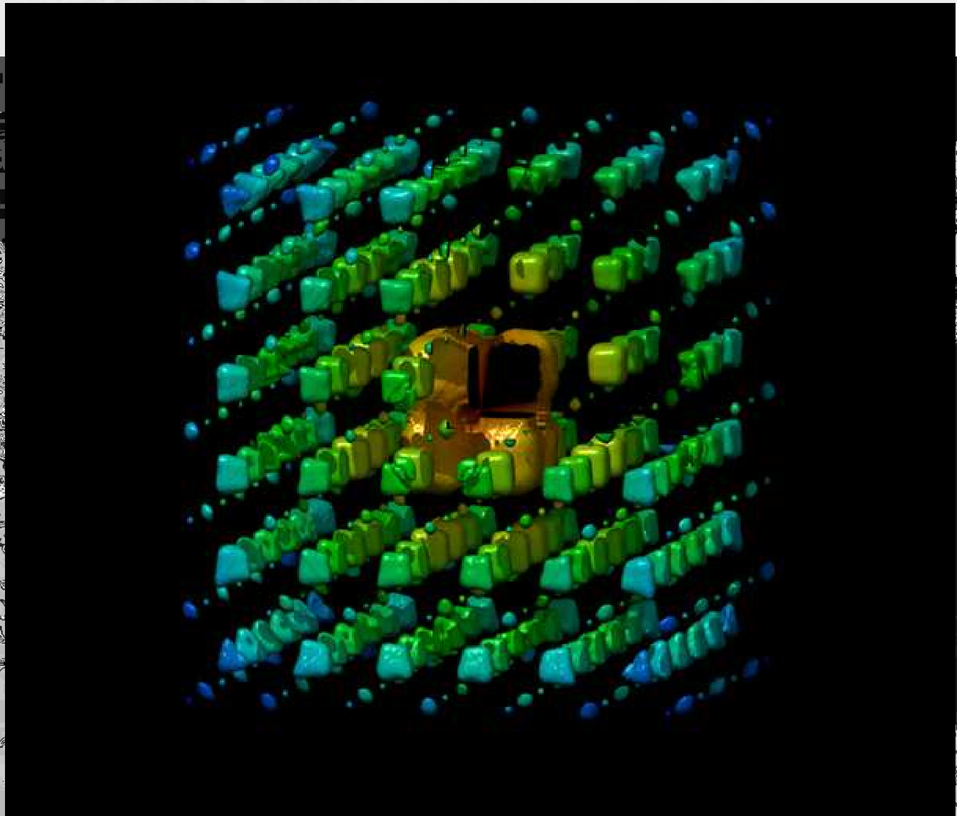

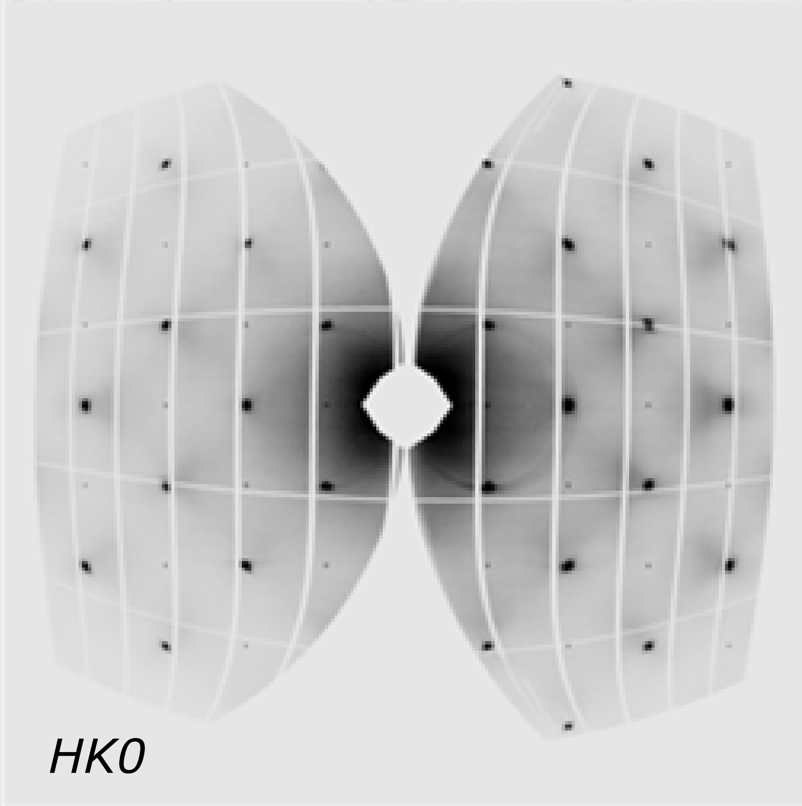

deformed cubes

characteristic intensity distribution close to Bragg reflections

=> Mg and Ta are displaced

first hints: Ta-Ta distance is larger than Mg-Mg is it general for non-relaxor disordered perovskites?

is calculating multi-site correlations useful?

to which physical properties we can access?

Joint use of diffuse scattering and inelastic scattering techniques is mutually beneficial

Acknowledgments

D. Chernyshov (SNBL at ESRF)

M. Krisch (ESRF)

A. Chumakov (ESRF)

M. Hoesch (ESRF)

B. Dorner (ILL)